Master's thesis

NTNU
Norwegian University of Science and Technology
Faculty of Information Technology and Electrical Engineering
Department of Electric Power Engineering

Maren Refsnes Brubæk

Battery Storage as Alternative to Grid Reinforcement in the Low-Voltage Network

A Case Study for a Cabin Field in the south of Norway

Master's thesis in Energy and Environmental Engineering
Supervisor: Magnus Korpås
June 2020

NTNU
Norwegian University of Science and Technology

Maren Refsnes Brubæk

Battery Storage as Alternative to Grid Reinforcement in the Low-Voltage Network

A Case Study for a Cabin Field in the south of Norway

Master's thesis in Energy and Environmental Engineering
Supervisor: Magnus Korpås
June 2020

Norwegian University of Science and Technology
Faculty of Information Technology and Electrical Engineering
Department of Electric Power Engineering

NTNU
Norwegian University of
Science and Technology

Abstract

Most of the Norwegian electrical grid was built in a period were the load patterns were less power demanding, and the requirements for the security of supply were lower than today. Since then, society has become more dependent upon electric power, and the implementation of power-demanding devices has increased, causing more stress on the grid. The low-voltage distribution grid is especially volatile for the increased power demand as this can cause significant voltage drops that can damage the system. One particular load type representing an area where such problems can occur is a cabin field. The low utilisation time of power and the high, unpredictable power peaks will stress the grid. An issue for the grid company in these areas is that upgrading the grid to satisfy the quality of supply often leads to an over-dimensioning of the network. As a result the investment becomes very costly relative to the number of customers. An alternative to grid reinforcement is to install a battery in the grid. The battery can provide power to the system during the most demanding hours and therefore avoid the most excessive voltage drops. At the same time, the installation can be a more cost-efficient solution, as well as a smaller intervention.

This thesis will investigate the utilisation of battery storage in a low-voltage distribution grid as an alternative to grid reinforcement. The objective is to perform a techno-economic analysis, to conclude upon the battery's ability to deliver the required services, as well as investigating the economic feasibility. Python has been used to develop a model that takes in hourly AMS data from a cabin field in the south of Norway. The model contains three main parts: a power flow model that uses the backward/forward sweep algorithm as solution method, a rule-based battery algorithm to control the battery operation, and at last an optimal charge/discharge algorithm to supply and withdraw the optimal power from the grid in each time-step. The basic operating principle of the model is that if the voltage in the system deviates more than 10 % of the nominal value, the battery will start providing power to keep the voltage level within the required limits. By using the results from the model to find the optimal size of the battery and the optimal cross-section for the line upgrade, the two alternatives can be compared economically during investment planning.

The results from the analysis show that if a battery with sufficient power and energy capacity is installed, the battery proves as an as good technical solution as the grid reinforcement. The annual costs of installing battery storage are, however, 77 % higher than the annual costs of the grid upgrade. For the alternatives to break even, the cost of battery capacity has to decrease with 43 % relative to the price level today, to a cost of energy capacity equal to 1164 NOK/kWh and a cost of power capacity equal to 3900 NOK/kW. Extensive sensitivity analyses investigate the impact of an increasing number of customers, several lengths of the main supply line, variations in the load profile and the economic impact from the C-rate of the battery. These studies reveal how dependant the required energy capacity of the battery is on the load profile, and hence the importance of an adequate data basis when investigating the use of grid-installed batteries. The results also confirm the costliness of using batteries for storing large amounts of energy. The study concludes upon batteries being a better solution than the grid reinforcement when the power peaks are not too high and only appear periodically.

Sammendrag

Mesteparten av det norske strømnettet ble bygget i en periode der lastprofilene var mindre kraftkrevende, og kravene til forsyningssikkerhet var lavere enn i dag. Siden den gang har samfunnet blitt mer avhengig av elektrisitet, og andelen effektkrevende enheter har økt, noe som gir økt belastning på nettet. Det lavspente distribusjonsnettet er spesielt utsatt ved økt effektbehov hos kundene, da dette kan forårsake betydelige spenningsfall som kan skade systemet. En spesiell lasttype som representerer et slikt område er et hyttefelt. Den lave brukstiden for effekt og de høye, uforutsigbare effekttoppene vil være belastende for nettet. En utfordring for nettselskaper i disse områdene er at oppgradering av strømnettet for å tilfredsstille krav til forsyningssikkerheten ofte fører til en overdimensjonering. Dermed blir investeringen veldig kostbar relativ til antall kunder. Et alternativ til nettforsterkning er å installere et batteri i nettet. Batteriet kan gi effekt til systemet i løpet av de mest krevende timene, og dermed unngå store spenningsfall i nettet. Samtidig kan installasjonen være en mer kostnadseffektiv løsning, samt et mindre naturinngrep.

Denne oppgaven studerer bruken av batterilagring i et lavspent distribusjonsnett som et alternativ til nettforsterkning. Målet er å gjennomføre en teknisk-økonomisk analyse for å undersøke batteriets evne til å levere de nødvendige nettrelaterte tjenestene, samt studere det økonomisk perspektivet. Python har blitt brukt til å utvikle en modell som tar inn timebaserte AMS-data fra et hyttefelt sør i Norge. Modellen inneholder tre hoveddeler: en lastflytmodell som bruker backward/ forward sweep-algoritmen som løsningsmetode, en regelbasert batterialgoritme for å kontrollere batteridriften, og til slutt en optimal oppladning- og utladningsalgoritme for å levere og trekke den optimale mengden effekt fra nettet i hver time. Det grunnleggende driftsprinsippet for modellen er at hvis spenningen i systemet minker med mer enn 10 % av den nominelle nettspenningen, vil batteriet levere effekt for å opprettholde spenningsnivået innenfor de gitte grensene. Investeringsplanlegging kan bli gjennomført ved å bruke resultatene fra modellen til å finne den optimale størrelsen på batteriet og det optimale tverrsnittet for linjen som skal oppgraderes.

Resultatene fra analysen viser at hvis et batteri med tilstrekkelig effekt- og energikapasitet er installert, viser batteriet seg som en like god teknisk løsning som alternativet, nettforsterkning. De årlige kostnadene for å installere batterilagringsløsning er imidlertid 77 % høyere enn de årlige kostnadene for nettoppgraderingen. For at alternativene skal være jevngode, må kostnadene for batterikapasitet synke med 43 % sammenlignet med prisnivået i dag. Det tilsvarer en kostnad for energikapasitet lik 1164 NOK/kWh og en kostnad for effektkapasitet lik 3900 NOK/kW . Omfattende sensitivitetsanalyser undersøker virkningen av et økende antall kunder, ulike lengder på hovedforsyningslinjen, variasjoner i lastprofilen og den økonomiske påvirkningen fra batteriets C-rate. Disse studiene avslører hvor avhengig den nødvendige energikapasiteten til batteriet er av lastprofilen, og derav viktigheten av et tilstrekkelig datagrunnlag når man undersøker bruken av nettinstallerte batterier. Resultatene bekrefter også hvor dyrt det er å investere i batterier med høy energikapasitet. Det konkluderes med at batterier er en bedre løsning enn nettforsterkningen når effekttoppene ikke er for høye og når de oppstår med jevne mellomrom.

Preface

This master's thesis concludes my five year Master of Science degree in Energy and Environmental Engineering at the Norwegian University of Science and Technology. The thesis was completed in the spring semester of 2020, written under the supervision of Professor Magnus Korpås at the Department of Electric Power Engineering at NTNU.

I want to thank my supervisor, Professor Magnus Korpås, for your availability, guidance and motivation throughout the work with this master thesis. Thank you for all our enlightening Teams-meetings. Further, I would like to thank my co-supervisor Kristin Rekdal at Lyse Elnett for providing valuable system data and for spending your time on this work. Also, a big thank you to PhD candidate at Department of Electric Power Engineering, Kasper Thorvaldsen, for excellent guidance, especially on the work with the specialisation report written during the autumn of 2019. Furthermore, I would like to thank Eivind Solvang at SINTEF Energi and Line Nyegaard at Hafslund Nett for sharing information I was unable to find myself.

Most important are all my friends through my five years in Trondheim. Thank you for making it clear from the start; that friendship is more important than master degrees. At last, my biggest appreciation goes to my family and my biggest fan for always cheering on me!

Trondheim, June 4th 2020
Maren Refsnes Brubæk

Contents

List of Tables

List of Figures

Abbreviations

AC	❖	Alternating current
BESS	❖	Battery Energy Storage System
BFS	❖	Backward/Forward Sweep
BTM	❖	Behind-the-Meter
CENS	❖	Cost of Energy Not Supplied
DC	❖	Direct current
DG	❖	Distributed Generation
DOD	❖	Depth of Discharge
DSO	❖	Distribution System Operator
EV	❖	Electric Vehicle
FACTS	❖	Flexible AC Transmission System
FDPF	❖	Fast Decoupled Power Flow
HP	❖	Heat Pump
IRENA	❖	International Renewable Energy Agency
KCL	❖	Kirchhoff's Current Law
KVL	❖	Kirchhoff's Voltage Law
LV	❖	Low-Voltage
NB	❖	Net Benefit
NPV	❖	Net Present Value
NREL	❖	National Renewable Energy Laboratory
NVE	❖	Norwegian Water Resources and Energy Directorate

- OPF — Optimal Power Flow
- PV — Photovoltaic
- SO — System Operator
- SOC — State of Charge
- TSO — Transmission System Operator

Nomenclature

The nomenclature shows the essential input and output parameters and variables used in the model and for the economic analysis.

B	❖	Set of branches in the system, indexed by b, $b \in B$
N	❖	Set of nodes in the system, indexed by n, $n \in N$
T	❖	Set of time periods, indexed by t, $t \in T$
$b_{battery}$	❖	Binary variable for inclusion of battery $b_{battery} \in \{0, 1\}$
$c_{E,batt}$	❖	Cost of energy capacity of BESS [NOK/kWh]
c_{el}	❖	Price of electricity [NOK/MWh]
c_{line}	❖	Cost per meter of new line [NOK/m]
$c_{P,batt}$	❖	Cost of power capacity of BESS [NOK/kW]
c_{spot}	❖	Spot price of electricity [NOK/kWh]
d	❖	Discount rate
E_{batt}	❖	Energy capacity of battery [kWh]
E^t_{batt}	❖	Energy capacity of battery in hour t [kWh]
P_{batt}	❖	Rated battery power [kW]/[pu]
P^t_{batt}	❖	Power injected to the battery in hour t [kW]/[pu]
P_{bbus}	❖	Power injected to the bus where the battery is located [kW]/[pu]
P^t_{ch}	❖	Power charged to the battery in hour t [kW]/[pu]
P^t_{dis}	❖	Power discharged from the battery in hour t [kW]/[pu]
P^t_n	❖	Real power injection at bus n in hour t [kW]/[pu]
Q^t_n	❖	Reactive power injection at bus n in hour t [kW]/[pu]
SOC^t	❖	Battery state of charge in hour t [pu]

- SOC_{start} — Initial SOC of the battery [pu]
- t — Time resolution. Each time step equals one hour [h]
- V_{min}^{t} — The lowest voltage in the system in hour t [V]/[pu]
- V_{n}^{t} — Voltage magnitude at bus n in hour t [V]/[pu]
- Z_b — Impedance value of branch b [Ω]/[pu]
- γ_{batt} — Economic lifetime of BESS investment [years]
- γ_{line} — Economic lifetime of line investment [years]
- δ_{n}^{t} — Phase angle at bus n in hour t [rad]
- $\epsilon_{\gamma,d}$ — Annuity factor for γ years and discount rate d [1/years]
- η_{ch} — Charging efficiency of battery [-]
- η_{dis} — Discharging efficiency of battery [-]
- η_{rt} — Round-trip efficiency of battery [-]
- κ_{BFS} — Maximum allowed mismatch in BFS-algorithm [-]
- κ_{V} — Maximum allowed mismatch in optimal charge/discharge algorithm [-]

1 Introduction

1.1 Background and Motivation

The Norwegian distribution grid is facing challenges as it is getting older, at the same time as the power demand is higher and the penetration of distributed generation is increasing. A large share of the Norwegian grid was built between the 1950s and the 1980s. Hence, the dimensioning of the grid was done from contemporary conditions [1]. Since then, the requirements for security of supply have increased, the society is more dependent on the electric power supply, and the power demand is relatively higher than the energy demand [2]. Grid enhancements are required, and as also the need for cost-efficient solutions is increasing, new technologies, like grid-installed batteries, can prove to be good alternatives to grid reinvestments.

1.1.1 Distribution Grid Development

The increasing demand for electric power pushes the development of the power system. Worldwide, there is a high focus on producing more renewable energy to cut the use of polluting fossil fuels and reach the common goal of performing climate change mitigation and reduce carbon emissions in all sectors. The fast development that is necessary to achieve these goals will intensify the stress on the power grid, and it is essential to develop the network to handle it. Developing an intelligent grid is the desired solution. Smart metering systems (AMS), power electronic equipment and digital control systems can solve the problems of the power system in an intelligent, cost-efficient manner, which is also a more efficient way of operating the system [1].

In Norway, there is an increasing power demand as a consequence of the high penetration of domestic electric vehicles (EV) and heat pumps (HP), along with the political will to electrify public transport, ferries, oil platforms and shortly also the aeroplanes. Distributed generation in the weaker parts of the grid also causes challenges for the system operators, as it is not dimensioned for the high power peaks [2]. Grid companies are obliged to deliver power of a certain quality, one of the criteria being sufficient voltage quality to avoid damaging electric equipment. With the increased power demand and with a grid that is not dimensioned to handle it, the

voltage drop may become too large.

The traditional way of dealing with stress on the grid has been to perform costly grid reinforcements. While this will still be necessary many places, the drawback of this solution becomes very clear in remote distribution grids, where upgrading may lead to an over-dimensioning of the network, and thus comes at a very high price relative to the number of customers. Cabin fields represent one of these types of areas with low utilisation time during the year and high power demand in specific periods. In such locations, a battery installation may be an as good technical solution and a more cost-efficient economic solution than a grid reinforcement.

1.1.2 The Value of Battery Energy Storage as a Grid Asset

Stationary batteries with monitoring and control can be one of the solutions to reach the goals for the future smart grid. It can provide grid services such as voltage regulation, balancing of phases, avoiding congestion, increasing short circuit current and local frequency control, and at the same time come at a lower cost and provide increased flexibility [3]. Besides the technical opportunities and the economic feasibility of installing batteries, another motivation is the fact that batteries and other energy storage systems will play a vital role in decarbonising the power sector in the world, which is essential to ensure a sustainable power system and to reach the climate goals[4].

Battery energy storage systems (BESS) used as an energy storage asset is predicted to be a suitable alternative to other grid investments in the Norwegian distribution grid. One of the main barriers is the still quite high price of power and energy capacity [5]. An economic analysis has to be performed to investigate the value of batteries in the grid. Many studies with various objectives and purposes have identified the related costs of battery installations, and rather few have found batteries to have a considerable economic advantage.

Studies that were conducted by H. Pandzic et al. [6] and Y. Zhang et al. [7] exploit arbitrage by letting the battery participate in the market. They aim to find the optimal battery size for its purpose. For both the studies, the investments costs have to be much lower than the market price today for the battery to be profitable. Y. Yang et al. [8] and P. Fortenbacher et al. [9] investigate the battery's ability to perform peak load shaving and voltage regulation when installed with photovoltaics (PV), and thus also reduce system costs. Yang et al. [8] do not find any profitable solution, while Fortenbacher et al. [9] find behind-the-meter (BTM) applications beneficial for low battery investment costs. P. Ahcin et al. [3] test the battery for various use cases, such as reducing grid charges, peak shaving with PV and grid support. It was found that using batteries for frequency regulation gives profitable economic outcome even for investment costs as high as 1500 EUR/kWh. As for the other use cases in this paper, they provide similar

results as the studies presented above.

B. Böcker et al. [10] and A. J. Aguado et al. [11] looks at larger systems and combine grid planning with the use of arbitrage for the battery, to investigate if exploiting arbitrage can reduce the grid costs. They find that the battery only used as a grid asset is not likely to be chosen due to the high prices, but when combining the use of arbitrage and grid support, batteries are viable options. However, these two studies also require low investment costs to obtain profitable results. Few studies investigate remote areas with loads with low utilisation time, where a battery will keep the voltage level up at hours with high demand as an alternative to grid reinforcement. When comparing the cost of the battery to the cost of a new line, the economic outcome may still favour the battery even if most of the above studies do not with the price level of today.

1.1.3 Batteries for Voltage Support in Low-Voltage Network

Residential photovoltaic (PV) systems may cause over-voltages when installed in a low-voltage (LV) grid, and EVs and other power demanding equipment typically produce under-voltages, both types which can damage connected equipment. Under-voltages also occur in highly loaded systems and in remote radial distribution systems where long lines cause large voltage drops. Various studies have been performed to investigate the use of batteries for voltage regulation in LV grids.

L. Wang et al. [12] propose a method for coordination of several batteries in a system, which purpose is to prevent voltage rise in an LV with PVs. The technique works for its purpose, and may also be used for peak-load shaving and under-voltage regulation. In two studies by P. Fortenbacher et al. [8] [13] AC grid models are used as a basis when installing BESSs in the LV grids with PVs to satisfy grid constraints, including avoiding overvoltages. In the study of I. Ranaweera et al. [14] over-voltages are avoided by setting a threshold for the power fed into the grid from the behind-the-meter (BTM) application. The voltage level is not included directly but represented as a function of active power. B. Böcker et al. [10] use a similar approach, where the voltage level is included as a function of the real power, used to set a limit on the transfer capacity in the lines.

M. Kashem et al. [15] propose a strategy for voltage support in the distribution grid by using batteries to export active and reactive power to the system. The strategy is optimised for voltage control to reduce the battery size and reduce the costs. M. Alam et al. [16] propose an approach for charging and discharging of the battery to solve voltage excursions. Both studies show that batteries can provide the necessary service for voltage regulation. M. Kabir et al. [17] propose a coordinated use of PV and batteries to address voltage rise and dip problems. They find that

support from the BESS is especially necessary for remote systems with high-resistance lines.

1.1.4 Power Flow Solution in Radial Grids

A complete power flow analysis will give the best basis for the study in terms of investigating the operation of the power system. This way the exact voltage magnitude and angle are found based on the real and reactive power levels in the system, resulting in a more precise solution, as also stated by P. Fortenbacher et al. [8][13]. For solving the power flow problem in radial distribution systems, the traditional Newton-Raphson method and the fast decoupled power flow (FDPF) method both have some shortcomings related to the ability to provide the power flow solution in radial grids [18].

A method that has proved as more reliable and robust for obtaining the power flow solution in radial grids is the backward/forward sweep (BFS) algorithm proposed by D. Shirmohammadi et al. [18]. There exist various modifications of the BFS method, such as inclusion of buses with distributed generation [19], voltage-dependent loads [20] [21] and three-phase systems [22]. Versions of the method have been adopted for optimal power flow models [8], methods for power flow in systems with multi-source and multi-type distributed generation (DG) [23] and power flow calculations in microgrids with droop-regulation [24], amongst others. M. Kabir et al. [17] use the BFS algorithm for power flow calculations in systems where BESS and PVs are installed with voltage regulating purposes. The extensive use of the method and its suitability for radial grids, enable the use of it for this study.

Based on previous research, it can be seen that the BESS operates as a suitable technical solution for grid services such as voltage support and load shifting. The most significant obstacle for the use of the BESS is the installation costs, making it harder to find use cases that return profitable solutions for the owner. This thesis will investigate the use of the battery in a weak grid, with large voltage drops due to high demand in parts of the year, for both technical and economic purposes. The analysis is performed from the distribution system operators perspective and utilises the robustness of the BFS method for power flow analysis. In an area with low utilisation time of power, a BESS may avoid an over-dimensioning of the line supplying the area.

1.2 Objective

The main objective of this master thesis is to perform a techno-economic analysis of installing a BESS in a weak, overloaded grid when comparing it to a grid reinforcement. The purpose of the BESS is to provide sufficiently active power during the hours with high power demand so that the voltage level in the system never drops below a specified limit set to 0.9 pu. in this case. The area to be investigated is a cabin field located in the outer part of the distribution

system in the southern part of Norway. The thesis has the following objectives:

- Give an introduction to the relevant theory and prerequisite knowledge used as the basis for the model development. The work should emphasis the low-voltage network operation, battery energy storage systems and the power flow solution method.
- Build a power flow model for a radial distribution system based on the principles of the backward/forward sweep algorithm. The model will include a rule-based algorithm to use BESS for hourly voltage regulation caused by voltage drop in the lines. Develop an optimal charging and discharging algorithm in order to limit the required BESS size and operate the BESS more efficiently.
- Find the optimal BESS size for the system so that it can handle the voltage drops at all time, and find the required line capacity in the case of a line upgrade. Both findings will be based on the results from the power flow model.
- Perform an investment planning analysis that compares the costs of the BESS installation with the cost of installing a new line.
- Investigate the operating differences with and without the BESS and compare them to the operation after a line upgrade.
- Perform sensitivity analyses on important system parameters to draw conclusions that are less dependent on this exact case study.

1.3 Limitations

Limitations on the scope of the thesis have been made to investigate the desired factors only and to keep the study within reasonable boundaries:

- The study focuses on normal operating conditions. All operation during a failure is neglected from the study, applying to both the technical and economic aspects.
- The analysis looks at the operating conditions in a one-hour perspective so that only the slow variations in the voltage are investigated. Other disturbances are neglected.
- The BESS is simplified to containing battery packages and one inverter; other components are neglected.
- Investment planning is comprehensive, with many cost factors included. Emphasis will be put on the investment costs of the investment alternatives. Operational costs, such as maintenance and the cost of battery degradation, are not taken into account.

- The data used in the study have been provided by Lyse Elnett, and one month of AMS data have been made available. The dimensioning of the BESS and the line is based on this operating month, assuming it is the most loaded month.
- The regulatory concerns have not been included in the economic analysis. It can be assumed that the grid operator is allowed to own or pay for a grid-installed BESS, and use it for voltage regulation.

1.4 Structure

This master thesis is strutured in the following way:

- Chapter 2, *Battery Installation in a Low-Voltage Network*, aims to give the reader the necessary background information about the concepts and the theory that underlies the work.
- Chapter 3, *Power Flow Algorithm*, gives an introduction to the power system operation and analysis, emphasising the theory behind the backward/forward sweep algorithm as a power flow solution method.
- Chapter 4, *Model Construction*, describes how the model used in the analysis is built, containing three main parts: a power flow model, a battery model and an optimal charge/discharge model.
- Chapter 5, *Investment Analysis*, contains information on the methodology of the performance of the investment analysis.
- Chapter 6, *Case Study Description*, introduces the system data provided by Lyse Elnett, and the development of a case study based on this data.
- Chapter 7, *Analysis of Results*, presents the technical results from running the model, as well as the economic outcome of the investigation. Results are analysed and compared through the chapter.
- Chapter 8, *Discussion*, focuses on discussing the main findings from the results, seen in a bigger picture.
- Chapter 9, *Conclusion*, summarises and concludes on the main findings.
- Chapter 10, *Further Work*, presents suggestions for further work.

2 | Battery Installation in a Low - Voltage Network

This chapter gives an introduction to the background and component theory that will affect the installation of a battery in the distribution grid. The section aims to provide the reader with an understanding of the basic working principles behind the research. It presents an overview of the Norwegian power system focusing on the radial distribution grid, with the purpose to explain the system where the BESS will be installed. A thorough description of the BESSs operation and composition will be presented, as well as the relevant regulatory aspects of the installation. The basic principles of investment planning are presented to enlighten a vital element of the technical-economic analysis performed in the study. The developed model of this thesis is based on the theory presented in this chapter and the upcoming chapter 3, that focuses on the power system operation.

Parts of this chapter are extracted from the specialisation project that was written by the author during the autumn of 2019 [25]. Most of the sections are re-written to better fit the objectives of this thesis, whereas section 2.2.3, 2.2.4 and 2.3 are direct excerpts from the specialisation report.

2.1 The Norwegian Power System

2.1.1 Features of the Power System

The three essential parts of the power supply system are production, transmission and trade [26]. The electrical grid is the infrastructure for supplying electricity to the end-users. Most of the customers are located far away from where the power is produced, and a well-functioning infrastructure for power transmission is essential to maintain the security of supply. The grid is dimensioned to handle continuous power flow, with daily and seasonal variations in peak power. Norway is also dependent upon power exchange with Europe, to export power when the water

reservoirs are filled up, and Europe needs power, and to import power during dry years and periods with high demand [26]. As opposed to the power producers the power grid is considered a natural monopoly, and it is therefore regulated by the Norwegian Water Resource and Energy Directorate (NVE) [27]. More information about the regulatory authority is given in section 2.1.2.

For grid stability, both active and reactive power must be balanced. At all time the power generated in to the system has to equal the power consumed from the system, including the system losses. A simplified power balance equation is formulated in equation (2.1):

$$\begin{aligned} P_{gen} &= P_{load} + \Delta P_{loss} \\ Q_{gen} &= Q_{load} + \Delta Q_{loss} \end{aligned} \tag{2.1}$$

The requirement of instant power balance is caused by the important electricity feature, that it can not be stored in its natural form [28].

2.1.2 Laws and Regulations

The Norwegian Power System is regulated by the Energy law §1-2 [29], translated to [1]:

> *"The law ensures that production, conversion, transmission, purchase, distribution and use of energy is made in a socially rational way, that include considering the public and private interests that are affected."*

NVE is the regulatory authority which job is to ensure that the Energy law is enforced. They regulate the grid companies' position as monopolies, ensure that the grid is used and developed in an efficient and rational socio-economic way, as well as verify that the power market is well-functioning and efficient [30].

Grid companies have to ensure the quality of supply. Quality of supply contains two main technical parts, voltage quality and the reliability of power supply. The reliability of supply tells how often the customer has access to electric energy. The voltage quality has to be ensured for the power to be usable and not in a condition where it may ruin electrical equipment [31]. The maximum voltage deviation in Norway is ± 10% of nominal value [32] and the nominal frequency of 50 Hz should not deviate more than 0.1 Hz in each direction [33]. Any frequency and voltage deviations should be adjusted back to their nominal values if any disturbances are introduced to the system. The law of a maximum voltage deviation of ± 10% refers to the slow variations in the effective value of the voltage. It is measured as the average over a minute. There are also laws for handling short voltage variations, and these variations are measured in

[1] Translated by the author

seconds. The inclusion of short voltage variations is out of the scope of the thesis, and will be neglected from the study [31].

There are no specified quantitative limits related to the regulations of the reliability of power supply. However, there are still strict rules for the regulations, regarding how the grid companies handle outages and requirements for improvements on the grid. The grid companies also have economic incentives for maintaining the grid. NVE sets a limit every year for how much revenue the grid companies can have. Their income is based on the grid tariffs that they set for the customers. The allowed revenue will cover all costs related to operation and depreciation, and will also give a reasonable return on investments. Any Costs of Energy Not Supplied (CENS) are subtracted from the annual allowed revenue. This gives incentives for the grid companies to maintain the network in good shape, and make the necessary investments to ensure safe and continuous operation [34].

As a consequence of the strict revenue rules and the monopolistic position, the grid companies are not allowed to do any speculations in the future power prices that can benefit them economically. All investments should be made based on the need for society, not what may benefit the grid company. Thus energy storage assets as batteries, are not allowed for the grid companies to own as they may provide economic benefits. By selling power when the cost of electricity is high, and buy power when the prices are low, a battery is seen as a participant in the power market, which is forbidden for any assets owned by a grid company.

Due to these regulations, installing a battery in the grid is not as easy as any other asset used for providing grid services. In the report that DNV GL has written for NVE [5], they conclude with the recommendation that batteries should not be owned by grid companies, as to avoid the possibility for them to misuse the position as monopoly, and to make it easier for NVE to regulate their activities. A third-party owner and operator of the battery may be one solution to deal with the regulatory limitations. Studies done on batteries in the grid show that the limitations from the regulatory framework is not insignificant regarding the economic feasibility of the battery. The regulatory framework, the market framework and the strategic behaviour may have decisive influence on the value of storage systems in the grid [35][36]. The economic study in this thesis will not include possible disagreements with the regulation authority, however to avoid the possibility, the BESS will only take the role as a grid asset and not as a participant in the market.

2.1.3 The Norwegian Distribution Grid

The Norwegian grid is divided into three levels, the transmission grid, the regional grid and the distribution grid. Table 2.1 shows how the grid is structured based on the different voltage

levels.

Table 2.1: Voltage levels for the grid division [37]

Grid level	Voltage level [kV]
Transmission system	420, 300, (132)
Regional system	132, 110, 66, 47, 33
Distribution system	22, 11, 0.4, 0.23

Statnett is the transmission system operator (TSO) in Norway, and owns most of the transmission grid, while the regional and distribution grid are owned by local distribution system operators (DSO)[26]. At the distribution level, the voltage level can be categorised as either high-voltage or low-voltage. The limit of which separates the levels is 1000 V, meaning that the low-voltage (LV) network is defined as having a voltage level below 1000 volts [38]. Most of the low-voltage network in Norway has a radial structure [39]. An example of a radial grid structure can be seen in figure 2.1. Radial networks have the advantage of being cheaper to install than the meshed networks, and it is also easier to limit fault currents from flowing in them, and thus reduce protection complexity.

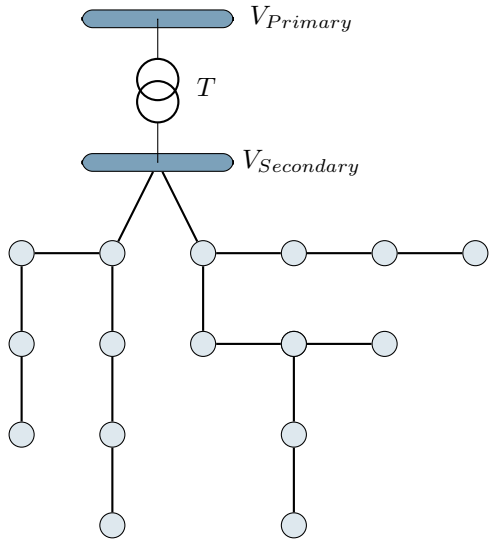

Figure 2.1: Radial grid structure

Another way of categorising the grid is using its physical condition and its capability of delivering power with the required quality. A grid can be seen as either a stiff or a weak grid, dependent on its short circuit capacity, impedance value and R/X-ratio. Stiff grids are defined by a high short circuit capacity, low impedance value and low R/X-ratio, while the opposite

is the case for a weak grid [40]. Weak grids are typically occurring in remote areas where the distance from the substation to the load is long, and the nominal voltage level is at 230V [41]. The low short circuit capacity makes it more challenging to detect fault situations, and the high R/X-ratio and high impedance may cause large voltage drops and poor voltage quality. The thesis will emphasise the issue of voltage drops in the distribution grid.

For stiff grids, the frequency in power systems is strongly related to the real power balance, and the voltage level is associated with the reactive power balance [42]. As for low voltage networks, the voltage level is highly responsive to changes also in the active power balance. The weaker the grid, the stronger is the relation between the active power and the voltage level. A power flow analysis can be conducted to get a precise evaluation of the "health status" of the power system [43]. More on the importance of power system analysis is given in chapter 3.

2.1.4 Mitigating Voltage Irregularities

Approximately 14% of customer complains are related to a too low voltage level. Voltage irregularities can be mitigated by using different technologies and techniques, and the method to be used will depend on the circumstances. For low-voltage distribution networks, active power management is more efficient than reactive power management, whereas the opposite is the case for transmission systems. Some ways of mitigating slow voltage deviations are given as follows [44]:

- **Network Reinforcement** - By upgrading the grid to a larger cross-section of the lines, the voltage drop and losses in the lines become smaller.
- **Replacement of Transformers** - If the transformer is not large enough to handle the power transfer, an upgrade to a larger transformer will be necessary to avoid voltage deviations.
- **Change of Transformer Tap Changing Setting** - Tap changing control is used to control the number of turns in the transformer windings so that the power and voltage output can be adjusted. DGs that returns inversed power flow cause problems for the tap-changing control.
- **Shunt/Series Compensation** - Capacitor banks and Flexible AC Transmission System (FACTS) devices are places in series or parallel at appropriate places in the grid to keep the voltage magnitude constant, amongst other uses [45][46].
- **Load Limitations / Peak Power Tariffs** - Trying to avoid the large power demand either by putting limitations on the total load demand in an area or by encouraging the customers to not use power during peak demand hours by giving price incentives. Utilise the flexibility in power demanding equipment like EVs and HPs.

2.2 Battery Energy Storage Systems

This section focuses on the battery composition and operation. It aims to provide knowledge of why a battery is chosen and how it is operated in a power system. Both a theoretical and a mathematical explanation will be given, as well as reviewing related research for better insight into the technical and economic possibilities and challenges. An illustration of a grid-connected battery energy storage system (BESS) can be seen in figure 2.2. The BESS is simplified to consist of a battery package and an inverter/converter. For the rest of the thesis, the terms converter and inverter will be used interchangeably.

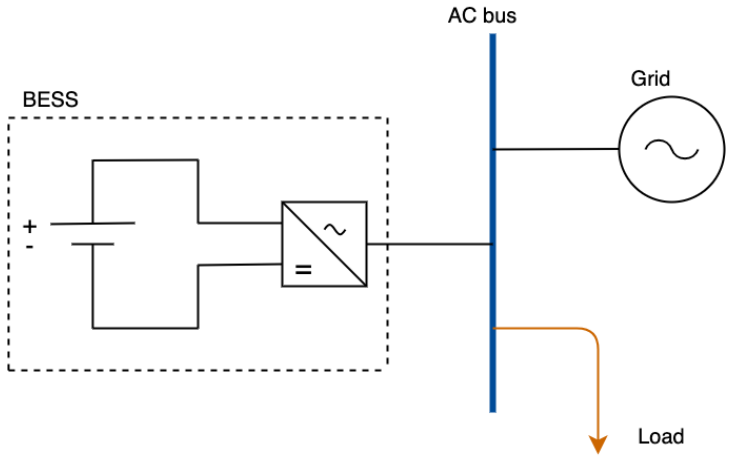

Figure 2.2: Grid-connected BESS

2.2.1 BESS characteristics

Batteries are storage devices that store energy chemically. Advantages of batteries are their fast response time, high energy efficiency and independency of geographical area, compared to, for instance, pumped hydro storage. A BESS includes monitoring and control systems, power conversion systems as well as the battery packages, as can be seen in figure 2.2. BESSs can be divided into mobile and stationary technologies, in which the stationary batteries can further be categorised as either utility-scale or behind-the-meter (BTM) applications. The different battery technologies available on the market vary greatly in their characteristics, based on their chemical composition. For further analysis, the characteristics and prices for the lithium-ion battery will be used. Important BESS terms used in this thesis are presented in table 2.2 [47].

Term	Unit	Description
Energy capacity, E_{batt}	kWh, MWh, Ah	The maximum amount of energy that can be stored in a battery.
Power capability, P_{batt}	kW, MW	The amount of power an installation can provide. Important for scaling of the converter.
Calendar life	Years	The number of years the battery can operate before losing considerable performance.
Cycle life	Number of cycles	The operational life of the battery. Measures how many complete charging and discharging cycles a battery can perform before losing too much of its performance.
Depth of discharge (DOD)	%, pu.	The amount of the battery's capacity that has been utilised at a given point. The deeper discharging, the shorter expected lifetime.
State of charge (SOC)	%, pu.	The amount of energy remaining in the battery at a given time. Often given as the percentage of the capacity. The inverse of the DOD. SOC = 1 - DOD
BESS efficiency, η	%	The efficiency of charging and discharging the battery. Can be separated into charging efficiency η_{ch}, discharging efficiency η_{dis} and round-trip efficiency η_{rt} being the product of the two.
C-rate	$\frac{kW}{kWh}$	The relation between rated power and rated energy capacity. A C-rate of 1 (C1) means that all the energy stored in the BESS may be utilised within one hour. C/5 refers to a BESS where the rated power is five times lower than the energy rating.

Table 2.2: Relevant BESS terms by IRENA [47].

Lithium-ion characteristics

Most of the stationary batteries bought for grid purposes the latest years are of the type lithium-ion, and they accounted for as much as 90% of new stationary battery capacity bought in 2017 [48]. Lithium-ion batteries are suitable as grid storage application due to their high cycle life and high power density compared to other battery types [49][50]. They also have a high power charge and discharge rate, excellent round-trip efficiency and low self-discharge rate [47].

Some definite drawbacks cannot be disregarded. Lithium-ion batteries are sensitive to heat, they come at a high initial cost, and the cycle life is highly dependent on the way of use [47]. As to avoid the cyclic ageing and rapid degradation, a lithium-ion battery should not be fully charged or discharged [51]. Batteries may also cause additional challenges for the system they are connected to, such as increased system losses caused by inverters and increased harmonic

development [4]. None of the operating characteristics of a lithium-ion battery will be included in the study, other than limiting the minimum SOC level in the BESS.

2.2.2 Cost of Capacity

The economic concern regarding batteries is still a major barrier to overcome before BESS can be a mainstream asset in the energy sector [52]. However, the increasing number of existing batteries and the upgrades in their design and functionality have pushed the battery costs down the latest years. The cost reduction is mainly caused by the high demand for electric vehicles, and by introducing batteries as a valuable asset in the power grid, it is forecasted that the costs will continue to fall [53] [54].

In a report from 2018 [55] the National Renewable Energy Laboratory (NREL) has investigated the cost projections from more than 25 publications for lithium-ion batteries used in the grid and in vehicles, and made cost projections curves based on the literature findings. Figure 2.3 shows bar graphs based on the resultant cost projections development, separated into cost of power capacity (figure 2.3a) and cost of energy capacity (figure 2.3b). The costs have been converted from American dollars to NOK by using the exchange rate from the Norwegian Central Bank the 8^{th} of April 2020. The exchange rate was such that 1 USD corresponded to 10.2971 NOK [56]. The high, mid and low bars in figure 2.3 represent the maximum value, the median value and the minimum value respectively. These costs will be used as reference when performing the economic analysis of the BESS.

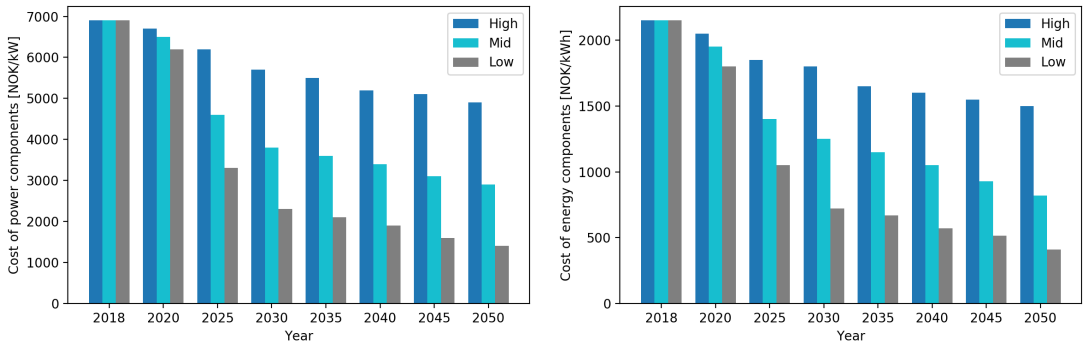

(a) Cost of power components

(b) Cost of energy components

Figure 2.3: Cost projections for power and energy components of lithium-ion system, based on numbers from NREL [55]

2.2.3 BESS Services

A BESS can provide multiple purposes and give additional opportunities to the power system. The type of services batteries can provide can be divided into grid services and market services. When looking at the grid services, the focus will be on the LV network and the challenges in distribution grids as presented in section 2.1.3. The market services and economic outcome of BESS investment will be presented in section 2.2.4. The combination of power and energy capacity that is suitable for a grid-installed BESS varies based on the services to be provided [7].

Voltage and Frequency Regulations

Two main technical criteria for power systems are frequency regulation and voltage stability. BESS can provide both active and reactive power within its capacity limits, and can thus be an asset in regulating both voltage and frequency in power systems [52][57]. In LV networks providing sufficient active power will be the most critical task for the battery as this will ensure both frequency and voltage regulation. BESSs used for frequency regulation do not require high energy capacity, while that may be the case for BESSs installed to regulate the voltage over a more extended period [7].

Short Circuit Currents

A grid-connected BESS may provide short circuit capacity by increasing the current flowing in the lines so that it exceeds the limit at which the protection devices will be activated. A battery whose primary purpose is to provide short circuit capacity should have high power density to be able to provide a sufficient current when needed. Also, a low self-discharge rate is beneficial [58].

Demand Reduction and Avoiding Congestion

A battery installation may provide increased flexibility for consumers and the grid. By storing energy when the demand is low, and release energy when the demand is high, the power peaks that cause violations in the network may be reduced. Peak-demand reduction will be of special relevance for weak grids with limited transfer capacity, especially with the increasing amount of high power-consuming devices [59].

Stabilising Renewable Energy Production

Solar and wind energy are strongly dependent on the weather conditions and will vary a lot during the day and for different seasons. Batteries have been accepted as one of the potential solutions to deal with these variations and avoid damaging the grid [52]. By using the same

principle as for load-shifting, the battery will store the energy produced by DGs when it is not consumed directly. A considerable amount of the newly integrated solar power is located behind the meter, in the weakest parts of the grid. Batteries can thus play an essential role in such areas, to avoid that all the produced power enters the electric grid at once, causing voltage rises the grid can not handle [59].

2.2.4 Economic Feasibility

By studying the economic feasibility of the different studies, as well as reading reports regarding BESS in the grid by NVE [53] and IRENA [54][47], there are three main ways a battery can become a profitable asset, all of them are presented below. Some observations to notice are that the base case scenario in which the battery investment is compared to have a clear impact on the profitability. The high installation costs of the batteries provided in the market today is still a great barrier to overcome. Most of the studies that conclude with profitable solutions have assumed low investment costs and few studies are including both the costs of energy and power capacity.

Increased Profit

By letting the battery participate in the market, it can utilise the arbitrage of the different price levels. Buying electricity and storing it in the battery when the prices are low, and selling electricity when the prices are high, can lead to increased profit for the battery owner. The battery owner may also get paid to deliver services, for instance, providing frequency regulation in the balancing market, as tested by Zhang et al. [7]. Many of the studies that exploit arbitrage only result in profitable solutions under certain circumstances. Nottrott et al. [60] show how the prices decrease for increased installed capacity, and that installing PV and BESS become economically feasible for all capacities when the cost of capacity decrease to 1800-3700 NOK/kWh. Ranaweera et al. [14] also exploit the arbitrage in the study and concludes that the sell-back price must be higher than the purchase price to gain profit. The mentioned studies emphasise the cost of energy capacity and not the cost of power capacity. For batteries providing these kinds of services and market participation, an optimal energy and power capacity that balances the investment costs and the operating costs of the BESS is important to maximise the profit.

Reduced Costs

In some cases, profitability may come as a result of decreased electricity bill, either by increased self-consumption or reduced peak-power consumption, typical for BTM installations. The master thesis written by F. Berglund [61] focuses on the use of BESS and PV to avoid the peak hour electricity prices and also utilises price arbitrage operation. Price arbitrage is, however, only

used to a small extent as excessive use at the BESS's capacity limits increases battery ageing, and this is to be avoided. BESS and PV for peak load shaving are also tested by Dagdougui et al. [62] and Yang et al. [8], but in these studies, no profitable solutions are found. Fortenbacher et al. [9] come to the conclusion that a distributed battery will reduce the electricity bill sufficiently to become profitable at an installation cost of 2300 NOK/kWh. The results from these studies lead to a similar conclusion that was presented for the cases with increased profit: that the price differences have to be significant in order to reduce the costs of investing in a BESS.

Reduced Grid Costs

The presumed most promising case in which the BESS could be the economically preferable option is when the cost of BESS is compared to investing in new lines or other types of grid upgrades. The installation cost of the battery may be lower than the necessary grid upgrades, or the operational costs of the grid may be reduced by installing a battery to provide voltage regulation. Two studies that are performed in a network expansion planning perspective, both are dependent on low investment costs to find profitable solutions [11][10]. Bocker et al. [10] propose a cost of capacity of 2000 NOK/kWh, and find BESS installations beneficial for some of the cases. However, if the price increases to 5000 NOK/kWh, only special operating conditions lead to profitable solutions.

2.2.5 Battery Operation

This section includes the mathematical formulations of the battery operation that are relevant for the study. The most important ones are related to the power and energy balance in the battery and the system. Clear boundaries are essential when putting up the mathematical formulation of the battery operation. The battery does not operate with a 100% efficiency, and the losses have to be included in an appropriate way to ensure the energy and power balance is included correctly. The losses are assumed only to be related to the conversion from AC to DC power and the inversion from AC to DC power. Figure 2.4 shows the grid-connected BESS with power flows and inverter-efficiency. It should be noted that the power flows from charging and discharging the battery are referenced to the battery-side of the inverter.

Power balance

The power balance in the system ensures that the power flowing into the bus is equal to the power flowing out of the bus. For the system shown in figure 2.4 the power balance at time t can be written as in equation (2.2):

$$\begin{cases} P^t_{grid,in} = P^t_{grid,out} + \frac{1}{\eta_{ch}} \cdot P^t_{ch} + P^t_{load}, & \text{if the battery charges} \\ P^t_{grid,in} + \eta_{dis} \cdot P^t_{dis} = P^t_{grid,out} + P^t_{load}, & \text{if the battery discharges} \end{cases} \tag{2.2}$$

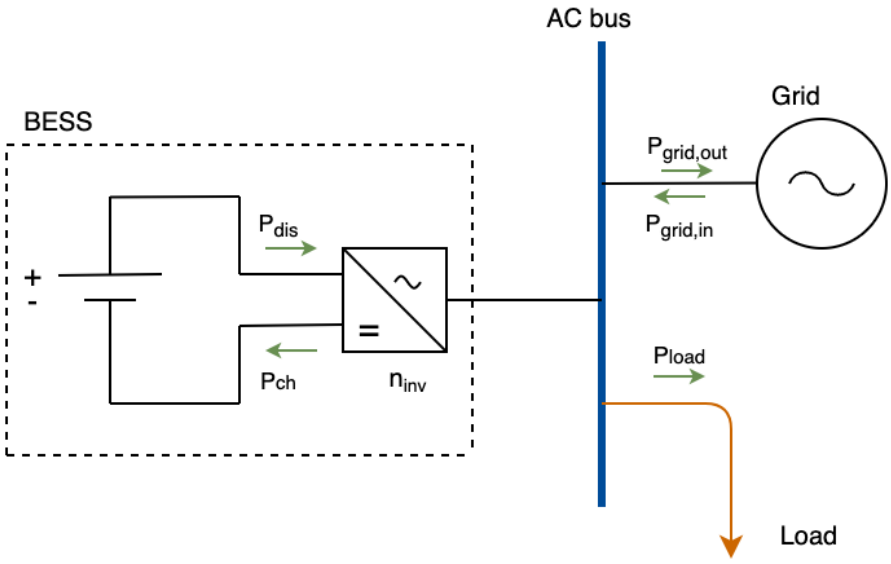

Figure 2.4: BESS connected to the grid, including power flows

When working with power flow analysis it is the bus-power that is of interest for obtaining the power flow solution. The AC-bus power is defined as positive for the power flowing in to the system. The power injected to an arbitrary bus with load and generation is defined to be [63]:

$$P_{bus} = P_{generated} - P_{load} \tag{2.3}$$

For the proposed system, the power injected to the AC bus becomes as in equation 2.4:

$$P^t_{bbus} = \begin{cases} -\frac{1}{\eta_{ch}} \cdot P^t_{ch} - P^t_{load}, & \text{if the battery charges} \\ \eta_{dis} \cdot P^t_{dis} - P^t_{load}, & \text{if the battery discharges} \end{cases} \tag{2.4}$$

Note that the bus power is defined as the power injected to the bus, as seen from outside the system. Thus, the power flowing in and out from the grid is not included. A complete description of power flow studies is given in section 3.1.

The efficiencies of the charge and discharge can be assumed to be equal, and to be determined by the round-trip efficiency:

$$\eta_{ch} = \eta_{dis} = \sqrt{\eta_{rt}} \tag{2.5}$$

The power output and input from the battery is limited by the rated battery power, P_{batt}. The minimum charge and discharge rate is equal to zero, and is increased continuously to P_{batt}, as

demonstrated in equation 2.6:

$$\begin{aligned} 0 \leq P_{ch}^{t} \leq P_{batt} \\ 0 \leq P_{dis}^{t} \leq P_{batt} \end{aligned} \tag{2.6}$$

Energy balance

The storage level of the battery at a given time is dependent on the storage level in the previous time step and the amount of energy that is either charged or discharged during the time interval. With the charging and discharging power defined at the battery side of the inverter, the energy balance of the battery becomes as in equation (2.7):

$$E_{batt}^{t} = \begin{cases} E_{batt}^{(t-1)} + P_{ch}^{t} \cdot t, & \text{if the battery charges} \\ E_{batt}^{(t-1)} - P_{dis}^{t} \cdot t, & \text{if the battery discharges} \end{cases} \tag{2.7}$$

A lithium ion-battery should not be fully charged or discharged as to avoid cyclic aging and rapid degradation [51]. The upper and lower energy level in the battery are defined by the maximum and minimum SOC the battery should have to avoid losing its performance. The SOC for a given time is defined as in equation (2.8). Equation (2.9) shows how the energy in time t is limited by the upper and lower SOC level, SOC_{min} and SOC_{max} respectively. For a lithium-ion battery the normal operation should be limited to having a SOC between 20% and 80% to comply with this requirement [51].

$$SOC^{t} = \frac{E_{batt}^{t}}{E_{batt}} \tag{2.8}$$

$$E_{batt} \cdot SOC_{min} \leq E_{batt}^{t} \leq E_{batt} \cdot SOC_{max} \tag{2.9}$$

2.3 Investment Planning Principles

By the regulators, the Norwegian grid companies are obliged to write a power system planning report (in Norwegian: Kraftsystemutredning (KSU)) that includes investment planning for the grid the next 20 years. An essential part of this report is to present various possible solutions for the development of the power system. The optimal socio-economic solution is to be chosen [64]. The grid has to be maintained at all time to sustain the need from the customers [65]. Traditionally there have not been a very wide variety of options when it comes to upgrading the power capacity to an area. The decision variables have mostly been to find the optimal cross-section of a new line or identifying whether or not a new investment is necessary. Expansion planning has become more complicated after the introduction of distributed generation and BESS [66][67].

The primary purpose of a socio-economic analysis is to map, highlight and systematise the consequences of initiatives and reforms before decisions are made. An essential rule in the socio-economic analysis is to describe all relevant alternatives and compare them with the basic alternative. As well as looking at the economic benefits, socio-economic analyses require the grid companies to, in the best possible way, describe the effects for all that are affected by the relevant initiative. That includes the quantitative effects as well as consequences for the environment [68]. In addition to the related costs, alternatives that are more flexible and that can postpone the more permanent decision making are valued.

When performing an investment planning analysis, all the present and future costs should be identified as best as possible. Firstly, the planning horizon, discount rate and all possible alternatives are to be identified, along with their related costs. In this study, all present and future costs will be annualised, and the options are compared by determining the annual net benefit of the BESS installation relative to the grid reinvestment. The net benefit (NB) and net present value (NPV) methods are explained in Appendix A.1. The method of calculating the annuity factor is explained in Appendix A.2. Optimal investment planning includes minimisation of the following five costs related to the power system investment and operation [69]:

- investment costs
- operation and maintenance costs
- cost of losses
- cost of an outage
- cost related to bottlenecks

This thesis will focus on the investment costs of the alternatives, and also include analysis of the cost of losses. The three remaining costs will be neglected for further investigation. The energy losses in the Norwegian power system account for about 8% of the annual energy generation, and the power losses at maximum load account for about 15% of the generated power. The cost of losses may thus account for a substantial part of the system costs, dependent on the utilisation time for losses and the power price [69].

3 | Power Flow Algorithm

While chapter 2 presented the structure and the theory behind the distribution grid, this chapter focus on the mathematical operation in a power system. The principles of power system analysis are presented, including an introduction to the power flow solution. An algorithm to solve the power flow problem, the backward/borward sweep (BFS) algorithm is explained in details, as it is a suitable solution method for radial distribution networks.

3.1 Power Flow Analysis

By H. Saadat [43], power flow analysis comprises the steady-state analysis of an interconnected power system during balanced operating conditions. Power flow studies create the basis for power system analysis and design. They are necessary for planning, operation, economic scheduling and control of existing power systems, as well as planning future expansion. The network consists of nodes and branches, with parameters and variables specified in per unit on a common VA basis. Each node or bus has four quantities associated with it. The real power P, the reactive power Q, the voltage magnitude |V| and the phase angle, δ. The combination of known and unknown bus quantities classifies the buses into different types, as presented in table 3.1. The power flow problem consists of determining the unknown quantities in the system.

Table 3.1: Classification of buses

Type of bus	Known	Unknown	Comment
Slack bus	|V|, δ	P, Q	The reference bus, where the magnitude and phase angle of the voltage are specified. This bus delivers the extra power needed to cover the system losses.
Load bus	P, Q	|V|, δ	Also called P-Q-buses, as the P and Q are specified at the bus.
Generator bus	P, |V|	Q, δ	P and V are specified at the bus, and it is also called P-V-bus. The bus has a reactive power limit.

3.1.1 Power Flow Solution

A set of non-linear equations have to be solved to obtain the power flow solution of a system. Solving them requires iterative procedures and the variety of computational methods is wide-ranging. The well-documented methods for solving the power flow problem can be divided into two basic classes, as presented by E. Bompard et al. [70]:

- The first class is composed of methods which require information on the derivatives of the network equations and is built upon Jacobian definitions.
- The second class includes the derivative-free and direct methods, using only the basic circuit laws.

The first class includes the traditional Newton-Raphson method and its modifications, as well as the various versions of the fast decoupled power flow (FDPF) method. The backward/forward sweep method belongs to the second class.

3.1.2 Power Factor

The power factor, pf, indicates how much of the average apparent power, S, consumed at the load that is active power, P. Customers with poor power factors draw a larger amount of reactive power, which is undesired as it causes voltage drop in the lines [71]. The power factor is defined as the cosine of the phase angle, θ, between the voltage and the current at a load, as seen in equation (3.1).

$$pf = \cos(\theta) \tag{3.1}$$

The average real and reactive power can be found by using the phase angle and the average apparent power, if these quantities are known. Equation (3.2) shows the relationship between the phase angle, the average apparent power and the average real and reactive power [72].

$$\begin{aligned} P &= S \cdot \cos(\theta) \\ Q &= S \cdot \sin(\theta) \end{aligned} \tag{3.2}$$

3.2 The Backward/Forward Sweep Algorithm

The BFS method was developed to cope with some of the shortcomings in the Jacobian-based methods [18]. The Jacobian matrix of vast distribution network with high R/X-ratio and radial structure often tends to singularity [73], and many of the assumptions made in the fast-decoupled Newton-Raphson method are usually not valid in distribution system [74]. For these types of networks, the BFS method was found to be more efficient and robust and has proven as a well-documented technique [17][23] [24][75] .

The algorithm presented is based on the method developed by D. Shirmohammadi et al. [18] in 1988. The effect of shunt elements in the lines is neglected in this study. Hence, it is not included in the proposed method, even if it is included in the original paper. The method presented here requires a radial network, one slack bus at the top node, and only load buses in the rest of the system.

3.2.1 Branch Numbering

The backward/forward sweep algorithm has a branch-oriented approach, in contrast to the more common node-oriented approach used in other power flow techniques. A radial distribution system has N nodes, $B = N - 1$ branches, and one single power source at the top node. An example of a typical distribution system can be seen in figure 3.1. The slack bus is numbered as bus 0.

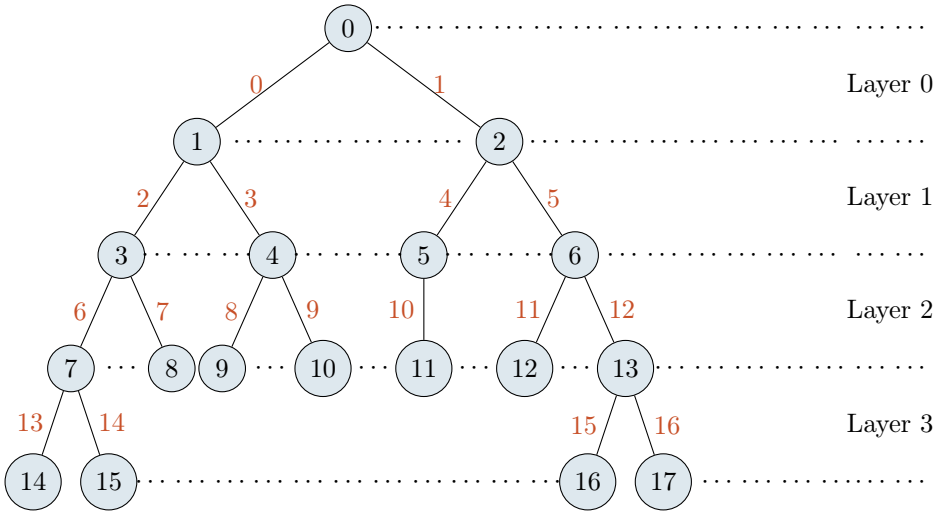

Figure 3.1: Branch numbering scheme

For the solution method of the BFS algorithm to work, the branches have to be numbered in a certain way that corresponds to the notation in equations used in the solution method. Numbering the branches is simple and straightforward, and it starts by numbering the layers away from the top node. When nodes are emanating from the parent node, a layer is defined between the parent node and the child nodes. The more generations of nodes, the more layers, as can be seen in figure 3.1. The numbering of branches follows the layers. All the branches in

layer 0 have to be numbered before the numbering of branches in the next layers starts. In the procedure presented further, the nodes are to be numbered using the same technique, starting from the top node, numbering the nodes from left to right in the upper generation before the next generation. In figure 3.1 the branch numbers are written in colours, and the node numbers are written inside each node.

3.2.2 Solution Method

The BFS algorithm uses an iterative procedure to calculate the unknown voltage magnitudes and angles in the system. The real and reactive loads at each node, except the reference node, are assumed to be known. The voltage angle and magnitude at the reference node are given, and the voltage profile is considered to be flat for all other nodes. The iterative solution algorithm consists of four steps when including the mismatch calculation as step four. Unless otherwise stated, all variables and parameters are complex numbers.

Step 1 - Nodal Current Calculation

At first, the node currents are calculated at each node. The nodes are numbered from 0 to N, and the nodal calculation starts with node one as the reference node is not included. As known from basic circuit theory, the current injection at a node n can be found as the complex conjugated of the apparent power divided by the node voltage [76]:

$$I_n^{(k)} = \left(\frac{S_n}{V_n^{(k-1)}} \right)^* \qquad n = 1, 2, \ldots, N \tag{3.3}$$

where,

$I_n^{(k)}$ - the nodal current injection at node n during the kth iteration.

$V_n^{(k-1)}$ - the voltage at node n calculated during the previous iteration, k-1.

S_n - the specified power injection at node n, defined as the difference between the power generated at the node, $S_{G,n}$ and the load withdrawn from the node, $S_{L,n}$:

$$S_n = S_{G,n} - S_{L,n} \tag{3.4}$$

The inclusion of shunt elements in the lines are neglected from the nodal current calculation presented here. They are included in the original method.

Step 2 - Backward Sweep

During the backward sweep, the branch currents are calculated using the direct application of KCL. KCL says that *the algebraic sum of all the currents at any node in a circuit equals zero* [77]. The branch currents, $J_b^{(k)}$, at branch b during iteration k, are calculated starting in the last layer, at branch B, and moving towards the layer closest to the reference node:

$$J_b^{(k)} = -I_{b+1}^{(k)} + \sum_{m \in \Omega_m} J_m^{(k)} \qquad b = B, B\text{-}1, \ldots, 0 \tag{3.5}$$

where,

- $I_{b+1}^{(k)}$ - the nodal current as calculated in equation (3.3), with a subnotation of b+1 instead of n, to show that the node of which the current, I, is referred to, is the node that the line current, J, is flowing towards. As seen in figure 3.1 and 3.2, this node will have a number that is one unit higher, b+1, compared to the branch b.
- Ω_m - Set of branches in the lower layer that are directly connected to branch, b
- $J_m^{(k)}$ - Line current in branch m, emanating from node b+1

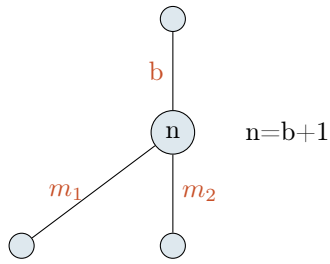

Figure 3.2: Illustration of Forward Sweep labeling

Step 3 - Forward Sweep

In the forward sweep, the nodal voltages are corrected, using the direct application of KVL, defined as *the algebraic sum of all the voltages around any closed path in a circuit equals zero* [77]. The updated nodal voltages, $V_m^{(k)}$, are calculated starting in the layer closest to the reference node and sweeping towards the last layer. It is calculated using the updated voltage from the previous layer and the branch current calculated in the backward sweep:

$$V_m^{(k)} = V_n^{(k)} - Z_{nm} \cdot J_{m-1}^{k} \tag{3.6}$$

where,

$V_m^{(k)}$ - the nodal voltage at the child node of node n that is located in the layer above node m. See figure 3.3.

$V_n^{(k)}$ - the nodal voltage at node n, calculated prior to the voltage at node m.

Z_{nm} - the series impedance of the branch connecting node n and m, being branch m-1.

J_{m-1}^k - the branch current flowing from node n towards node m, as calculated in equation (3.5). Here having the subnotation of m-1 instead of b to illustrate the connection to node m.

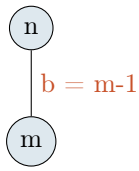

Figure 3.3: Illustration of Backward Sweep labeling

Step 4 - Convergence Criterion

The convergence criterion is the maximum real and reactive power mismatch at the nodes. The power mismatch is found as the absolute value of the difference between the specified power injection at the nodes, S_n and the calculated power injection at the nodes, $S_{calc,n}$. The power injection at node n at iteration k is calculated as in equation (3.7) when neglecting the shunt elements:

$$S_{calc,n}^{(k)} = V_n^{(k)} \cdot (I_n^{(k)})^* \tag{3.7}$$

where $V_n^{(k)}$ and $I_n^{(k)}$ are found from equation (3.6) and (3.3) respectively.
The real and reactive power mismatches at node n are then calculated as:

$$\begin{aligned} \Delta P_n^{(k)} &= |\Re e[S_n - S_{calc,n}^{(k)}]| \\ \Delta Q_n^{(k)} &= |\Im m[S_n - S_{calc,n}^{(k)}]| \end{aligned} \tag{3.8}$$

The four steps are repeated until convergence is achieved when the maximum mismatch is smaller than the pre-set limit, κ_{BFS}.

A flowchart of the solution algorithm of BFS is drawn in figure 3.4 giving a clear overview

of the method. Included in initial data input are the real and reactive loads at all the nodes, the system configuration, the branch and node numbering, the maximum mismatch limit, and the maximum number of iterations that are to be performed before breaking the loop and printing diagnostics.

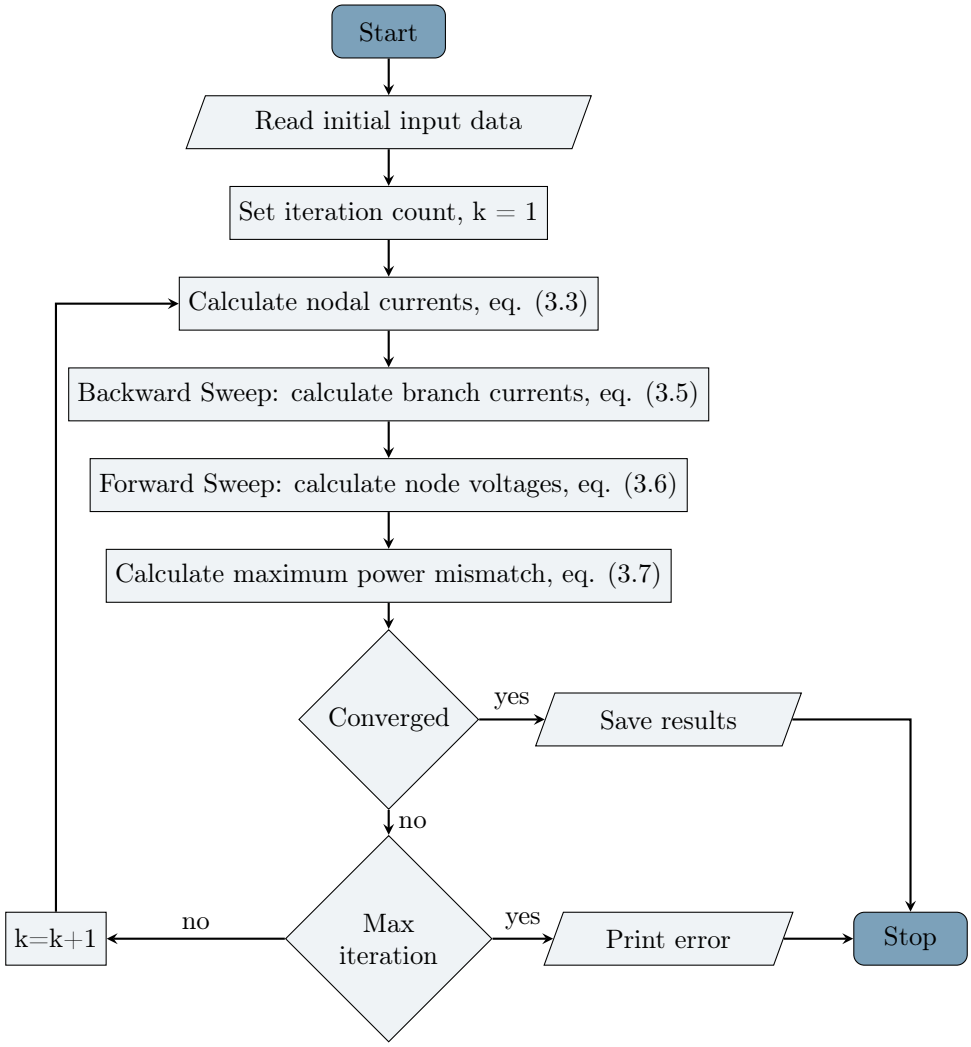

Figure 3.4: Flowchart Backward/Forward Sweep Algorithm, as presented by Shirmohammadi et al. [18]

4 | Model Construction

This chapter consists of a thorough description of the model that has been developed for the master thesis. Necessary limitations and assumptions will be explained, and the tools used to create the system model will be introduced.

4.1 Methodology

The developed model contains three main parts: 1) the BFS-algorithm to solve the power flow at a given hour, 2) a battery model to determine and perform the required battery operation of the hour, and 3) an optimal charge and discharge model to find the optimal charging or discharging power for the given hour. The objective is to solve the power flow for each hour with a given hourly-based load, and further to include a battery to deal with too large voltage drops when that is the case. This model will create the basis for finding the needed battery size and line cross-section, as will be explained in chapter 5. The model is primarily a technical model focusing on the physical parts of the system. However, there are some economic reasoning that underlies some of the decisions taken in the development of the model. These will be explained.

4.2 Analysis Tools

4.2.1 Python

The model is developed by using the programming language Python to construct algorithms for solving the problems. Python was chosen for its free availability for everyone and because it is a friendly programming language that is easy to understand. To be able to exploit more of the mathematical tools in Python, some additional packages have to be used to be able to perform more advanced mathematical calculations, such as using complex numbers or doing calculations with sine and cosine. Python's built-in packages Numpy and Cmath make these computations possible. To handle the input and output data more smoothly, Excel has been used for storing data. For Python to be able to read and import the data from Excel, the Python-package Pandas is used.

4.2.2 Excel

Excel is a powerful calculation tool, that can easily visualise and handle data in a convenient way. The orderly layout is suitable to keep a good overview of large data and to make changes and handle the data manually easily.

4.3 Assumptions

- The load data and system topology are known before the analysis.
- Assuming normal operating conditions and that no fault will occur.
- Only one BESS will be installed in the grid.
- It is assumed that the battery can be fabricated as to deliver any required combinations of power and energy capacity.
- The battery will only deliver and consume real power from the grid.
- The time t refers to the end of the current time-step. Meaning that the data at the beginning of time-step t is equal to the data at the end of time-step $(t-1)$.

4.4 Power Flow Model

The power flow model represents the main and outer loop of the model. It is developed to handle hourly-based load data and to give the power flow solution of the problem as the output for each hour. If no battery is connected to the system, the loop has no control organ, and the power flow solution will be delivered based on the BFS-algorithm presented in chapter 3. However, if there is a battery connected, this will operate as a voltage regulating device, delivering or consuming the required power for the system voltage to not deviate more than 10% of the rated voltage level. The output will both contain the updated power flow solution solved with the BFS-algorithm, as well as the battery operation data.

The grid that is to be analysed has to have a radial structure. Further, it has to follow the BFS numbering scheme presented in section 3.2.1. The numbering of buses and branches is done before the model runs. As described in section 3.2, the slack bus is the only bus where the voltage magnitude and angle are known, and the other buses in the system are load buses. The slack bus is numbered as bus 0.

The input data to the power flow model can be seen in table 4.1.

Table 4.1: Input data to the power flow model

Parameter	Description
N	Number of buses in the system, numbered based on system topology.
B	Number of branches, B = N - 1, in the system, numbered based on system topology.
V_0^t	Voltage level at slack bus $\forall\ t \in T$. Set to be 1 pu
δ_0^t	Phase angle at slack bus $\forall\ t \in T$. Set to be 0 rad.
Z_b	The impedance value of all the branches in the system, given in per unit values based on the system apparant power basis.
T	Total number of operating hours, including the starting and ending hour.
P_n^t	Real power injection at every hour t for all the load buses in the system. $n \in$ {1,N}
Q_n^t	Reactive power injection at every hour t for all the load buses in the system. $n \in$ {1,N}
$b_{battery}$	Binary variable for the model to know if the battery is to be included. Will be equal to 1 if battery is included and 0 if not.
κ_{BFS}	Maximum allowed mismatch between the specified and the calculated power injections at the load buses.
Battery data	Information about the battery to be further included in the battery model. See table 4.3.

4.4.1 Solution Method

The solution method of the power flow model is divided into three steps, where the first step will be carried out for all situations, and the second and the third step will only take place if the BESS is connected. A flowchart of the model algorithm can be seen in figure 4.1.

Step 1 - Solve the Power Flow Problem

The power flow solution is found by solving the BFS-algorithm. The iterative power flow procedure is modelled in Python following the solution method presented in section 3.2.2. Within the BFS-model there is included a limit of the maximum allowed iterations before the loop breaks, to avoid infinite loops to run.

Step 2 - Determine the Lowest System Voltage

If a battery is included in the system, its primary goal is to regulate the voltage to avoid situations with very high voltage drops caused by high load demand. It is also desired that the battery is being charged if the system voltage allows it. The basis for what role the battery will have in a given hour, is the lowest voltage level in the grid, V_{min}^t. If the lowest voltage level is

precisely 0.9 pu., the battery will not be operated for this hour, and step 3 will not be carried out.

Step 3 - Run Battery Model

If the lowest voltage level is below 0.9 pu., the battery will deliver power to the system, given that the battery state allows it. And if the voltage level is above 0.9 pu., the battery will consume power from the system, if the battery state requires it. Details about the charging and discharging of the battery will be explained in section 4.5 and 4.6. The battery model returns the updated system data, based on the appropriate charging or discharging level found. The update relevant for the power flow model involves the change in the power delivered or consumed at the bus where the battery is installed, P^t_{bbus}.

After the system data is updated from the battery algorithm, step number 1 is repeated, to deliver the updated power flow solution. The loop will continue until the last hour is operated. The power flow model output data is presented in table 4.2. The output data from both the power flow model and the battery model will be stored in python dictionaries during the operation, and when the power flow model is completed, all data will be exported to Excel.

Table 4.2: Output data from power flow model

Variable	Description
V^t_n	Voltage level each hour for all the load buses, $n \in \{1,N\}$
δ^t_n	Phase angle at every hour for all the load buses, $n \in \{1,N\}$
P^t_0	Total active power delivered from slack bus every hour
Q^t_0	Total reactive power delivered from slack bus every hour
Battery output	Output data from the battery operation, if the battery is included. See table 4.4

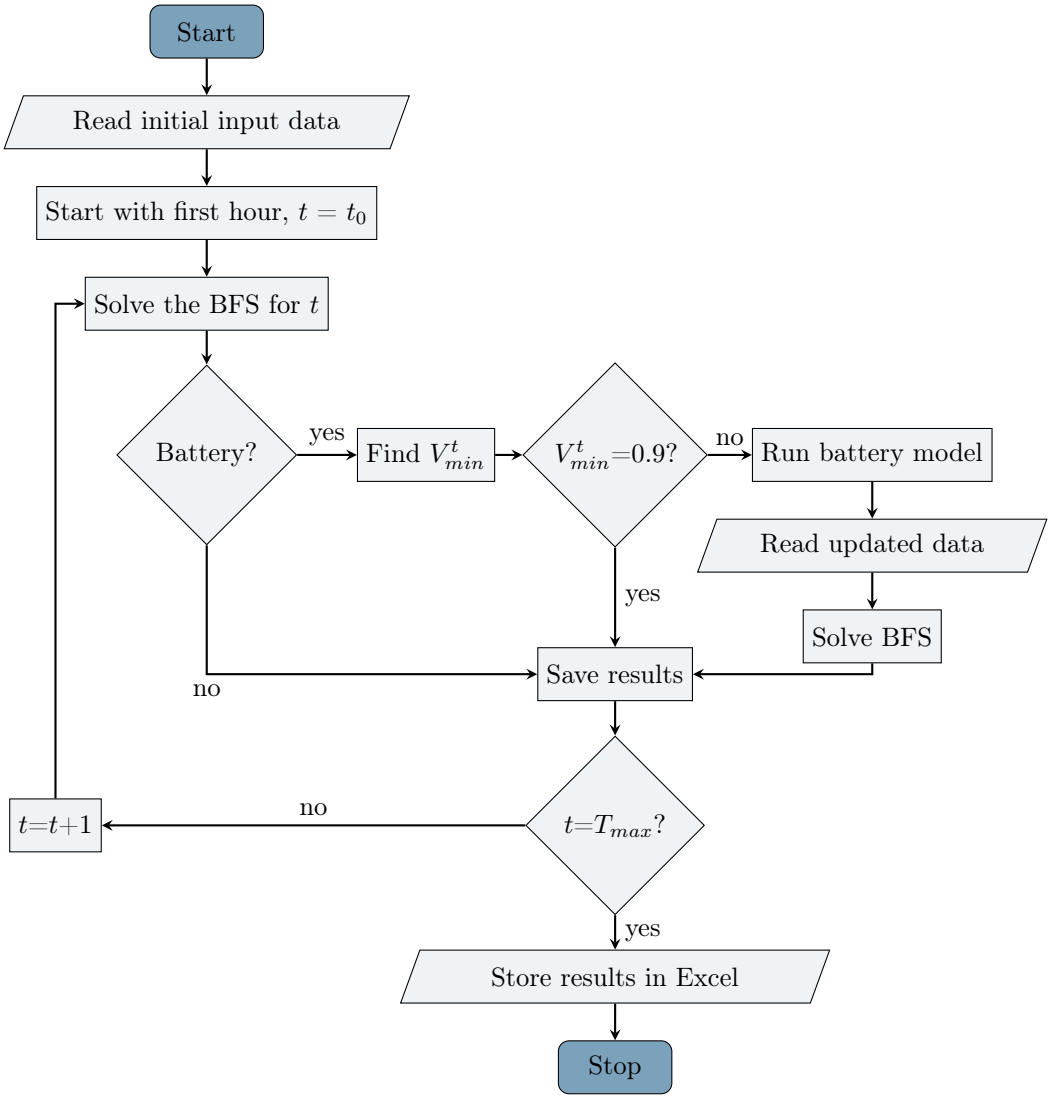

Figure 4.1: Flowchart power flow model

4.5 Battery Model

The battery model is an inner loop of the main power flow model. The battery is connected to one of the buses in the system, where it is suited for handling voltage issues at all the buses that need it. Based on the input information received from the main model, the battery is charged or discharged while keeping the voltage level above the limit of 0.9 pu. It returns the updated system data after the battery is operated, and the power flow model will continue to run. The input data to the battery model is shown in table 4.3.

Table 4.3: Battery input data

Parameter	Description
E_{batt}	Battery energy capacity.
P_{batt}	Rated battery power. Maximum power possible to withdraw from or supply to the battery.
SOC_{start}	Initial SOC of the battery.
$E_{batt}^{(t-1)}$	Energy stored in the battery the previous time-step.
$SOC^{(t-1)}$	SOC of the battery in the previous time-step.
V_{min}^{t}	The lowest voltage level in the system at time t.
P_{bbus}^{t}	The power injected to the bus where the battery is placed at time t.
η_{ch}, η_{dis}	Charging and discharging efficiency of battery.

4.5.1 Solution Method

The battery model algorithm is divided into three steps. Step 1 will be carried out for all scenarios, step 2 will be done it the system status indicates that the battery should be discharged, and step 3 if the battery should be charged. A flowchart of the battery model can be seen in figure 4.2.

Step 1 - Check Status of Input Data

From the outer loop, it was clarified that the battery model would only start running if the minimum voltage level in the operating hour were not equal to 0.9 pu. As such, the battery model need only to check if the minimum voltage level is above or below 0.9 pu. The status of the lowest voltage level, along with the SOC-level of the battery, will determine if the battery should be charged, discharged or remain unused. The requirement for starting discharging the battery is that the voltage level is below 0.9 pu. and that the SOC of the battery is above 0.2. The requirement for starting charging the battery is that the voltage level is above 0.9 pu. and that the SOC of the battery is below 1.0. The minimum SOC level of 0.2 was chosen based on

the knowledge of optimal battery operation. However, the upper SOC limit is not restricted by these recommendations. It was more convenient for the model development to have a lower threshold than an upper threshold, and as the battery operation cost is not taken into account, the maximum SOC of 1.0 will not affect the results in a negative way.

If neither of the requirements for charging nor the requirements for discharging are fulfilled, the battery will not be used, the system data will remain unchanged, and none of the following steps will be completed. This should only occur if the battery is fully charged or if the installed battery capacity is too low to handle the voltage problems throughout the entire period of analysis. The last scenario is not the desired outcome, and as it will be shown in chapter 5, the optimal battery size will be found to avoid such situations.

Step 2 - Discharge Battery

If the battery discharges, the required amount of power to be drawn from it has to be determined. For financial reasons, it is of the interest to not deliver more power to the grid than what is required to maintain the voltage level above 0.9. pu. By avoiding a too large power discharge, the total size of the battery can be limited, and as will the system costs. An optimal discharge algorithm has been developed for this purpose and will return the optimal P_{dis} to the battery model. The discharge algorithm is explained in detail in section 4.6.

Once the optimal discharge power is obtained, the system data is updated within the battery model. The power injected at the bus where the battery is placed is updated as in equation (4.1):

$$P^t_{bbus} = P^t_{bbus} + \eta_{dis} \cdot P^t_{dis} \tag{4.1}$$

Further the battery energy and SOC level is updated as in equation (4.2) and (4.3) respectively:

$$E^t_{batt} = E^{(t-1)}_{batt} - P^t_{dis} \cdot t \tag{4.2}$$

$$SOC^t = SOC^{(t-1)} - \frac{P^t_{dis} \cdot t}{E_{batt}} \tag{4.3}$$

The three equations above, showing the updated system data, are formulated using the system boundaries presented in figure 2.4. The minimum SOC level was earlier set to 0.2, and it should be noted that this limit is not finite. The battery may be discharged as to have a lower SOC than 0.2, as long as the SOC before the discharging starts is above 0.2. In a "worst case scenario" this could lead to a discharging close to a SOC of 0 for certain circumstances. However, this will not occur with the method used for determining BESS size. This method will be explained in section 5.1.2, and ensures that the SOC will not decrease to a level below 0.2.

Step 3 - Charge Battery

The most important battery operation is to ensure that the voltage level in the system at all time stays above 0.9 pu, as this is a law-defined requirement. The reason why the battery is charged for every hour where the lowest system voltage is above 0.9, is to take advantage of all the opportunities of re-charging that are given. This strategy will also avoid the need of installing a battery with too much energy capacity. An optimal charge algorithm is developed based on the same principles as the discharge algorithm, and they are both explained in section 4.6. The returned optimal charging power, P_{ch}^{t}, is used to charge the battery and update the system data as in the following equations ((4.4), (4.5), (4.6)), similar to the procedure of step 2, using the same boundaries from figure 2.4:

$$P_{bbus}^{t} = P_{bbus}^{t} - \frac{1}{\eta_{ch}} \cdot P_{ch}^{t} \tag{4.4}$$

$$E_{batt}^{t} = E_{batt}^{(t-1)} + P_{ch}^{t} \cdot t \tag{4.5}$$

$$SOC^{t} = SOC^{(t-1)} + \frac{P_{ch}^{t} \cdot t}{E_{batt}} \tag{4.6}$$

Both for step 2 and step 3, E_{batt}^{t} and SOC^{t} are updated concerning the status the previous hour. The P_{bbus}^{t} is, however, updated referring to the initial status of the same operating hour.

As already mentioned, the battery can be charged to the full SOC of 1.0. If the battery is close to fully charged and the grid allows it to charge at the maximum rate, the battery model needs a strategy to avoid a situation where the SOC exceeds the limit of 1.0, while still charging the remaining power for the battery to become fully charged. The battery model receives the optimal P_{ch}^{t} the grid can handle from the optimal charge algorithm. If this power is so high that the battery will be fully charged before the elapsed time of one hour, the battery will be charged at this rate for the minutes until the SOC is 1.0. However, the grid will be loaded as if the power demand lasted for the entire hour. This strategy was chosen since a significant power demand will not affect the system in a negative way as long as it can handle the voltage drop, and that was assured before the charging.

After the algorithm is completed, the model returns the updated system data to the outer loop. Along with the updated P_{bbus}^{t}, E_{batt}^{t} and SOC^{t}, the model will also return either P_{dis}^{t} or P_{ch}^{t} if step 2 or 3 have been completed. These values will be stored along with the rest of the output data. P_{dis}^{t} will be stored as a positive value, to illustrate the view from the grid perspective. A complete list of the returned variables from the battery model is written in table 4.4.

Table 4.4: Battery output data

Parameter	Description
E^t_{batt}	Energy stored in the battery at time t.
SOC^t	SOC of the battery at time t.
P^t_{bbus}	Updated power at bus where battery is located at time t.
P^t_{dis}	Discharging power at time t. Returned as a positive value.
P^t_{ch}	Charging power at time t. Returned as a negative value.

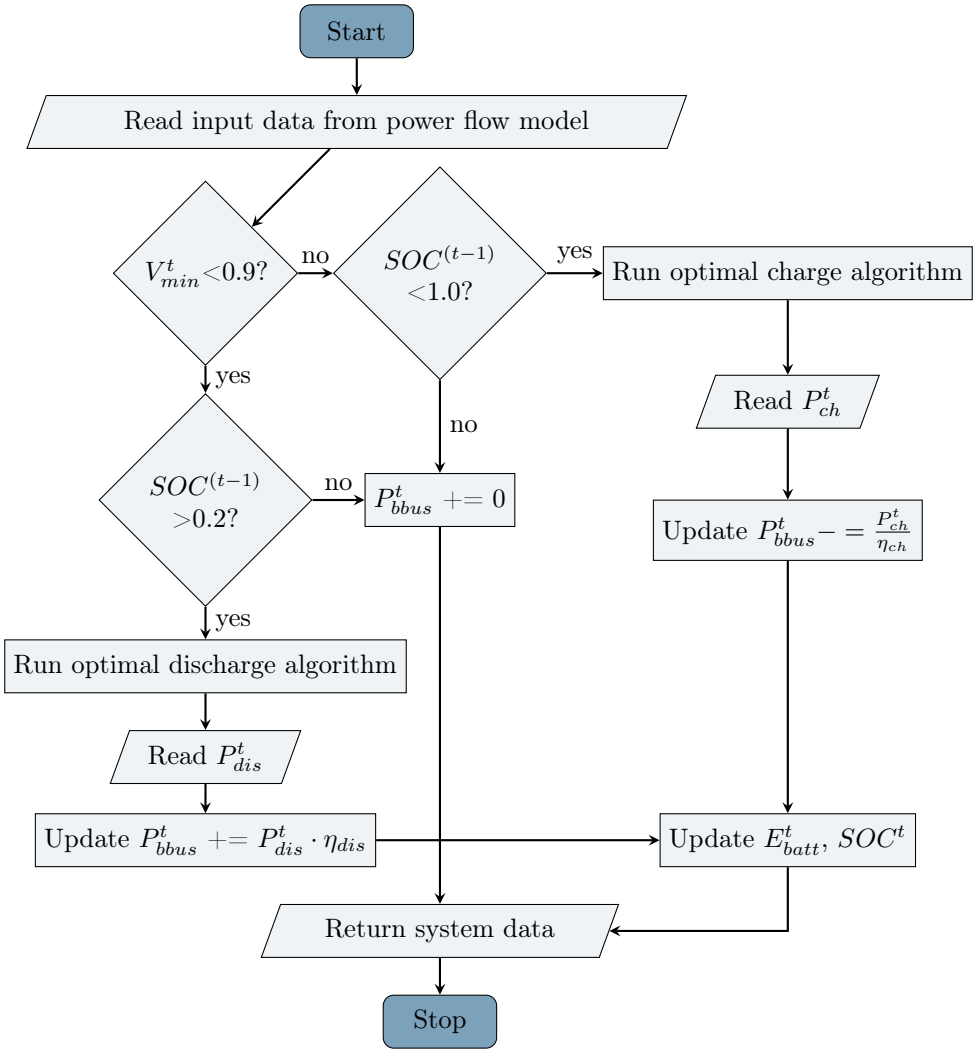

Figure 4.2: Flowchart battery model

4.6 Optimal Charge/Discharge Model

Within the battery model, there are optimal charging and discharging algorithms to avoid loading the battery more than necessary and to charge the battery as much as possible without exceeding the voltage limit in the grid. The input data to this algorithm is almost the same as for the power flow model and the battery model. Within the algorithm, the data is converted to temporary variables not to affect the actual variables while the iterative solution procedure is ongoing. The only value that will be returned from the model is the optimal charge/discharge power; all other variables in the algorithm will be reset and not used further. The optimal charge and the optimal discharge models include both running of the BFS algorithm and charging and discharging of the battery.

4.6.1 Solution Method

In the code, the discharging algorithm and the charging algorithm are written as two separate functions. They are based on the exact same principles, and only minor details differ them from one another. As such, they will here be explained simultaneously, and their differences will be specified. A flowchart of the proposed model can be seen in figure 4.3. The actions only applying to the charging algorithm is written in blue, while the actions only applying to the discharging algorithm is written in orange. All other commands have black writing.

The algorithm is developed based on the principles of the bisection method described in appendix B.1. But instead of finding the root of a function, the P_{dis}^t or P_{ch}^t giving the voltage level closest to 0.9 pu is found. P_{dis}^t and P_{ch}^t are given as P_{test}^k in the algorithm to avoid mixing it with the values of the two outer loops. The algorithm runs with the following five steps:

Step 1 - Clarify the Variables

First of all the range of the charge/discharge rate has to be identified as P_{high} and P_{low} to give the starting point for the algorithm. For both the charging and discharging algorithm they will be defined as in equation (4.7):

$$\begin{aligned} P_{high} &= P_{batt} \\ P_{low} &= 0 \end{aligned} \tag{4.7}$$

that is also the range of which the battery can be charged/discharged as described in equation (2.6).

The iteration count, k, will be given the start value of $k = 0$, to indicate that the iterative procedure has not yet started. The variable, P_{test}^k, that in the end of the algorithm will give the

optimal charge or discharge power for the time t, is first set to be equal to P_{high}, as this is the maximum power that can be charged/discharged. Furthermore $P_{bus}^{temp,k}$ is found by updating P_{bus}^{t} the same way as done in equation (4.1) and (4.4), here given in equation (4.8):

$$P_{bbus}^{temp,k} = \begin{cases} P_{bbus}^{t} - \frac{1}{\eta_{ch}} \cdot P_{test}^{k}, & \text{for charging the battery} \\ P_{bbus}^{t} + \eta_{dis} \cdot P_{test}^{k}, & \text{for discharging the battery} \end{cases} \tag{4.8}$$

It is important to notice that during the algorithm, P_{bbus}^{t} is a constant value, and only the temporary copy $P_{bus}^{temp,k}$ will change during the iterations.

Step 2 - Identify if a Solution Exists

With the P_{test}^{k} and P_{bbus}^{temp} defined, the BFS algorithm can be used to find the power flow solution of the system, and thus also the lowest temporary system voltage, V_{min}^{k}, the same way it was done in the power flow model in section 4.4.1. Before the iterative part of the bisection method can start, it has to be clarified if there exist any possible solution to the problem, for $P_{test}^{k} \in [P_{low}, P_{high}]$. This test will be different for the charging and the discharging algorithm:

- **Optimal charge algorithm:** Check if $V_{min}^{k} \geq 0.9$ pu. If the lowest system voltage V_{min}^{k} still is higher than 0.9 pu even with the maximum possible power, P_{batt}, withdrawn from the grid to charge the battery, no solution exists close to 0.9 pu, and the loop will break and return P_{test}^{0}.
- **Optimal discharge algorithm:** Check if $V_{min}^{k} \leq 0.9$ pu. If the lowest voltage level in the system is lower than 0.9 pu. even when the maximum possible power, P_{batt}, is supplied to the grid, no solution exists close to 0.9 pu., and the loop will break and return P_{test}^{0}.

This test also finds if the solution exists for exactly $P_{test}^{k} = P_{high}$, which will also break the loop. If there exist a solution within the given interval, that is not $P_{test}^{k} = P_{high}$, the iterative procedure starts and the iteration count is updated, $k = k + 1$.

Step 3 - Find the Arithmetic Mean

P_{test}^{k} will be updated by finding the arithmetic mean between $P_{high}^{(k-1)}$ and P_{low}^{k-1}, of the previous iteration, as shown in equation (4.9):

$$P_{test}^{k} = \frac{P_{high}^{(k-1)} + P_{low}^{(k-1)}}{2} \tag{4.9}$$

A new $P_{bbus}^{temp,k}$ is found as in equation (4.8). This will be completely independent of $P_{bbus}^{temp,(k-1)}$, and all earlier values. Then again will the BFS algorithm run to find the power flow solution with this value for P_{test}^{k}, and following can the minimum system voltage, V_{min}^{k} be found.

Step 4 - Convergence Criterion

The convergence criterion is given as the mismatch between the temporary minimum system voltage and the desired voltage level of 0.9 pu. The mismatch value, ΔV_{mis}^k, has to be smaller than the pre-set limit κ_V, for the loop to break. To ensure that the returned voltage level from the algorithm is not below 0.9 pu., which may be the case when solving equations numerically, the minimum voltage level is set to be 0.9 pu + κ_V. The mismatch calculation is given in equation (4.10):

$$\Delta V_{mis}^k = |V_{min}^k - 0.9 + \kappa_V| \tag{4.10}$$

If the convergence criterion is not met, step 5 will be conducted and then step 3 - 5 will be repeated until it is.

Step 5 - Update Upper/Lower Power Rate

New boundaries for the upper and lower power rate have to be set to narrow down the search area further. The new boundaries are dependent on the value of V_{min}^k, and will be different for the charge and the discharge algorithm:

- **Optimal charge algorithm:** Check if $V_{min}^k > 0.9$ pu. If that is true, the following updates will be carried out: P_{low}^k will take the value of P_{test}^k, while P_{high}^k will remain unchanged, shown mathematically in equation (4.11).

$$\begin{aligned} P_{low}^k &= P_{test}^k \\ P_{high}^k &= P_{high}^{(k-1)} \end{aligned} \tag{4.11}$$

  If the voltage level is not higher than 0.9 pu, P_{low}^k will be unchanged, and P_{high}^k will take the value of P_{test}^k, as shown in equation (4.12):

$$\begin{aligned} P_{high}^k &= P_{test}^k \\ P_{low}^k &= P_{low}^{(k-1)} \end{aligned} \tag{4.12}$$

- **Optimal discharge algorithm:** Will also check if $V_{min}^k > 0.9$ pu. The dicharging algorithm will deliver the opposite boundary update of those given in the charging algorithm. If the V_{min}^k has a higher value than 0.9 pu., P_{high}^k will take the value of P_{test}^k as showed in equation (4.12). If the opposite is the case, than the P_{low}^k will take the value of P_{test}^k, just like in equation (4.11).

The iteration count is then updated to $k = k + 1$ before step 3 is repeated. When the iterative process is completed, the function will return the optimal charge or discharge power to the battery model, such that the minimum voltage level is as close as possible, but above to 0.9 pu.

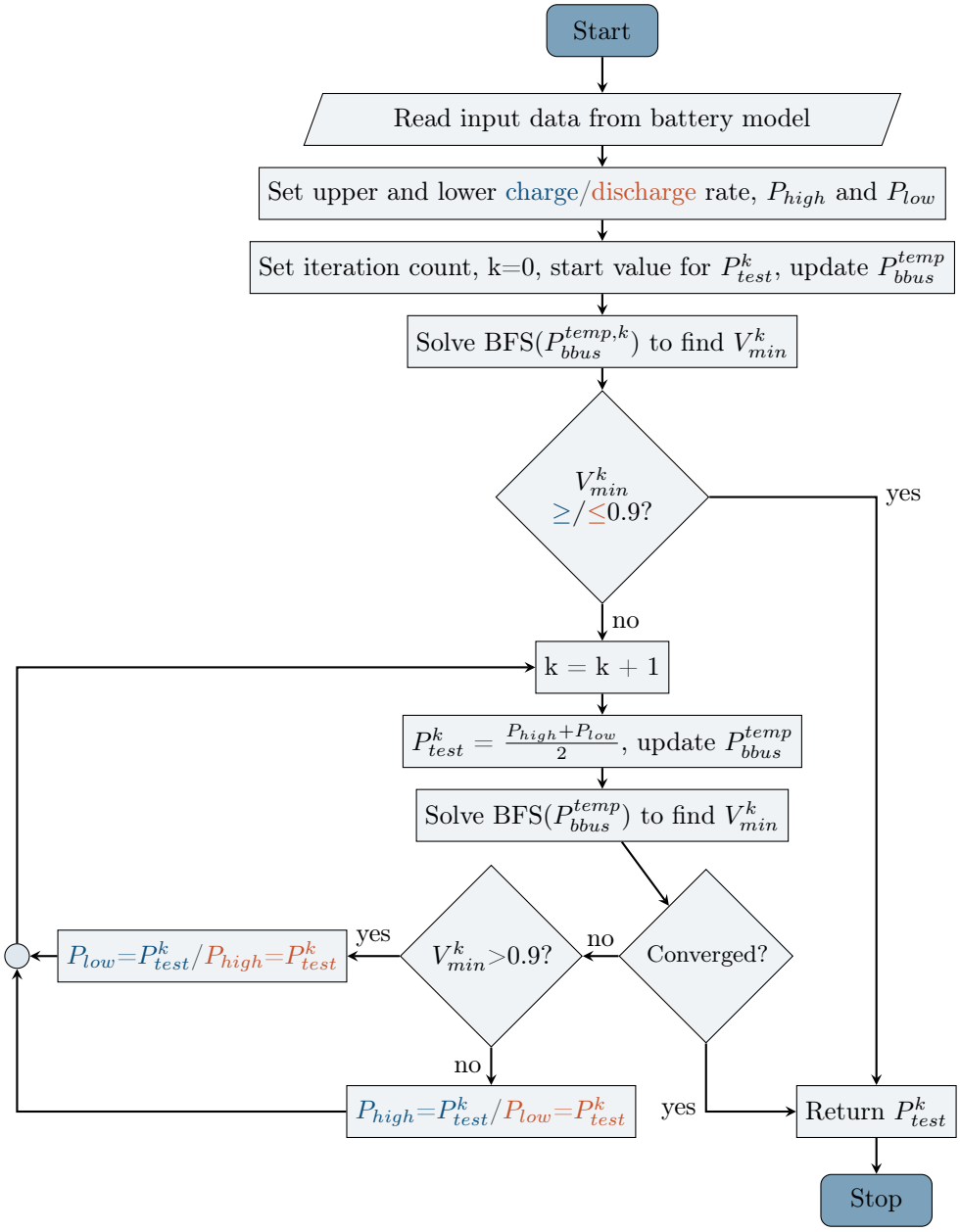

Figure 4.3: Flowchart of optimal charge/discharge algorithm. Charging algorithm is written in blue, discharge algorithm is written in orange, seperated with /.

5 | Investment Analysis

This chapter presents the method of performing the economic analysis of the study. The most important factor regarding the costs of the investments is related to the sizes of the different alternatives. Hence, a presentation of the method for finding the optimal sizes will be given. Furthermore, the investment planning method used for comparing the economic outcome of the line and the BESS will be presented.

5.1 Determining Locations and Sizes of Line and BESS

The size determination process includes finding the optimal cross-section for the line and finding the close to optimal energy capacity and power rating. Finding the right placement for the investments can also greatly affect the sizing, and deciding on the right branch or bus for the installations should be done wisely. The method of finding the optimal sizes includes running the model presented in chapter 4.

The locations, the power and energy ratings of the battery and the impedances in the lines have to be defined before running the model. As such, the optimal sizes and placements are found by testing various values, and systematically narrow down the scope until a solution close to optimal is found. It can be assumed that only one line upgrade or one BESS is needed.

5.1.1 Method of Finding Optimal Cross-Section

The goal is to find the optimal cross-section for a line that needs an upgrade, such that the installation costs are the lowest. That procedure also includes finding the right branch to perform the upgrading. Deciding on the optimal cross-section of a line investment depend on the maximum power flow in the line. There exist methods for calculating the optimal cross-section directly. However, in this study, the necessary upgrading will be found by testing different impedance values in the lines and run the load flow model presented in section 4.4 to check the minimum voltage level. If the requirements for the voltage level are fulfilled, a line with characteristics that correspond to the impedance value of the test case will be chosen. The

resultant optimal line impedance, Z_{line}, is determined as in equation 5.1:

$$Z_{line}\left[\frac{\Omega}{m}\right] = \frac{Z_{pu,opt}[pu.] \cdot Z_{base}[\Omega]}{l_{line}[m]} \tag{5.1}$$

where $Z_{pu,opt}$ is the per-unit impedance value found through the testing, Z_{base} is the impedance base value and l_{line} is the length of the line in kilometres. The value of Z_{line} is compared to impedance values for various overhead lines. The obtained impedance value of the chosen line will for the further study be given as the resistance, r_b, and reactance, x_b, values of the branch, b, where the upgrade is performed. These technical parameters are needed to run the model with the updated line information. However, only the cost and the length of the line is needed for performing the economic analysis.

5.1.2 Method of Finding Energy Capacity and Power Rating of BESS

The method for finding the optimal energy capacity and power capacity for the BESS installation uses a similar testing approach as used for finding the optimal cross-section. Initially assumed high values are set as input values in the model for both the energy and power capacity. The load flow and battery model is then to run to see how much of the proposed capacity that is needed during the analysis. The rated energy and power can be directly scaled down to fit the need of the system. This procedure will be carried out for various locations in the grid where the BESS can perform its required tasks.

Power Rating P_{batt}

Primarily, the power rating of the BESS will be determined. The power rating will be equal to the maximum discharge power P_{dis}^{t} that was found from the optimal discharge model, only rounded up to the closest integer. This will be the maximum needed power to maintain the voltage requirements in the grid. The reason why the maximum charging rate is not chosen is that this rate can be much higher during the low-demand periods than the needed maximum discharge rate during the high-demand periods. This could lead to an over-dimensioning of power capability.

Energy Capacity E_{batt}

After the power rating is decided and the input value for P_{batt} is updated, the energy capacity will be chosen so that the battery can supply power to the grid whenever needed. For the battery to be considered as an equally good technical solution as the grid investment, it has to have a large enough energy capacity to provide the required power at all time. With a large initial battery capacity tested, along with the optimal power ratings of the BESS, the maximum withdrawn energy amount can be found, i.e. the minimum energy level during the period of

analysis. The difference between the test-capacity $E_{batt,test}$ and the minimum energy level during the operation, $E_{batt,min}$, will make the needed energy for the analysis period. Dividing this value by 0.8 also takes into account the minimum allowed SOC-level of 0.2, and will give the minimum energy need of the battery, found as $E_{batt,ex}$. The calculation is presented in equation 5.2. The value found will be rounded up to the closest integer divisible by five, and this will be the close-to-optimal E_{batt} used in the further analysis.

$$E_{batt,ex} = \frac{E_{batt,test} - E_{batt,min}}{0.8} \tag{5.2}$$

It should be noted that the value of $E_{batt,test}$ has to be set high enough to handle the voltage problems throughout the analysis period. If this is not accomplished, a larger value will have to be tested.

5.2 Economic Analysis

The economic analysis will be performed based on the investment planning principles presented in section 2.3, using economic factors as the annuity factor presented in appendix A.2. The analysis will include the investment costs and the cost of losses from the consumer perspective, all other costs are neglected from the study. The input parameters needed to perform the economic analysis that applies to both investment alternatives are presented in table 5.1:

Table 5.1: Input values for the economic analysis

Parameter	Description
d	Discount rate
c_{el}	Electricity price $[\frac{NOK}{kWh}]$

The investment alternatives will be compared on a basis of the annual costs, c. This way the salvage value is not needed. The costs are annualised by first finding the total costs, C, and multiplying it with the annuity factor $\epsilon_{\gamma,d}$, as showed in equation 5.3:

$$c\left[\frac{NOK}{year}\right] = C[NOK] \cdot \epsilon_{\gamma,d}\left[\frac{1}{year}\right] \tag{5.3}$$

Since the annuity factor depends on the economic life of the asset, here noted by γ, the value will not be the same for the two investment alternatives. The discount rate, d will be the same in both cases.

The method of calculating cost of losses is the same for both alternatives and is included as

the costs seen from the consumers as they have to pay for all power delivered from the grid. The cost of losses is given in equation (5.4):

$$c_{loss} = E_{loss} \cdot c_{el} \tag{5.4}$$

The total costs for each alternative will be found by summarising the cost of losses over a year and the annual investment costs. The investment cost calculations for each alternative are presented in below.

5.2.1 Cost of Line Upgrade

The values needed prior to performing the economic analysis of the grid reinforcement are presented in table 5.2. The values are needed for both the investment cost-calculation and for determining the cost of losses.

Table 5.2: Input values for the economic analysis of line upgrade

Parameter	Description
$E_{loss,l}$	Energy losses over the analysis period in the system with line upgrade [kWh]
l_b	Lenght of the line in the branch, b, to be upgraded [m]
c_{line}	Cost per meter of new line [$\frac{NOK}{m}$]
γ_{line}	Economic lifetime of the overhead line [years]
$\epsilon_{\gamma_{line},d}$	Annuity factor for line investment [$\frac{1}{years}$]

The total investment cost of the line, C_{line}, is determined as in equation (5.5):

$$C_{line} = c_{line} \cdot l_b \tag{5.5}$$

By using equation (5.3) the annual line costs can be determined, and the cost of losses is calculated as in equation (5.4).

5.2.2 Cost of Installing BESS

The total investment costs of installing the BESS are related to both the cost of energy and power capacity, as presented in section 2.2.2. The input parameters needed to calculate the total annual BESS costs are presented in table 5.3.

The total capitalised investment costs of installing the BESS can be found as in equation (5.6):

$$C_{batt} = P_{batt} \cdot c_{P,batt} + E_{batt} \cdot c_{E,batt} \tag{5.6}$$

Table 5.3: Input values for the economic analysis of the BESS

Parameter	Description
E_{batt}	Energy capacity of BESS [kWh]
P_{batt}	Power capacity of BESS [kW]
$E_{loss,batt}$	Energy losses over the analysis period in the system with BESS [kWh]
$c_{P,batt}$	Cost of power capacity of BESS $[\frac{NOK}{kW}]$
$c_{E,batt}$	Cost of energy capacity of BESS $[\frac{NOK}{kWh}]$
γ_{batt}	Economic lifetime of the BESS [years]
$\epsilon_{\gamma_{batt},d}$	Annuity factor for the BESS investment $[\frac{1}{years}]$

5.2.3 Economic Comparison

Annual Net Benefit (nb)

The annual net benefit, nb, from installing the BESS compared to the line upgrade is given as in equation (5.7):

$$nb = c_{line,a} - c_{batt,a} \tag{5.7}$$

Where $c_{line,a}$ and $c_{batt,a}$ are the total annualised costs of the line and the BESS, respectively, calculated as shown in equation 5.3. The BESS is economically profitable if the net benefit has a positive value.

Break-Even Cost

The break-even cost for the BESS is defined as the cost of capacity required for the BESS to have the exact same annual costs as the line upgrade. If the net benefit is positive, these values will be higher than the price level today. If the net benefit is found to be negative, these values will be lower than the price level today, showing how much the costs have to decrease. The method of determining the break-even costs of the BESS are as follows:

- Set the annual costs of the BESS equal to the annual costs of BESS:

$$c_{batt,a,BE} = c_{batt,l} \tag{5.8}$$

- Find the resulting capitalised costs of the BESS:

$$C_{batt,BE} = c_{batt,a,BE} \cdot \epsilon_{\gamma_{batt},d} \tag{5.9}$$

- When finding the equal increase/decrease for the cost of power and energy capacity, the factor x is here given as the percentage required cost increase/decrease. It can be found

by solving the following equation for x:

$$C_{batt,BE} = x \cdot P_{batt} \cdot c_{P,batt} + x \cdot E_{batt} \cdot c_{E,batt} \tag{5.10}$$

6 | Case Study Description

In this chapter, the case study is presented. Section 6.1 contains information about the system and load data that are provided by Lyse Elnett. Section 6.1.3 describes how the given information is combined in a suitable way to develop an interesting present situation. Further, section 6.2 presents the investment alternatives that create the basis for the performance of the case study.

6.1 Cabin Field in Southern Norway

A case study is to be performed in a remote distribution grid in southern Norway. Lyse Elnett has provided information about the system topology and load profiles of the customers. They have requested research on the possibility of installing a BESS in a weak grid with cabins located in southern Norway. However, due to privacy concerns and lack of available data, information about the actual area can not be given. Information about a similar type of grid and data from similar loads, being independent of each other, is presented below. Section 6.1.1 and 6.1.2 describes the information on the grid and the loads respectively. In section 6.1.3, the information is composed into one system in an appropriate way for the analysis.

6.1.1 The Grid

The area to be investigated is a cabin field located remotely in the distribution grid. The grid distribution network can be described as a weak grid with radial structure. A figure of the grid, as provided by Lyse Elnett, can be seen in figure 6.1. There are two main radials with a total of ten customer connection points. Three of them are located at the left radial, and seven at the right. The substation connects the system to the main grid. It has a capacity of 230 kVA and a secondary voltage level of 235V. The lines in the system are mostly overhead lines of the type EX with different cross-sections. Two Cu-cables connects two of the customer points in the left radial. A summary of the network data is presented in table 6.1. Information about the conductivity in the different types of lines, listed in table 6.1a, is provided by Hafslund Nett.

Table 6.1: Network data

(a) Line data

Line	r [Ω/km]	x [Ω/km]	R/X
EX3x95	0.32	0.074	4.3
EX3x50	0.64	0.077	8.3
EX3x25	1.20	0.081	14.8
Cu3x16	1.15	0.088	13.1

(b) Substation data

	Rated value
Apparent power	230 kVA
Secondary voltage	235 V

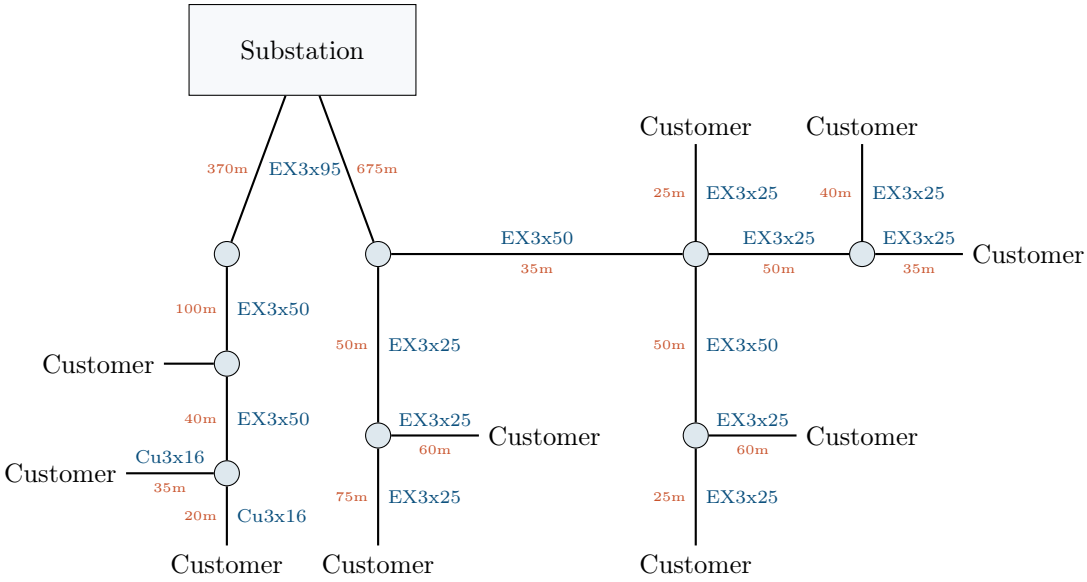

Figure 6.1: The grid topology

6.1.2 The Loads

Cabins represent a particular type of load. Their load profiles are less predictable than, for instance, the load profiles of households or the industry. Most of the year they remain unused with low power demand, and there can be expected high and sudden power peaks once they are in use.

Lyse Elnett has provided AMS-data for eight cabins located in an area with similar conditions as for the grid presented above. The data is from the 720 hours of April 2019. A summary of the maximum, minimum and average load demand for each of the eight cabins is presented in table 6.2 and in figure 6.2. The hourly load demand for April 2019 at each cabin is presented in four graphs in figure 6.3. The different colours each represent one load profile for one unique cabin. The load profiles are printed in four different charts, two cabin loads in each, for better visualisation. Note that the y-axis is scaled differently in the four charts.

The AMS-data only contain information about the active power consumption for the loads. Lyse Elnett also did provide information about the maximum, average and minimum active and reactive power for different cabins over a year. By using the relationship presented in equation (3.2) the power factor was found to be approximately pf = 0.98 for all the loads. This power factor was further used to develop an approximated reactive power-profile at the cabins, with basis in the same relationship of equation (3.2). This way the reactive power is 0.2 times the active power in a given hour. The reactive power is included in the study, but emphasis will be put on the active power demand.

Table 6.2: Load data at cabins

Cabin nr.	P_{max} [kW]	P_{min} [kW]	P_{avg}[kW]
1	6.119	0.243	1.097
2	2.018	0.625	1.035
3	5.718	0.091	0.588
4	3.800	0.018	0.902
5	3.414	0.002	0.253
6	5.191	0.088	0.895
7	4.233	0.131	0.858
8	4.067	0.047	0.570

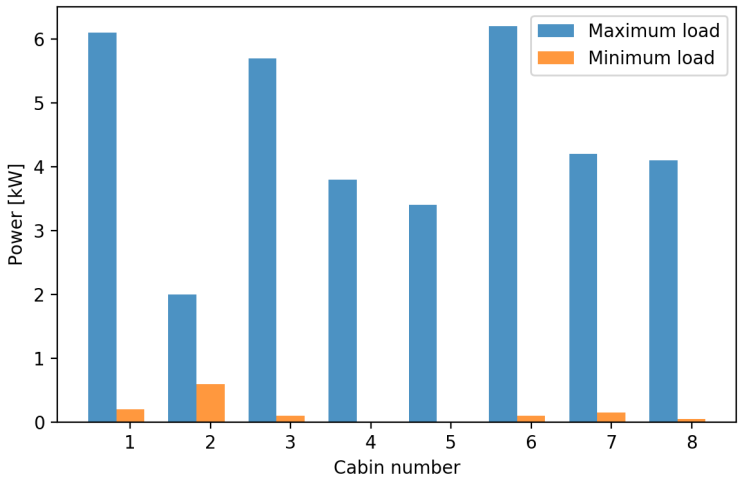

Figure 6.2: Maximum and minimum load demand at the cabins

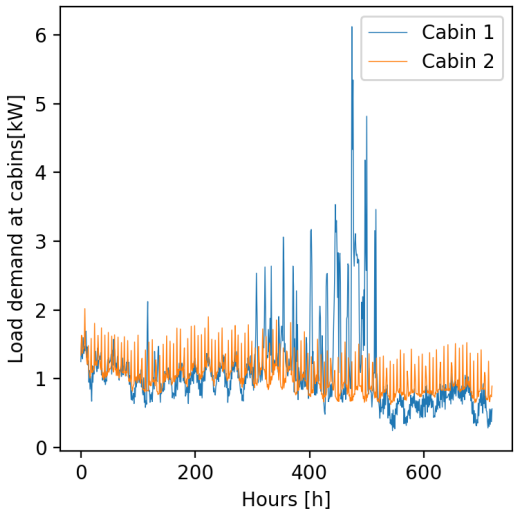

(a) AMS data from cabin 1 and 2

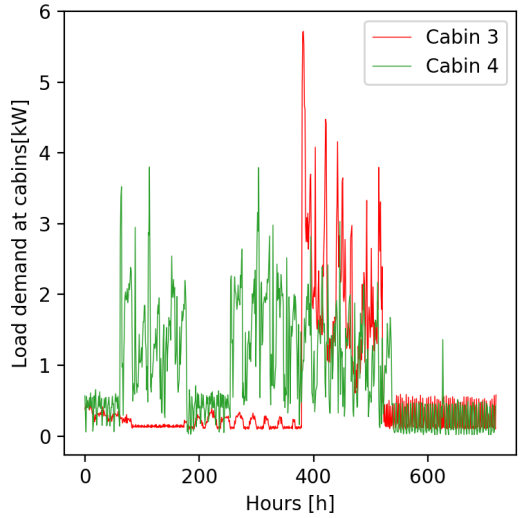

(b) AMS data from cabin 3 and 4

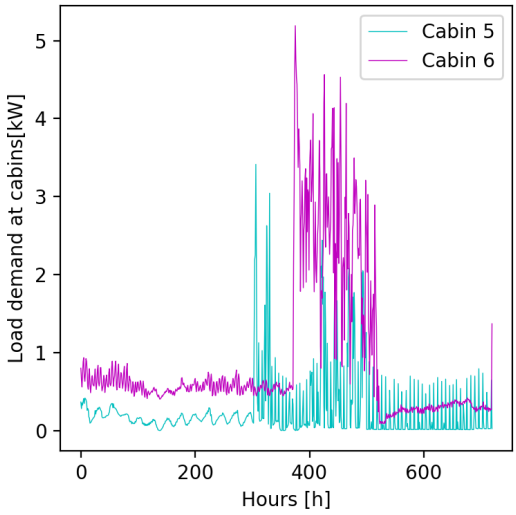

(c) AMS data from cabin 5 and 6

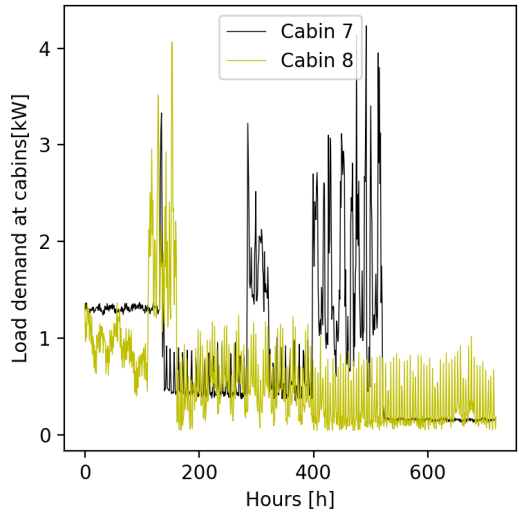

(d) AMS data from cabin 7 and 8

Figure 6.3: Hourly load profile from April 2019

6.1.3 Development of the Present Situation

The present situation has been developed to illustrate the operation of a weak, radial distribution grid with high voltage drops. It is created based on the data and information described in the sections above, as well as including the required structure for using the BFS-algorithm.

Per-Unit Basis

The common per unit basis developed for the system, uses the system information provided in section 6.1.1 and 6.1.2. The base voltage V_{base} and base apparent power S_{base} are decided upon and used to calculate the corresponding base impedance Z_{base} as shown in equation (6.1):

$$Z_{base} = \frac{V_{base}^2}{S_{base}} \tag{6.1}$$

The per unit values are summarised in table 6.3.

Table 6.3: System base values

Base variable	Base value
S_{base}	1 kVA
V_{base}	235 V
Z_{base}	55.225 Ω

The base voltage is set equal to the voltage level at the substation in the system, so that the slack bus has the value of 1.0 pu. For convenience, the base apparent power is set to 1 kVA. This way 1 pu. of power in the model corresponds to 1 kW power, and it will be easier to keep track of the consumed power at the buses during operation of the model.

The Grid Structure

First of all the grid has been structured after the principles of the BFS-numbering scheme presented in section 3.2.1. Figure 6.4 shows the grid in figure 6.1, with the branch and node numbering that will be used in the analysis. Node 0 is the slack bus where the substation is located. All the other buses are load buses, but not all of them have customer connection points. The buses where the loads are connected are marked with a deeper blue colour. Further, the left radial that constitutes bus number 1, 3, 6 and 7, is named radial A. The right radial is called radial B and includes the rest of the load buses. A summary of information about the lines is presented in table 6.4. It includes the branch and node numbers, the types of lines, the length of the lines and the total line impedance calculated based on the information presented in section 6.1.1. It can be noted that branch 0 contains two different line types.

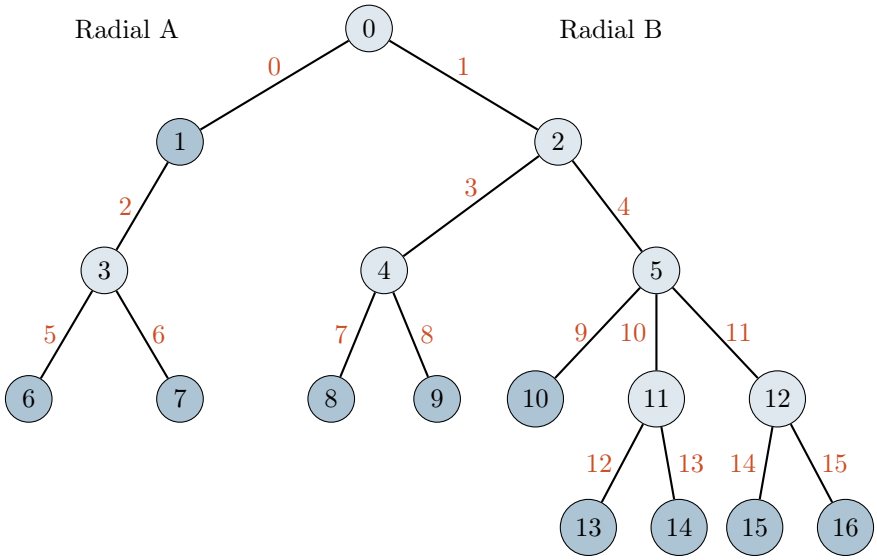

Figure 6.4: Nodes and branches in the grid numbered after the BFS numbering scheme

Table 6.4: Line information

Branch	From n	To n	Length [m]	Line type	R [Ω]	X [Ω]
0	0	1	370 + 100	EX3x95+EX3x50	0.1824	0.035
1	0	2	675	EX3x95	0.216	0.050
2	1	3	40	EX3x50	0.026	0.003
3	2	4	50	EX3x25	0.060	0.004
4	2	5	35	EX3x50	0.022	0.003
5	3	6	35	Cu3x16	0.040	0.003
6	3	7	20	Cu3x16	0.023	0.002
7	4	8	75	EX3x25	0.090	0.006
8	4	9	60	EX3x25	0.072	0.005
9	5	10	25	EX3x25	0.030	0.002
10	5	11	50	EX3x25	0.060	0.004
11	5	12	50	EX3x50	0.032	0.004
12	11	13	40	EX3x25	0.048	0.003
13	11	14	35	EX3x25	0.042	0.003
14	12	15	25	EX3x25	0.030	0.002
15	12	16	60	EX3x25	0.072	0.005

The Load Demand

The different cabin loads are placed at the buses in the system, with intent to load the weakest part of the system the most. This is to provoke an overloaded system with too high voltage drops at peak load hours. As there is only available information about the load of eight cabins, six extra load profiles are created based on the existing profiles. The load profiles are shifted a few hours back in time to avoid the peak hours of coinciding too much, while still the cabins are in use the same days to illustrate the high-season for cabin usage. Table 6.5 shows the details of how cabin nr. 9 - 14 were created.

Table 6.5: Creation of additional load profiles

Cabin nr.	Based on cabin nr.	Comment
9	6	Load profile shifted one hour back in time
10	6	Load profile shifted two hours back in time
11	3	Load profile shifted one hour back in time
12	7	Load profile shifted one hour back in time
13	1	Load profile shifted one hour back in time
14	5	Load profile not shifted

The 14 cabins are placed at the buses in the grid with customer connection points. Cabin 1 - 3 are connected to the left radial, while the 11 remaining are connected to the buses in the right radial. Table 6.6a summarises which of the cabins that are connected to what bus, and includes the peak power demand at the buses. In table 6.6b interesting information about the total system load is presented, including the peak power and total energy demand in the area for April. The same information is also given for radial A and B separately.

The total load profile for the area becomes as presented in figure 6.5. It can be seen from the graph that the average load demand is higher from around hour number 350 to hour number 510, than it is during the rest of the month. These hours corresponds to the dates from April 15^{th} to April 22^{nd} 2019. The high power demand can be explained by the Easter break of 2019 that coincided with these dates. It is to be assumed for the analysis, that April is the month of the year with the highest power demand. This can be justified as the Easter break attracts many Norwegian people to their cabins, also a higher amount than other weekends, which is also the trend seen from figure 6.5. Another argument for this assumption is that the power demand at cabins may not be as related to domestic heating as normal households. Cabins are often installed with wood stoves that limits the need for electricity for heating. With this assumption as basis, the electricity use in the cabins may not vary as much throughout the seasons, and a

Table 6.6: Total load demand in the system and at buses

(a) Load connected to the buses

Bus nr.	Connected cabin(s) nr.	P_{max} [kW]
1	1	6.119
6	2	2.018
7	3	5.718
8	4 & 11	6.662
9	5	3.414
10	6	5.191
13	7 & 13	7.979
14	8 & 14	5.457
15	9 & 12	5.473
16	10	5.191

(b) Total system load data

Term	Value
Maximum power	29.71 kW
Energy consumption	7762.20 kWh
Peak power hour	403
Maximum power A	8.57 kW
Energy consumption A	1958.02 kWh
Peak power hour A	403
Maximum power B	23.85 kW
Energy consumption B	5804.18 kWh
Peak power hour B	448

high number of users at the same time will cause higher power peaks than cold winter days.

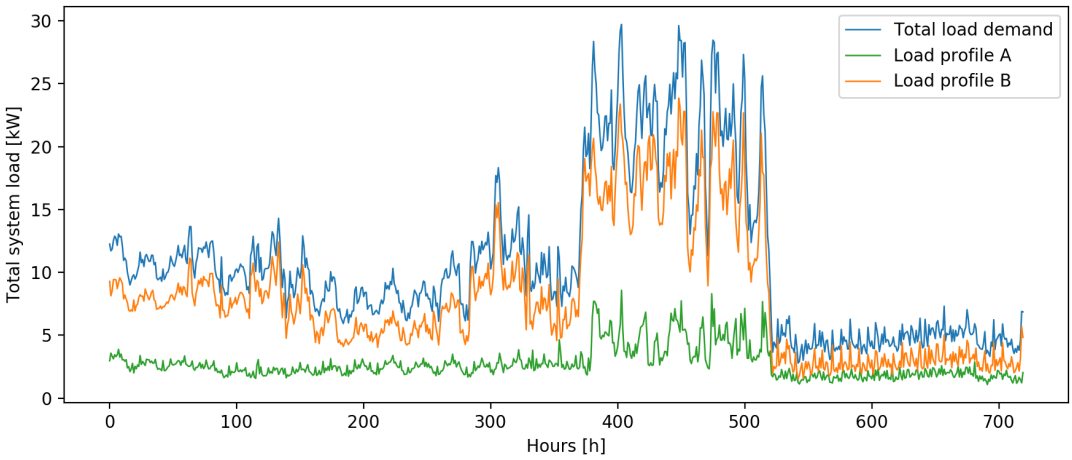

Figure 6.5: The total load demand in the area for April 2019

The present situation was developed so that the right radial B was much higher loaded than the left radial A. For the further investigation of the focus will be put on radial B, as this is the part of the system where it will be necessary to upgrade the grid or install a BESS. Also it can be noted that the maximum total load demand is around 30 kW, and the substation is dimensioned for 230 kVA. As such, there will not be any problems with delivering the required

power to the slack bus, and the two radials can be analysed independent of each other.

6.2 Investment Alternatives

Since the current status of the grid is that it is overloaded during the peak hours, the only viable option is to upgrade the system. The two alternatives that are to be investigated and compared are alternative 0 - line upgrade and alternative 1 - BESS installation. This section will present the decisions, costs and parameter values used for the investment alternatives. Those parameters regarding only one of the alternatives are will be presented in section 6.2.1 (A0) and 6.2.2 (A1).

The parameter values for conducting the analysis can be divided into model parameters required to run the model, and economic parameters needed to perform an economic investment analysis based on the technical results from the model. Table 6.7 and 6.8 show summaries of the model and economic parameters used in the study. They will all be described in more detail.

Table 6.7: Model Parameters

(a) Values for both alternatives

Parameter	Value
B	16
N	17
T	720 hours
P_n^t	AMS data
Q_n^t	AMS data
t	1 hour
V_0^t	1 pu.
δ_0^t	0 rad
Z_b	Line data
κ_{BFS}	0.0001

(b) Values for alternative 0

Parameter	Value
$b_{battery}$	0
r_b	-
x_b	-

(c) Values for alternative 1

Parameter	Value
$b_{battery}$	1
E_{batt}	-
P_{batt}	-
SOC_{start}	100%
SOC_{min}	20%
SOC_{max}	100%
κ_V	0.001
η_{ch}	0.95
η_{dis}	0.95

As for the values that are needed for both the alternatives, most of the system description has already been presented in the previous section, whereas the rest will be presented briefly. The convergence criterion for the BFS algorithm has been set to 0.0001. This way the results are precise without taking too much capacity. The electricity price needed to calculate the cost of losses was chosen to be equal to the average day-ahead price for April 2019, found at Nordpool to be 397.82 NOK/MWh [78]. The discount rate used for the economic analysis has been set to

Table 6.8: Economic Parameters

(a) Both alternatives

Parameter	Value
c_{el}	397.82 $\frac{NOK}{MWh}$
d	6 %

(b) Values for alternative 0

Parameter	Value
γ_{line}	40 years
$\epsilon_{\gamma_{line},d}$	0.06646
c_{line}	-
l_b	-

(c) Values for alternative 1

Parameter	Value
γ_{batt}	15 years
$\epsilon_{\gamma_{batt},d}$	0.10296
$c_{P,batt}$	6'900 $\frac{NOK}{kW}$
$c_{E,batt}$	2'060 $\frac{NOK}{kWh}$

6% based on instructions given to NVE from the Norwegian Ministry of Petroleum and Energy [79].

6.2.1 Investment Alternative 0 - Line Upgrade (A0)

The base case scenario for the analysis is to invest in a new line in to the over-loaded area. It can be assumed that the high load hours can cause a potential risk during operation, and that some action has to be taken. Grid reinforcement is a common way for grid companies to handle high voltage drops and increasing load demand. The lowest requirement for the line upgrade is that the minimum voltage in the system is above 0.9 pu. However, when a grid upgrade is performed it is likely that the grid company will invest in a grid that also can handle future load increases. This will be taken into account when choosing the line that is to be installed.

All the costs related to the line upgrade are provided by SINTEF Energi AS, from "Planleggingsbok for kraftnett" [80]. The cost is dependent on the cross-section of the line and includes all the related cost of the installation. Since line upgrades are well-known technologies, there are little uncertainties related to their costs. The line is assumed to have an economic life of 40 years. Hafslund Nett has provided information about the impedance values in the different line types. A summary of the required input parameters to run the model and to perform the economic analysis for alternative 0 are presented in table 6.7b and 6.8b. Two of the input parameters needed to run the model for alternative 0 are the resistance and reactance value of the line to be upgraded. These columns are left empty and will be presented as results in chapter 7. The same applies to the length of the line, l_b, needed to perform the economic analysis, and the per-meter cost of the line as this value is associated with the specific line cross-section.

6.2.2 Investment Alternative 1 - Installation of BESS (A1)

A summary of the model and economic parameters for alternative 1 are given in table 6.7c and 6.8c. Firstly, it can be assumed that the grid company is allowed to install a BESS for the given purpose. Furthermore, when analysing the effects of the BESS in the system, decisions

have to be made regarding the BESS characteristics. This includes the minimum and maximum SOC-level, already presented in chapter 4 as 20% and 100%, respectively. Furthermore, the charging and discharging efficiency are set to be equal and to have the value of 0.95. The Tesla Power Wall has a round-trip efficiency of 0.9 [81], which gives a charge and discharge efficiency of 0.949 if they are assumed to be equal.

The initial SOC level for the BESS has been set to 100%. That means that the battery is fully charged at the start of the analysis period. That assumption may not be realistic if the starting hour is the actual first time the BESS is operated. However, it can be assumed that April is a sample month of operation, and given the relatively low demand at the start of the month, it is realistic to assume that the BESS is fully charged. This assumption also limits the period where the battery is operated, and the first operating hour will be when the voltage level is below the critical limit.

The convergence criterion for the optimal charge and discharge model has been set to 0.001. A higher convergence criterion was chosen for this model than for the BFS-algorithm to lower the computational time. Also, less precise results are required from this model. Empty spots have been left in the table of model parameters for the BESS also. The optimal energy and power capacity will be presented in the results in section 7.2.

The economic life of the BESS has been set equal to 15 years, as suggested by NREL [55]. Their report presented in section 2.2.2 has also formed the basis for the BESS capacity costs used in this thesis. The price level from 2018 has been used, giving the cost of energy capacity a price of 2060 NOK/kWh, and the cost of power capacity equal to 6900 NOK/kW. It can be assumed that these costs are the only ones related to the installation of the BESS and that they take into account all economic factors from purchase to installation. Since batteries are a new technology there are larger uncertainties related to the costs, and as opposed to the line, the BESSs are not specially developed for Norwegian distribution grids and the Norwegian nature.

7 | Analysis of Results

This chapter presents the main results from the case study, along with sensitivity analyses and some variations of the input data to test how the results react to small changes in the operating conditions. Firstly, the main findings from the present situation will be introduced to visualise the challenges in the grid today. Furthermore, alternative 0 will be presented and compared to the present situation. The operational and economic results from alternative 1 will be emphasised, and these findings will be analysed and compared with the cases mentioned above, focusing on alternative 0. One month of simulation, i.e. 720 time steps, takes between 24 and 27 seconds, on a MacBook Air with macOS Mojave v10.14, Intel Core i5 1.4 GHz CPU and 4 GB of RAM.

7.1 The Present Situation (PS)

Operational results from the present situation are presented to illustrate the voltage problems that exist in the system now, and that have to be handled by the two investment alternatives. Some key-quantities are also presented to easier compare the investment alternatives with the present situation. Table 7.1 shows the technical results from the simulations, along with the needed system information for easier comparison with coming results.

It can be seen from the results in table 7.1 that the lowest voltage level for radial A is 0.9651 pu., while the lowest voltage in radial B is 0.8586 pu. This finding verifies the assumption about radial B being the part of the grid with voltage problems. Low voltage in radial B does not affect the voltage level in radial A. As such, the further presentation of results will only focus on radial B. Figure 6.4 from section 6.1.3 shows how the system is divided into two main radials. The total energy loss over the month in radial B is relatively small compared to the largest power losses during the peak hour operation. 6.1% of the energy delivered by the slack bus is lost. During the most extensive peak demand hour, 13% of the power delivered from the slack bus was lost in transmission.

Table 7.1: PS: Results for the present situation

The Present Situation		
Peak power demand in radial A	8.57	kW
Lowest voltage level in radial A - bus 7	0.9651	pu.
Energy consumption in radial B	5804.18	kWh
Energy delivered from slack bus to radial B	6181.35	kWh
Energy losses in radial B	377.17	kWh
Peak power demand in radial B	23.85	kW
Peak power delivered from slack bus to radial B	27.39	kW
Lowest voltage level in radial B - bus 13	0.8586	pu.

The voltage profiles of the buses in the system are plotted for 100 of the total hours in figure 7.1. Many of the buses experience a voltage drop below the critical limit, and bus number 13 most often reaches the lowest voltage levels due to the high power demand at this bus. Hence, this bus will be used to demonstrate how the voltage level is affected during the various operating conditions presented through the report. The resultant voltage profiles at all the other buses in the system are presented for both investment alternatives in appendix D.1.

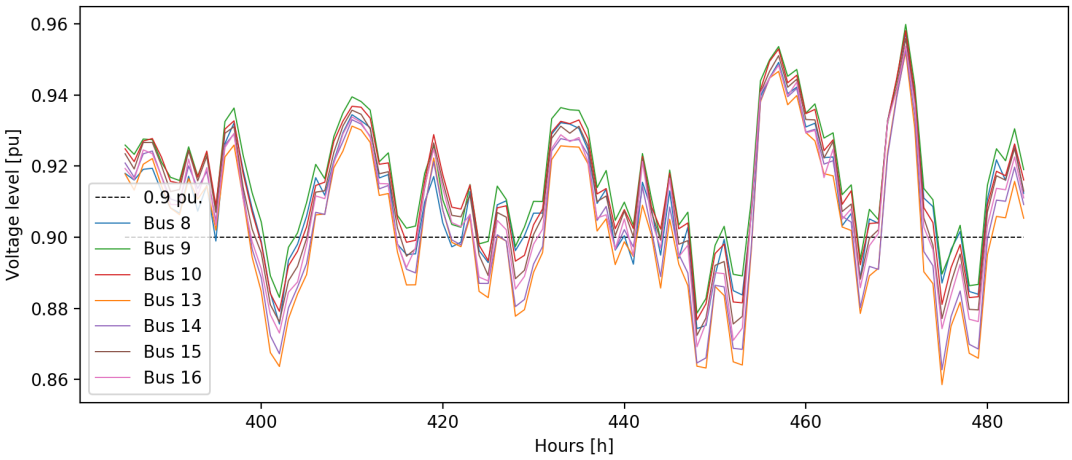

Figure 7.1: PS: The voltage profiles of the seven load buses in radial B

Figure 7.2 shows the relationship between the load demand in radial B and the voltage level at bus 13. The voltage problems occur when the load demand is high, and when the load profile of

bus 13 coincides with the demand at the other buses, resulting in high total load demand in the system. From the figure, it can be seen that the critical operating hours are from hour number 373 to 510. The voltage level drops dramatically to levels much below 0.9 pu. during many periods within this time frame. These are the issues that have to be managed by the investment alternatives.

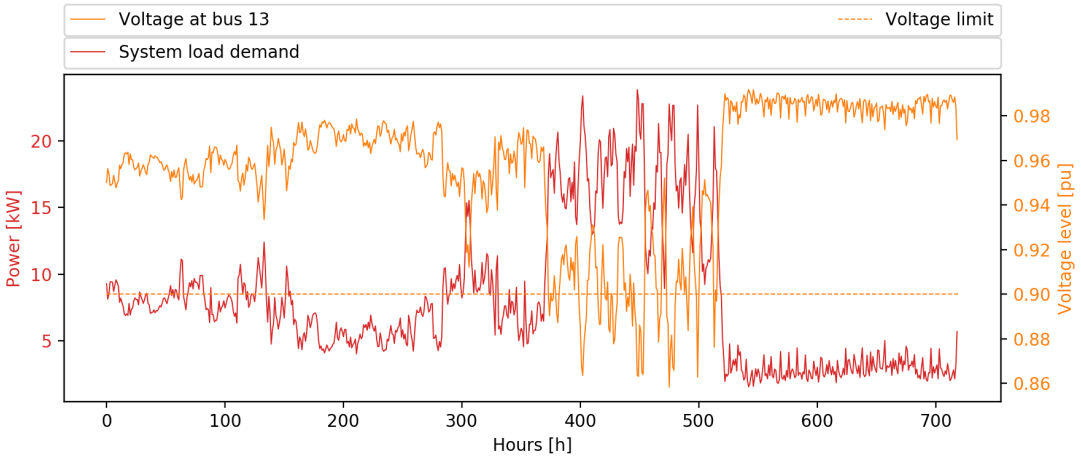

Figure 7.2: PS: The load demand in radial B and the voltage level at bus 13 for the present situation

7.2 Alternative 0 - Line Upgrade (A0)

The results from the line upgrade are divided into finding the required cross-section of the line and presenting the operational and economic results.

7.2.1 A0: Deciding on the Cross-Section of Line

The line of branch 1 is the line that connects radial B to the substation. This line also has the highest total resistance. By reducing the resistance on this line, the voltage drop will be lower in the entire radial, and this line is thus chosen to be upgraded. By still using the existing, the upgrade does not have to be as big as if the line had to be shifted. Assuming that it is only the limited transfer capacity that causes the voltage problems and that there is no damage on the existing line, it is valid to consider it to be further in operation. A suitable upgrade is to install an extra line of the already existing type, being a line of the type EX3x95mm^2. Installing this line will reduce the impedance in branch 1 with 50%, and limit the voltage drop at all the buses in branch B. The updated input parameters of the line can be seen in table 7.2, and details of the operating results are presented in section 7.2.2.

Table 7.2: A0: Updated Input Parameters

(a) Model Parameters

Parameter	Value
$b_{battery}$	0
r_b	0.108 Ω
x_b	0.025 Ω

(b) Economic Parameters

Parameter	Value
γ_{line}	40 years
$\epsilon_{\gamma_{line},d}$	0.06646
c_{line}	263.1 $\frac{NOK}{m}$
l_b	675 m

7.2.2 A0: Operational Results

As a result of the lower impedance values, the voltage level in the entire system has improved. Figure 7.3 shows the voltage profile of the exposed bus 13 before and after the line upgrade. The voltage drops still exist, but they are considerably improved and are never below the critical limit of 0.9 pu. The voltage fluctuations have also become smaller.

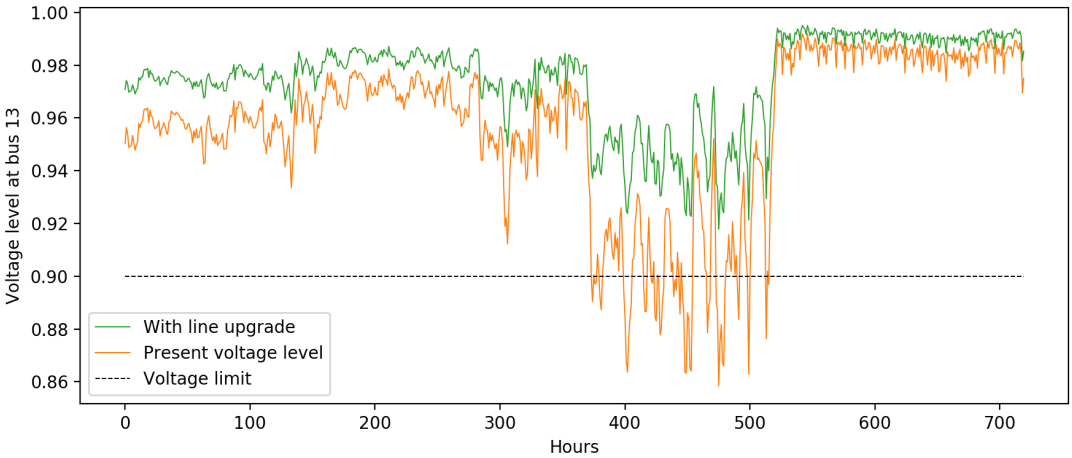

Figure 7.3: A0: Improved voltage level at bus 13 after upgrading the line in branch 1

The main technical results from the simulations are presented in table 7.3. Both the energy and power losses have been reduced compared to the situation today, and the maximum power drawn from the grid is lower, as was expected. The lowest system voltage at bus 13 during the operation is found to be 0.9187 pu. This level provides some flexibility regarding possible load increases in the area in the future, without excessively over-dimensioning the line for the current situation.

Table 7.3: A0: Technical results from upgrading the line

Technical Results Alternative 0				
Energy drawn from the grid	6006.00	kWh		
Compared to present situation	*−175.35*	*kWh*	*−2.84*	*%*
Energy losses	201.82	kWh		
Compared to present situation	*−175.35*	*kWh*	*−46.49*	*%*
Maximum power drawn from the grid	25.60	kW		
Compared to present situation	*−1.79*	*kW*	*−6.54*	*%*
Lowest voltage level at bus 13	0.9178	pu.		

7.2.3 A0: Economic Results

In table 7.4 the economic results from alternative 0 are presented. With the length of the needed line being 675 meters, the total investment cost comes at 177'597 NOK, with an annualised cost of 11'803 NOK per year. The cost of energy losses in the system is found to be small compared to the investment costs for this alternative. As mentioned in section 2.3, the cost of losses may in some situations account for a large part of the costs when doing investment planning research and are therefore not neglected initially. However, a monthly cost of 80.29 NOK, only accounts for 7.5% of the total annual costs in this situation, and it is therefore valid to not emphasis the cost of losses in the further analysis.

Table 7.4: A0: Economic results from upgrading the line

Economic Results Alternative 0			
Cost of losses in April 2019	80.29	$\frac{NOK}{month}$	
Total investment costs of line	177'597	NOK	
Annual investment costs of line	11'803	$\frac{NOK}{year}$	

7.3 Alternative 1 - Installation of BESS (A1)

The presentation of alternative 1 is divided into four parts, starting with the sizing of the BESS, followed by section 7.3.2 that gives an overview of the operating results, and comparing the main findings with with alternative 0. Furthermore, the economic results are presented in section 7.3.3, including the net benefit calculation. Section 7.3.4 addresses more of the details in the operation of the BESS and the rest of the system, when taking a closer look at a 48-hour

perspective.

7.3.1 Deciding E_{batt}, P_{batt} and the placement of the BESS

Bus 2 is connected to the entire right radial, and by placing the BESS here voltage issues can most easily be handled at all the buses emanating from bus 2. As also explained in section 7.2.1, the voltage drop will be the largest in this branch due to the length and high impedance value. The maximum required power drawn from the battery was determined and resulting in the need of a 10 kW power capacity of the BESS. This equals to 1/3 of the total system load demand, and around 40% of the power demand in radial B. The required energy capacity when considering a minimum SOC of 20% and maximum SOC of 100% was found to be 65 kWh. This accounts for 1.1 % of the total energy demand in radial B the given month. With an energy capacity of 65kWh and a power capability of 10kW, the C-rate of the battery becomes equal to C/6.5. The updated system parameters when including the findings from this section are presented in table 7.5.

Table 7.5: A1: Updated Input Parameters

(a) Model Parameters

Parameter	Value
$b_{battery}$	1
E_{batt}	65 kWh
P_{batt}	10 kW
SOC_{start}	100%
SOC_{min}	20%
SOC_{max}	100%
κ_V	0.001
η_{ch}	0.95
η_{dis}	0.95

(b) Economic Parameters

Parameter	Value
γ_{batt}	15 years
$\epsilon_{\gamma_{batt},d}$	0.10296
$c_{P,batt}$	6'900 $\frac{NOK}{kW}$
$c_{E,batt}$	2'060 $\frac{NOK}{kWh}$

7.3.2 A1: Overview of Operating Results

The parameters presented in table 7.5a were used to run the simulation model with the inclusion of the BESS located at bus number 2. The operating results from investment alternative 1 are presented in figure 7.4. The graphical plotting focuses on the time period from hour number 350 to 550, as these are the hours when voltage problems occur in the system. Since the battery follows the strategy to only operate when there are too large voltage deviations, these are the most interesting hours of the battery operation. The battery is initially fully charged, so that the battery is not operated until the voltage problems occur in hour 373. One can argue that it

is more likely to start the analysis with an empty BESS. However, it will not affect the results in any way and is thus not given any further discussion.

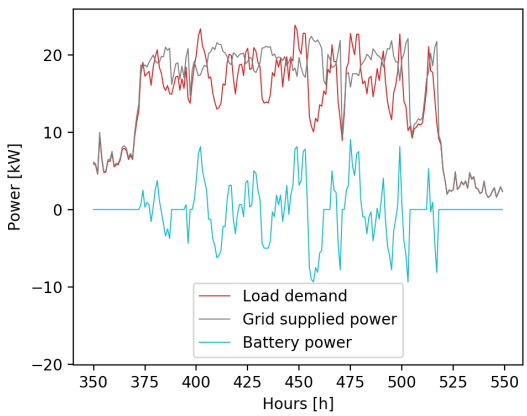

(a) System operation

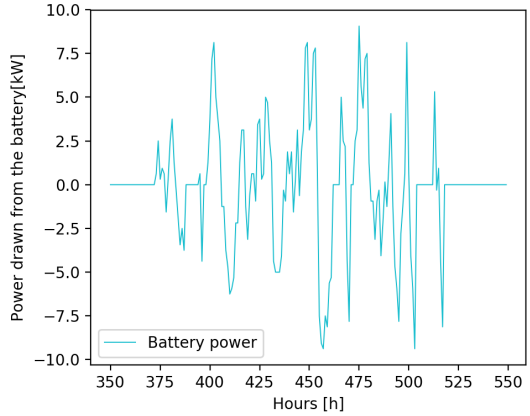

(b) Battery operation

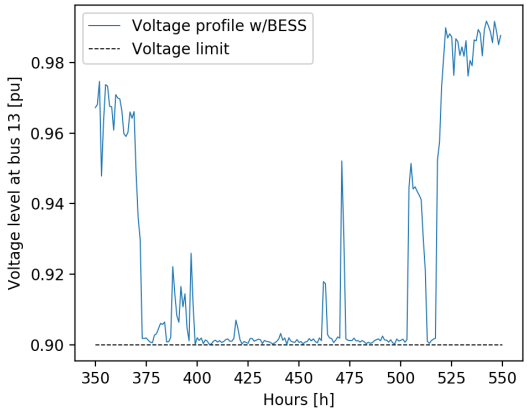

(c) Voltage profile at bus 13

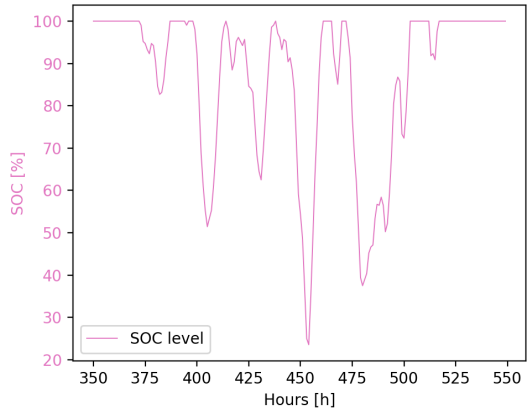

(d) State of charge of BESS

Figure 7.4: A1: Operating results from alternative 1

Figure 7.4a shows the system operation of the power consumption and supply in the area. In this graph both the power supplied from the slack bus and the load profile are plotted as positive values, for more easily comparison. The battery power is defined as positive as seen from the grid, meaning that positive values are plotted when the battery is discharging and supplying power to the grid. These definitions for positive and negative power will be used consistently throughout the report.

In figure 7.4b, only the battery operation has been plotted for a more precise view. The figure

shows the power drawn from and delivered to the battery at the battery side of the inverter. The BESS losses are thus not included in the plot. With the inclusion of the efficiency, the power profile would show the power as seen from bus 2, and the power delivered to the grid would be 0.95 times lower, while the power drawn from bus 2 to the battery would be 1.053 times higher than in the plot. Figure 7.4c shows the voltage profile at bus 13 when the BESS is included with its optimal charging and discharging strategy. Only bus 13 is shown here, and the voltage profile of the other buses in the system can be seen in appendix D.1.2. Lastly, figure 7.4d shows the state of charge of the BESS during the operation.

A presentation of the essential technical results of the system operation is given in table 7.6. More details on the battery operation will be given in table 7.9. Due to battery inverter losses, the total system losses and amount of energy drawn from the grid has increased. The changes are small compared to the present situation, with an increase of 10% in energy losses. When comparing the losses to alternative 0, they are more than doubled, which could be of interest if the energy losses accounted for a more substantial part of the total energy drawn from the grid than the current 6.7%. The comparison of losses with the present scenario can be of relevance in the decision-making, as it is the customers that have to pay for the system losses, and if they are significantly increasing, the willingness to pay for the BESS may be less popular.

While the energy demand is increasing with a BESS in the system, the peak power demand is significantly decreasing, compared to both previous scenarios. That finding comes as expected as the battery will supply the loads with power during the hours of high load demand, so the maximum power demand from the substation becomes lower. This effect illustrates how the battery has a peak-shaving capability.

Due to the fact that the charging and discharging strategy in the battery model is programmed to discharge the battery as little as possible, the lowest voltage level in the system is exactly 0.9 pu. It can also be seen from figure 7.4c, that during the operating hours of the battery, the voltage profile is stable slightly above 0.9 pu., both if the battery is being charged and discharged. A deeper look into the battery operation and the correlation of the different factors will be given in section 7.3.4.

Figure 7.5a compares the voltage profiles at bus 13 in the three presented scenarios. When the battery is not in operation, the voltage level of A1 and present situation are coinciding, while the voltage level of A0 sustains a higher level for all hours. The figure clearly shows how the battery improves the voltage level when this is required, and how it uses the periods with higher voltage level to recharge, and this way keeps the voltage level stable and low over a longer period.

Table 7.6: A1: Technical results from installing BESS

Technical Results Alternative 1				
Energy drawn from the grid	6221.16	kWh		
Compared to present scenario	*+39.81*	*kWh*	*+0.64*	*%*
Compared to alternative 0	*+215.16*	*kWh*	*+3.58*	*%*
Energy losses	416.98	kWh		
Compared to present scenario	*+39.81*	*kWh*	*+9.55*	*%*
Compared to alternative 0	*+215.16*	*kWh*	*+106.61*	*%*
Maximum power drawn from the grid	22.39	kW		
Compared to present scenario	*−5.00*	*kW*	*−18.25*	*%*
Compared to alternative 0	*−3.21*	*kW*	*−12.54*	*%*
Lowest voltage level at bus 13	0.9000	pu.		

In figure 7.5b the power drawn from the main grid is plotted as a function of time for the two investment alternatives. Even if the peak hour demand was reduced when installing a new line, it is even lower with a BESS in the system. The BESS causes both the voltage profile and the grid power demand to be less fluctuating, and stabilised at a lower level, compared to the grid upgrade alternative. Since the only objective in this analysis is to keep the voltage level above 0.9 pu., the peak-shaving and stabilising ability of the BESS will not impact the economic results to be investigated in section 7.3.3.

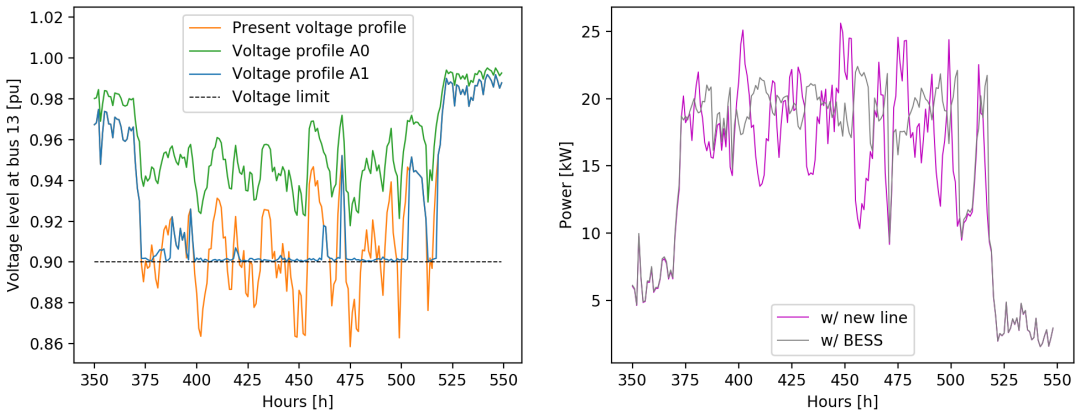

(a) Voltage profiles of scenarios

(b) Power supplied from grid for A0 and A1

Figure 7.5: Comparing operating results of PS, A0 and A1

7.3.3 A1: Economic Results

As the BESS has proven as an as good technical solution for this case study as the line upgrade, the results from the economic analysis is vital for the decision making. The main economic results are presented in table 7.7.

Table 7.7: A1: Economic results from installing BESS

Economic Results Alternative 1			
Cost of losses in April 2019	150.06	$\frac{NOK}{month}$	
Compared to alternative 0	*+69.77*	$\frac{NOK}{month}$	*+86.90 %*
Total investment costs of BESS	202'853	NOK	
Compared to alternative 0	*+25'256*	NOK	*+14.22 %*
Annual investment costs of BESS	20'886	$\frac{NOK}{year}$	
Compared to alternative 0	*+9'082*	$\frac{NOK}{year}$	*+ 76.95 %*
Resultant net benefit of BESS	-9'082	$\frac{NOK}{year}$	

From the annual net benefit given in the last row, it can be seen that alternative 1 is not a feasible solution compared to alternative 0. The net benefit has to be positive for an investment alternative to be economically beneficial. The annual costs of installing a BESS are 76.95% higher than the grid installation, so the differences are significant. The short calendric life of the battery, being only 15 years compared to the 40 years of the line, constitutes a large deal when comparing annualised costs. However, it can be seen that also the total investment cost of the BESS is higher than the total line cost, though only 14.22% higher.

As a result of the increased energy losses in the system presented in section 7.3.2, the cost of losses is also higher for A1. As April is considered to be the "worst" operating month by means of poor voltage quality and high power demand, this cost of losses is not representative for all 12 months. And even if it were, it would only account for 8% of the annual costs, so neglecting it from the study is valid. The operating costs have been neglected when calculating the net benefit, and further analyses will focus on the investment costs only.

Break-Even Cost of BESS

When the net benefit of the BESS installation was found to be negative, the break-even cost of the BESS can be determined as the cost of capacity required for the BESS and the line to become equally economic alternatives. Since the alternatives are compared on an annual basis, the annual costs of BESS and line are set to be equal. The break-even costs for energy and

power capacity are found based on this. The results are presented in table 7.8.

Table 7.8: Break-even cost of the BESS

BESS Break-Even Cost			
Annual break-even cost for BESS	11'803	$\frac{NOK}{year}$	
Capitalised break-even cost for BESS	114'641	NOK	
Break-even cost of power capacity	3'900	$\frac{NOK}{kW}$	
Break-even cost of energy capacity	1'164	$\frac{NOK}{kWh}$	
Compared to current costs from A1			-43.49 %

The power and energy capacity are determined when assuming that the cost reduction will be equal for both of the costs, here found to be a reduction of 43.49% compared to today's prices. When looking at the price development projections from NREL, presented in table 2.3, these price levels may be realistic already before 2025, if the development follows the low-cost curve. By looking at the mid-cost projection curve, the battery will reach the break-even costs sometime between 2030 and 2035. And if the prices keep a level as high as the high-cost projections, economically beneficial BESS prices will not be reached by 2050.

7.3.4 A1: 48-Hour Operation

To get a more detailed view of the system operation, the results from 48 operating hours have been studied closer. First an overview of some of the key numbers from the results of the battery operation over the entire period is given in table 7.9.

Table 7.9: A1: Summary of BESS operating results

Summary of BESS operation alternative 1			Hour(s)
Maximum charging power P^t_{ch}	9.38	kW	457
Maximum discharging power P^t_{dis}	9.06	kW	475
Lowest state of charge level SOC^t	23.56	%	454
Lowest level of energy stored in BESS E^t_{batt}	15.31	kWh	454
Longest discharging period	9	hours	446-452
Energy demand from BESS these hours	44.06	kWh	446-452
Available energy capacity of BESS, $E_{batt} \cdot SOC_{min}$	52.0	kWh	

The chosen 48-hour period was from hour number 432 to 480, corresponding to Friday 19^{th} and Saturday 20^{th} during the Easter week. An overview of the system operation during these hours along with the resultant voltage profile at bus 13 can be seen in figure 7.6. The hours were chosen because of the large fluctuations in both the battery SOC and the voltage profile, as well as the high power demand. The battery is both operating as fully charged, and with the larges depth of discharge of the month. Figure 7.7 includes four different plots of operating characteristics worth investigating, including load demand, voltage profile, SOC and battery operation.

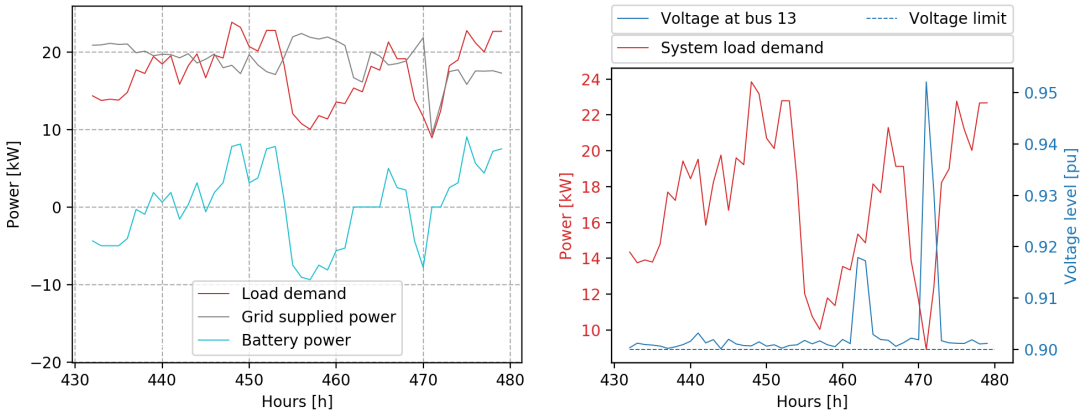

(a) System operation

(b) Load and voltage profile

Figure 7.6: A1: 48 hours of system operation

The three power plots in figure 7.6a clearly demonstrate how the battery operates to handle the load peaks so that the grid is less loaded. The power drawn from the grid is the largest when the battery is charging, and always lower than the load demand during peak hours since the battery contributes these hours. It can also be seen how the battery utilises the hours of lower load demand to charge. How much the battery is allowed to charge depend on the load demand for the given hour.

For the present situation and alternative 0, a clear dependency between the load profile and the voltage profile during operation is observed. Such a relationship can not be found when investigating only the load profile and the voltage profile of alternative 1, as shown in figure 7.6b. A more interesting study is to see how the voltage level is regulated by the battery operation, plotted in figure 7.7a. The orange line shows the voltage level in the system without the BESS connected, while the blue stippled line shows the voltage level with the BESS. The cyan-coloured battery operation can be seen as almost a mirror of the voltage level without the

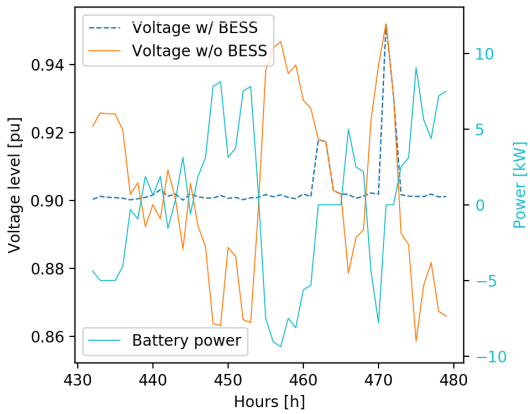

(a) Voltage level regulated by BESS

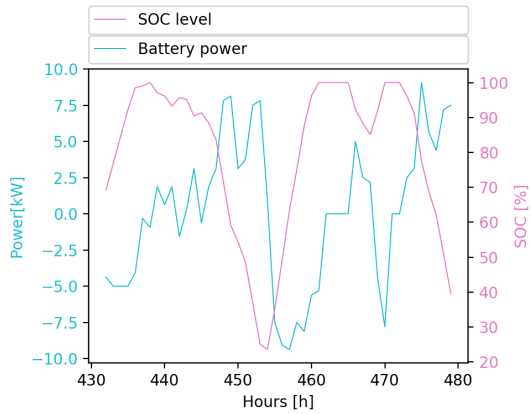

(b) Battery operation vs. SOC level of BESS

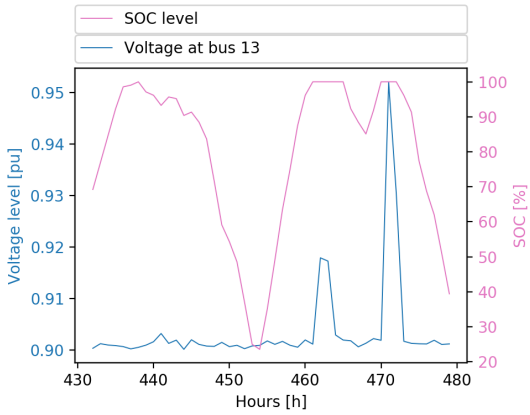

(c) Voltage profile at bus 13 vs. SOC level of BESS

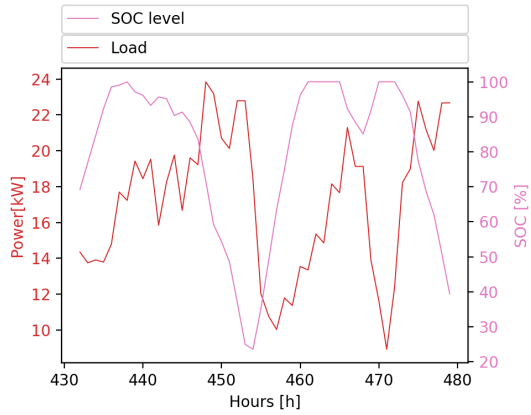

(d) Load profile vs. SOC level of BESS

Figure 7.7: A1: Display of interesting operating relationships

BESS. It is discharging the most when the voltage level is the lowest and charging as much as possible when the voltage level is above 0.9 pu. Either way, the voltage level with BESS is kept stable above 0.9 pu. as long as the battery is in operation.

If the battery is not operated during an hour, two reasons can explain why. Either the lowest voltage level in the system is precisely 0.9 pu., giving no opportunities for charging or discharging. Or the battery is fully charged, and the lowest voltage level is above the critical limit. Figure 7.7b and 7.7c show how the state of charge of the battery affects the battery operation and the voltage level, respectively. While the voltage level is kept more or less stable from hour 430 to 460, in hour number 462 and 469 the voltage level rises suddenly as a result of the battery state of charge being equal to 100%. From figure 7.7b, it can be seen that the battery power is

equal to 0 when it is not in operation, and the SOC level is at its maximum.

During these 48 hours, the system experiences the most extensive peak load hour, as well as the highest power demand over time. Those events cause the most significant drop in the battery state of charge of the entire analysis period. The relation between power demand and the SOC can be seen in figure 7.7d. From hour 439 to 454, being from 7 to 22 Friday the 19^{th} of April, the battery is being charged only two of the 16 hours, with the most prolonged discharging period being 9 hours in a row. The load profile these 16 hours, is what decides on the installed energy capacity of the battery. If the period of high demand had lasted even longer, this would require a larger installed battery capacity, changing the economic outcome of the analysis. A more thorough investigation of the sensitivity of the battery size as a result of the load profile will be performed in section 7.4.4.

The operation of the battery is dependent upon the lowest voltage level in the system, which in turn is dependent on the load demand in the system. It should be noted that the resulting charging and discharging power is also dependent on where the bus with the highest load demand is located in the system. The total system power demand is the largest in hour number 448, with a peak demand of 23.85 kW. The power drawn from the battery at this hour equals 7.81 kW. While the simulated battery discharging power is at its peak, 9.06 kW in hour 475, the total system demand this hour is only 22.77 kW. However, the load demand at bus 13, that is located far out in the grid, is very high this hour. In the hour with the highest system peak power, the demand was distributed more evenly between the buses, so the voltage level will not drop as dramatically at one bus in particular.

7.4 Sensitivity Analyses

The goal of performing sensitivity analyses is to see how sensitive the results are to changes in parameter values. These changes can be related to both the economic parameters, as well as the physical components like sizes, line-length and number of customers, which all of them will be investigated in this section. The pure economic investigations, like changes in costs and discount rate, do not require for the model to run with updated parameters. This will be necessary when updating some of the physical factors.

7.4.1 S0: Sensitivity to BESS costs

Since the battery costs are rapidly decreasing and somewhat unpredictable, it may be interesting to take a closer look at the sensitivity to cost reduction. From the break-even calculation in section 7.3.3 the required cost of capacity for the BESS to compete economically with the line-upgrade was found. These values were determined for an equal decrease in the cost of power

and energy capacity, and found to be equal to a reduction of 43.49% compared to the current price level.

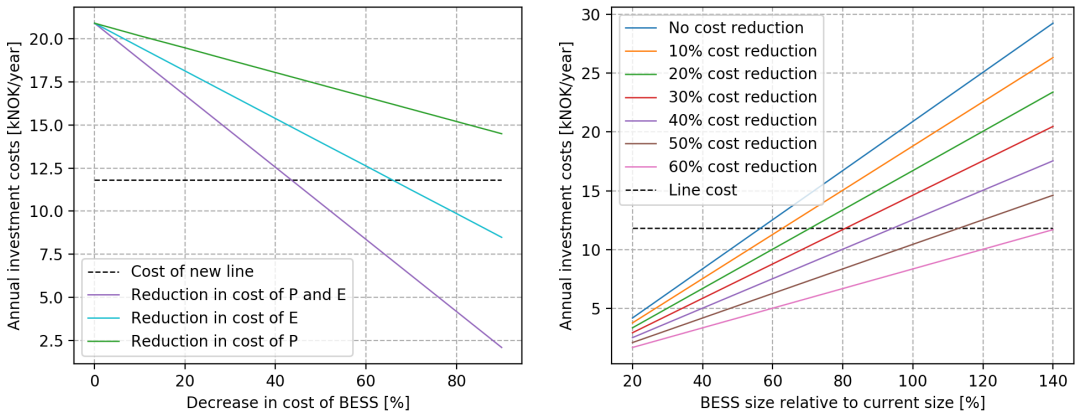

(a) Decrease in costs of P_{batt} and E_{batt}

(b) Varying the cost and size of BESS

Figure 7.8: S0: Sensitivity to the BESS costs

Figure 7.8a shows the annual investment cost as a function of a percentwise decrease in BESS costs related to only P_{batt}, only E_{batt} and both seen as one, which was the case in break-even calculation. The BESS will be profitable for all scenarios below the black-stippled curve showing the current line-upgrade cost as given in alternative 0. Even if the costs are higher per power capacity than per energy capacity, reducing the power costs to 0 will still not make the BESS installation profitable. This factum is due to the low C-rate and that the power capacity is 15.38% of the energy capacity. A cost reduction of 65.9% for the energy capacity is required if only the energy capacity is to be reduced. Such a reduction equals a cost of capacity of 702 NOK/kWh.

The graphs in figure 7.8a would be the same if they showed the decrease of the sizes of E_{batt} and P_{batt}. A battery capacity reduction of 65.9% gives an installed capacity of 22kWh. With a power capacity of 10 kW and an energy capacity of 22 kWh, the resultant C-rate becomes C/2.2. Such a small size it not realistic with the energy demand in the system presented, as the voltage requirements would not have complied, but the value should be kept in mind for the upcoming sensitivity analyses and discussion.

Figure 7.8b shows the annual investment costs as a function of BESS size for various cost reduction scenarios, all of them which look at an equal decrease in energy and power capacity costs. Also here the BESS will be profitable for all scenarios below the black-stippled line. Since

the battery size can not be decreased without changing the operating conditions, the most interesting scenarios for this exact case are related to the current size of 100%, and a size increase for a higher safety margin. There are few profitable scenarios for this system configuration, but in systems where an even smaller BESS capacity is needed, there are larger economic possibilities for BESS installations.

7.4.2 S1: Sensitivity to the Discount Rate

An important economic factor in investment planning is the discount rate. The discount rate may be decisive when it comes to comparing investment alternatives, and deciding on the best option, as the economic outcome changes with the discount rate. Figure 7.9a shows the relationship between the annual costs and the discount rate, for the line and the BESS. Figure 7.9b shows how the break-even cost for the power and energy capacity changes as a function of the discount rate.

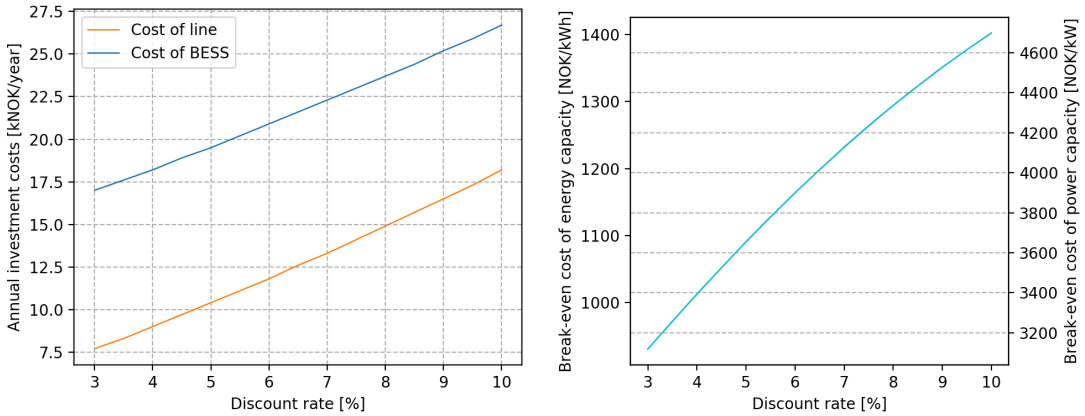

(a) Annual costs as a function of discount rate (b) Break-even cost as a function of discount rate

Figure 7.9: S1: Sensitivity to the discount rate

Since the total capitalised cost of the BESS is also higher than the total cost of the line, changing only the discount rate will not affect the economic outcome of this case, as figure 7.9a shows. The difference becomes smaller for a higher discount rate, but the changes are so small they are difficult to detect from figure 7.9a.

The difference becomes clearer in figure 7.9b when observing how the break-even cost increases for an increasing discount rate. A higher break-even cost will give the BESS a better position, as the market price does not have to become so low before the BESS turns profitable. The discount rate was set to 6%, by recommendations from NVE and the ministry of oil and energy.

Higher discount rates are normally used for investments that require high returns, and that is not necessarily the goal for the grid company.

7.4.3 S2: Sensitivity to Load Increase

While S0 and S1 focus on the economic outcome by changing parameters without running the model, the three upcoming sensitivity analyses will go more into details on how some factors affect the size determination and thus also the economic outcome. This section will study how sensitive the system is to a load increase and decrease. Additional cabins will be added to the system, using the same procedure that was used to create the present situation, presented in section 6.1.3. Some of the created cabin-loads were also removed from the system for study of a load decrease. One additional cabin, nr. 15, had to be created to have enough data, in addition to using the load profiles of radial A directly. Five load scenarios were created, including a range of 7 to 15 cabins connected in the system. The combination of new loads for the five load scenarios can be seen in table 7.10. The information about the cabin loads are given in table 6.2 and 6.5. The five resultant total load profiles in the system for each of the scenarios are presented for a fragment of the operating hours in figure 7.10. It can be seen that the more loads that are connected in the system, the less sensitive does the total profile become to additional load increase.

Table 7.10: S2: Number of the cabin loads connected to each of the buses for the five load scenarios

Bus nr.	7 cabins	9 cabins	11 cabins (PS)	13 cabins	15 cabins
8	4	4 & 11	4 & 11	4 & 11	4 & 11
9	5	5	5	5 & 1	5 & 1
10	6	6	6	6 & 2	6 & 2
13	7	7 & 13	7 & 13	7 & 13	7 & 13
14	8	8	8 & 14	8 & 14	8 & 14 & 15
15	9	9	9 & 12	9 & 12	9 & 12
16	10	10	10	10	10 & 3

Table 7.11 shows an overview of the operating results from the five load scenarios. Note that the 11-cabin scenario is the system as developed for the present situation in section 6.1.3. It can be seen that for the scenario with only seven cabins connected, there is no need for upgrading since the minimum voltage level is above 0.9 pu. for all the 720 operating hours. Upgrades are needed for the four remaining scenarios. The line type EX3x95 that was used in A0 is large enough to be used for all the load scenarios. Thus, the operating conditions and the costs of line upgrade remain the same as in A0. Significant differences are, however, occurring for the

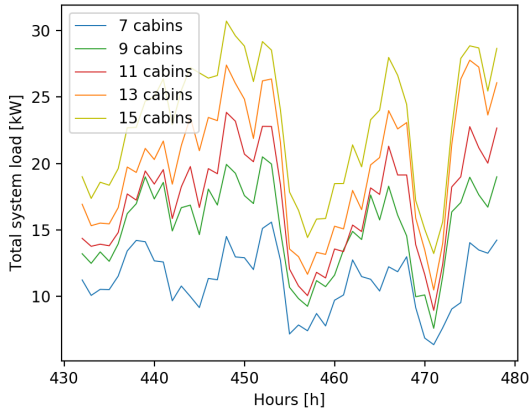

Figure 7.10: S2: Total load demand for each load scenario, 48 hours operation

Table 7.11: S2: Operating results for different load scenarios

Scenario	$V_{min,PS}$	$V_{min,A0}$	$P_{load,max}$[kW]	E_{batt}[kWh]	P_{batt}[kW]	E_{tot}[kWh]
7 cabins	0.9033	-	16.92	-	-	3'793
9 cabins	0.8819	0.9330	20.09	15	5	5'415
11 cabins	0.8586	0.9178	23.85	65	10	5'804
13 cabins	0.8290	0.9092	27.78	430	14	7'339
15 cabins	0.8184	0.9036	30.73	1140	17	8'412

battery size determination.

The relationship between the size for energy capacity and power capacity as a function of the system peak power (figure 7.11a) and the number of cabins (figure 7.11b) are presented in figure 7.11. While the required power capacity increases almost linearly with the load increase, the energy capacity demand increases exponentially. Hence, the optimal energy capacity for the scenario with 15 cabins becomes 18 times as big as the optimal size found for 11 cabins in A1, while the power capacity needed for that scenario is not even doubled. With fewer cabins in the system, both the energy and power capacity of the BESS decrease. For the scenario with 9 cabins the energy capacity has been reduced with 77%, to a capacity of 15 kWh.

The large increase in energy capacity relative to the power capacity and thus also line cross-section, can be explained by the upward-shift in the power demand curve. With an increasing number of hours where the BESS power is needed, the fewer hours are available for re-charging the battery, and the energy that has to be stored in the battery over time increases. In addition, the power peaks become higher, so that the battery is drained for energy faster. More details

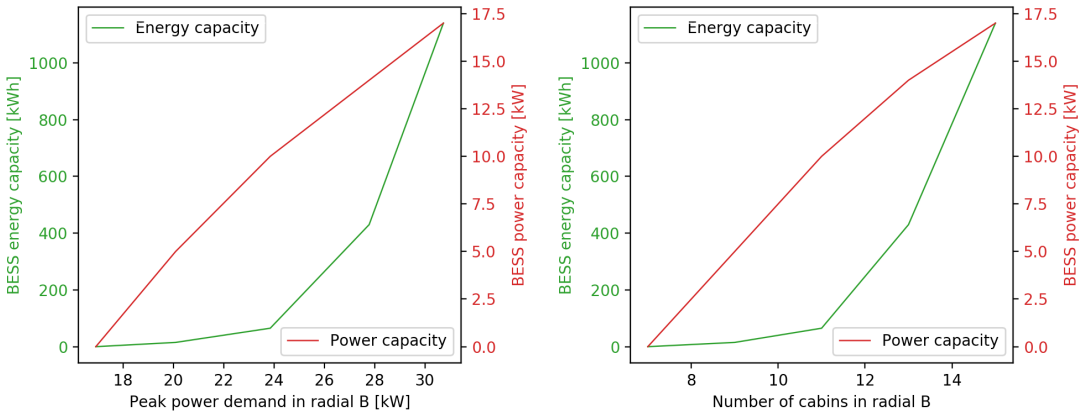

(a) Size as a function of system peak power

(b) Size as a function of number of cabins

Figure 7.11: S2: BESS energy and power capacity as functions of load increase

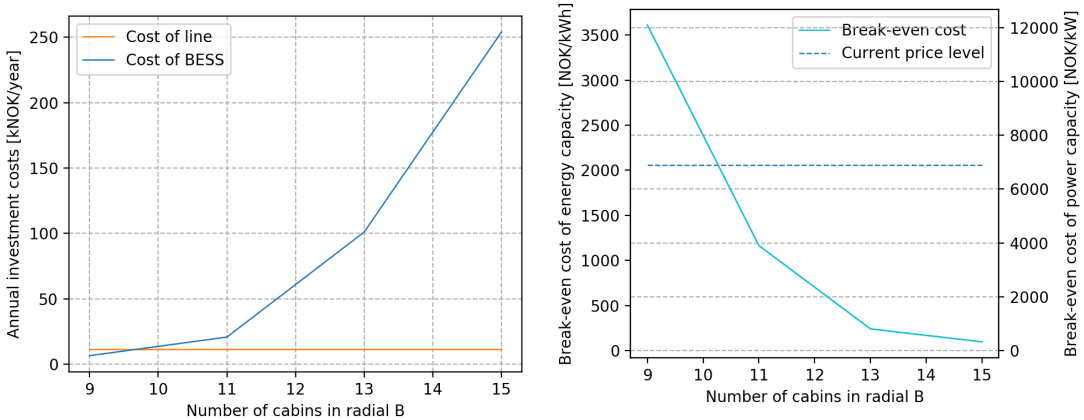

(a) Annual costs for BESS and line

(b) Break-even costs for power and energy capacity of the BESS

Figure 7.12: S2: Costs as functions of the number of cabins in radial B

of the impact from the load profile will be studied in section 7.4.4.

The economic outcome of this sensitivity analysis has been illustrated in figure 7.12. Figure 7.12a shows how the annual costs of the BESS installation increase dramatically as the number of cabins increases and thus also the energy capacity requirement of the BESS. Figure 7.12b shows the break-even cost of the BESS, decreasing as a result of increased load demand. The plot illustrates how the break-even cost of the battery is higher than the prices today when the energy requirement of the BESS is low. Hence, the BESS is the preferred solution for the

scenario with only 9 cabins in the system. The annual costs of BESS have decreased to 6732 NOK/year, resulting in an annual NB equal to 5071 NOK/year.

7.4.4 S3: Sensitivity to the Load Profile

As explained in section 5.1.1 deciding on the optimal cross-section of a line investment depend on the maximum power flow in the line. The decision-making is more comprehensive when finding the required battery size. As already explained, both the energy and power outputs have to be determined. From the 48-hours plots in figure 7.6, it could be seen that the battery was closest to a SOC level of 0.2 when the power demand over a longer period was high. Not only the power peaks in the system affect the dimensioning of the battery, but also the variety in the load has a significant impact on the required energy capacity. This factor, however, is indifferent to the line investment.

The load profiles have been adjusted without changing the maximum power demand to study this effect in more detail. Adjustments are made in two directions: a more stable load profile over time for S30 and a more fluctuating load profile for S31. Since the maximum power demand in the system is kept the same, the power output of the BESS will not change, nor will the cross-section of the line.

S30: Less Fluctuating Power Demand

This scenario looks at how a less fluctuating power demand affect the case. The hours from 432 to 480 were looked deeper into, and the load profiles at the cabins were adjusted so that the power demand becomes high during the entire day from 7 to 23, and the battery gets to charge the same amount as before during the nights. This way the battery has to deliver power to the system for 17 hours in a row at its maximum, being 8 hours longer than for A1, whereas the re-charging time remain unchanged. The updated energy capacity was determined as presented in section 5.1.2. The updated BESS operating results are given in table 7.12

The required energy capacity of the BESS has increased with 46.15%, to a storage value of 95kWh in order to cope with the voltage drops for the new power demand profile. Some of the operating characteristics from the analysis can be seen in figure 7.14. The model has been run for all the 720 hours of the month, but only a fragment of the operating hours, the same 48 hours used in section 7.3.4, have been plotted to get a better view of the details.

Figure 7.13a shows how the load profile has changed to being more stably high during daytime, while still considerably low during night time. The battery is deeply discharged during the days, obtaining a SOC close to 0.2 at the end of each day. From figure 7.13b it can be seen that the voltage profile without BESS now has a lower average value, almost laying at 0.9 pu. for all

Table 7.12: S30: Summary of BESS operating results

S30: Summary of BESS operation				
Installed power capacity	10	kW		
Installed energy capacity	95	kWh		
Compared to A1	*+30*	*kWh*	*+46.15*	*%*
Lowest state of charge level SOC^t	21.05	%		
Longest discharging period	17	hours		
Energy demand from BESS these hours	60.0	kWh		
C-rate	C/9.5			

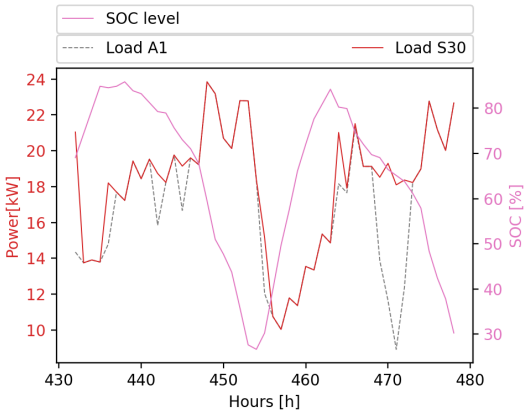

(a) SOC and the less fluctuating power demand

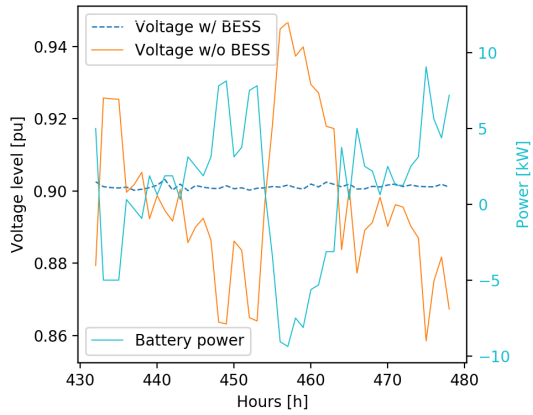

(b) Battery operation and voltage profiles

Figure 7.13: S30: System and BESS operation

the 48 hours. That outcome is caused by the battery having to charge at all hours possible, not letting the voltage level rise more than required. With a higher load demand, the voltage level without the BESS is also lower over a longer period, and consequently, the BESS has to discharge during that period.

The resultant cost increase caused by the upgraded energy storage capacity becomes equal to 30.46% compared to alternative 1, with an annual battery cost of 27'247 NOK/year. The net present value calculation has worsened to −15'444 NOK/year for the BESS installation. The rest of the economic results are presented in table 7.13. It is worth noticing how the break-even cost of the BESS has decreased significantly. With this energy capacity the costs of power and energy capacity have to be as low as 2'990 NOK/kW and 890 NOK/kWH respectivley,

Table 7.13: S30: Economic results

S30: Economic Results				
Annual investment costs of BESS	27'247	$\frac{NOK}{year}$		
Compared to A0	*+15'444*	$\frac{NOK}{year}$	*+ 130.85*	*%*
Compared to A1	*+6'361*	$\frac{NOK}{year}$	*+30.46*	*%*
Break even cost of power capacity	2'990	$\frac{NOK}{kW}$		
Compared to A1	*−910*	$\frac{NOK}{kW}$	*−23.35*	*%*
Break even cost of energy capacity	890	$\frac{NOK}{kWh}$		
Compared to A1	*−273*	$\frac{NOK}{kWh}$	*−23.35*	*%*

for the BESS to become an equally good economic option as the line investment. Looking at the mid-development cost curve from figure 2.3, this will not happen until 2050. From the low-development curve it may be realistic between 2025 and 2030.

S31: More Fluctuating Power Demand

By adjusting the power demand to a more fluctuating profile, while maintaining the peak power as 10 kW, a smaller energy capacity is needed. The load profile was adjusted arbitrary so that the maximum discharge period was decreased to 3 hours. As a results, the requirement for energy capacity of the BESS was reduced to 35 kWh, equal to a 46.15% reduction compared to the initial size of 65 kWh. The results from running the model are presented table 7.14. Extracts from the system and BESS operation are presented in figure 7.14.

Table 7.14: S31: Summary of BESS operating results

S31: Summary of BESS operation			
Installed power capacity	10	kW	
Installed energy capacity	35	kWh	
Compared to A1	*−30*	*kWh*	*−46.15* *%*
Lowest state of charge level SOC^t	23.21	%	
Longest discharging period	3	hours	
Energy demand from BESS these hours	14.7	kWh	
C-rate	C/3.5		

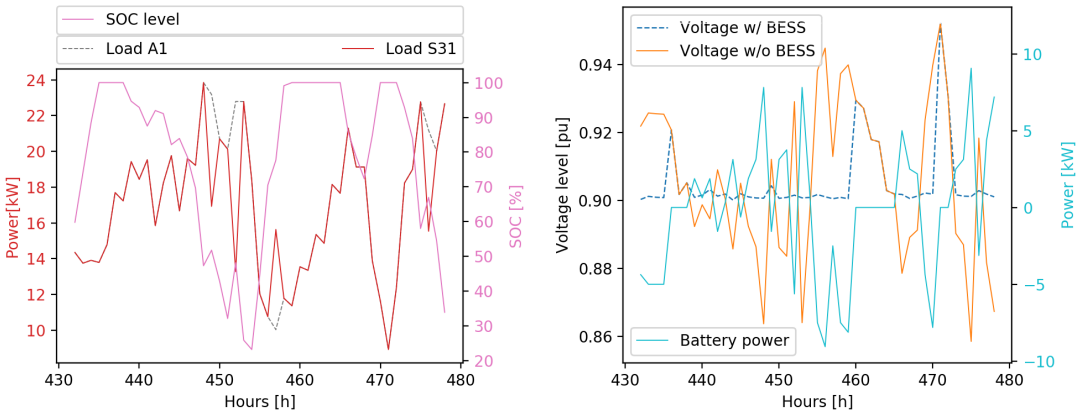

(a) SOC and the more fluctuating power demand (b) Battery operation and voltage profiles

Figure 7.14: S31: System and BESS operation

From figure 7.14a it can be seen that the power profile has become more fluctuating, providing more opportunities for the battery to charge. The maximum required discharge rate is still 9.06 kW, but the continually changing load profile, between high and low demand, decreases the need for storage capacity. As a result, the voltage profile and battery power profile also become less stable. Figure 7.14b shows how the voltage level has a higher average value over the operating hours.

The economic results are presented in table 7.15. The battery costs for this scenario are decreased by 30.46% to an annual cost of 14'525 NOK/year. An annual cost that is still not low enough to compete with the annual line costs, resulting in a net present value of −2'722 NOK/year. From the findings in section 7.4.1 an energy capacity reduction of 65.9%, to 22 kWh, was necessary for the line and BESS to break even with today's prices. For that to be realistic the BESS would need to operate even more as a peak-shaving asset for high power peaks occurring periodically, than as an asset for evening out the load demand during the day.

The costs for the BESS and the line to break even with an energy size of 35 kWh have increased to 5'610 NOK/kW for power capacity and 1'673 NOK/kWh for the energy capacity. These are values that may be realistic before 2025 following both the mid- and the low-development profiles from NREL, seen in figure 2.3.

The demonstration of S30 and S31 show how dependent the total BESS-costs are to the load profiles of the cabins. The case of S30 is almost twice as expensive as the case in S31, causing a load profile of stable high power demand over time to become a potential deal-breaker for a BESS grid-installation. The line investment remains unaffected and comes at the same costs for

Table 7.15: S31: Economic results

S31: Economic Results				
Annual investment costs of BESS	14'525	$\frac{NOK}{year}$		
Compared to A0	*+2'722*	$\frac{NOK}{year}$	*23.06*	*%*
Compared to A1	*−6'361*	$\frac{NOK}{year}$	*−30.46*	*%*
Compared to S30	*−12'722*	$\frac{NOK}{year}$	*−46.69*	*%*
Break even cost of power capacity	5'610	$\frac{NOK}{kW}$		
Compared to A1	*+1'710*	$\frac{NOK}{kW}$	*+43.80*	*%*
Break even cost of energy capacity	1'673	$\frac{NOK}{kWh}$		
Compared to A1	*+500*	$\frac{NOK}{kWh}$	*+43.80*	*%*

all scenarios, A1, S30 and S31.

7.4.5 S4: Sensitivity to the Length of Branch 1

One last effect that could affect the outcome of the study, both physical and economic, is the length of the line into the main distribution point in radial B, being branch 1 from figure 6.4. Since this exact grid topology used for this study will not be representative for all distribution grids, doing some changes to the system may give solutions that can be more relevant for other systems. In S2 and S3 only the BESS size was affected by the changes that were done. This analysis may also affect the dimensioning of the line as the voltage drop will be more significant when the line is longer, and the impedance in the line is bigger.

The original length of the line in branch 1 is 675 meters. Analyses have been performed for various line lengths between 500 and 900 meters. An overview of the results from the dimensioning of the line and the BESS, and some of the operating results are presented in table 7.16.

As expected, the minimum voltage level in the system drops as the line length increases. This can be seen both for the present situation voltage level, $V_{min,PS}$, and for the voltage level after an additional line has been installed, $V_{min,A0}$. For the 900-meters scenario a line with a larger cross-section, EX3x150mm^2 was needed to handle the voltage drops. As for the sizing of the BESS, a similar development as for the case with the increased load demand in section 7.4.3 can be found. Figure 7.15 shows graphically how the sizing of the BESS is dependent on the length of line.

In figure 7.15a the power and energy capacity requirements of the BESS are plotted as function

Table 7.16: S4: Operating results for different lengths of branch 1

Length [m]	$V_{min,PS}$	Line	$V_{min,A0}$	E_{batt} [kWh]	P_{batt} [kW]	$V_{min,A1}$
500	0.8904	EX3x95	0.9319	3	3	0.9001
550	0.8815	EX3x95	0.9279	20	6	0.9002
600	0.8725	EX3x95	0.9239	35	7	0.9000
675	0.8586	EX3x95	0.9178	65	10	0.9000
700	0.8538	EX3x95	0.9157	110	10	0.9000
750	0.8440	EX3x95	0.9116	255	11	0.9000
800	0.8340	EX3x95	0.9075	430	12	0.9000
900	0.8131	EX3x150	0.9113	725	14	0.9000

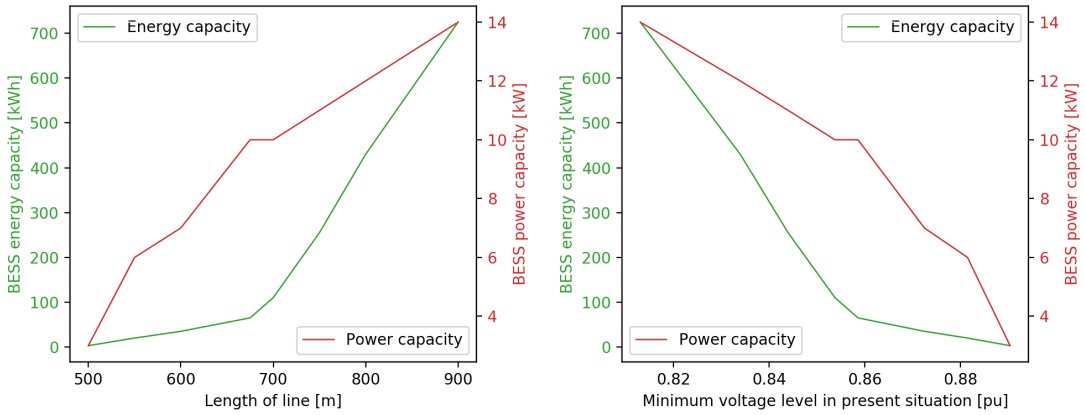

(a) Size as a function of line length

(b) Size as a function of voltage drop during PS

Figure 7.15: S4: BESS energy and power capacity with increasing line length

of the line length. The profile is similar to ones in the graphs presented in figure 7.11, showing the relation between the load increase in the system an the BESS size. The same conclusion can be made, that the energy capacity increases exponentially with the line length, while the power capacity is close to linear, with a tendency of flattening out. In figure 7.15b the BESS size is plotted as a function of the lowest system voltage for the present situation. This illustrates the importance of the voltage drop in the dimensioning process.

For all the eight scenarios presented, the voltage in the present situation and the load demand will have the same profiles as in the original system. The voltage profile will be shifted upwards or downwards along the y-axis as the line length decreases or increases. The load profile will remain the same. A downward shift in the voltage profile will lead to an increase in the amount

of operating hours with voltage exceedings. Two examples are illustrated in figure 7.16. Hence, is it not the low voltage level in itself that causes the increase in the energy capacity requirement of the BESS, but rather the increased duration with voltage exceedings.

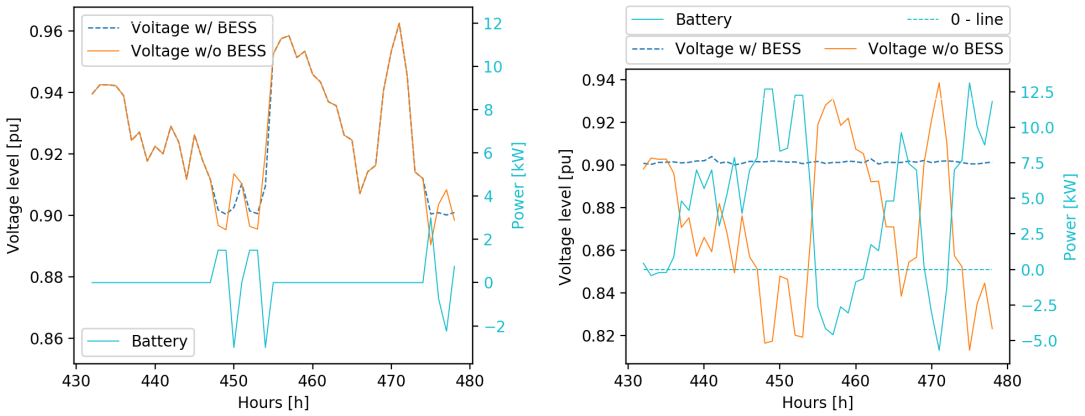

(a) Branch 1 = 500 meters

(b) Branch 1 = 900 meters

Figure 7.16: S4: Battery operation and voltage profiles

Figure 7.16a and 7.16b show the voltage profiles and the resulting battery operation profiles for the line length of 500 meters and 900 meters respectively. The orange voltage profiles showing the voltage levels without the BESS-installation are the same for both scenarios, only shifted along the Y-axis. Consequently, there are large differences in the operation of the BESS. While the BESS in figure 7.16a only has to operate for some peak-load hours, the BESS in figure 7.16b is operated for all the 48 hours plotted, where only 13 of them are used to charge the battery. With this type of load and voltage profile, the battery has to store a large amount of energy over time, to compensate for the low ability to re-charge during some peak-demand days.

Also, the cost development curves of this analysis are similar to those presented for the load-increase analysis in figure 7.12. Figure 7.17a shows the annual cost profile of the BESS and the line as a function of the line length of branch 1. The annual costs of the BESS are increasing dramatically as the energy capacity becomes much bigger. The line-costs are also increasing since a longer line is needed. The slope is however much less steep than the battery-cost curve. The break-even cost of the BESS relative to the line is plotted in figure 7.17b. All values above the blue stippled line, marking the price level today, are profitable solutions for the BESS. As such, line lengths shorter than approximately 580 meters and minimum voltage levels above 0.8780 pu. will return profitable solutions for the BESS.

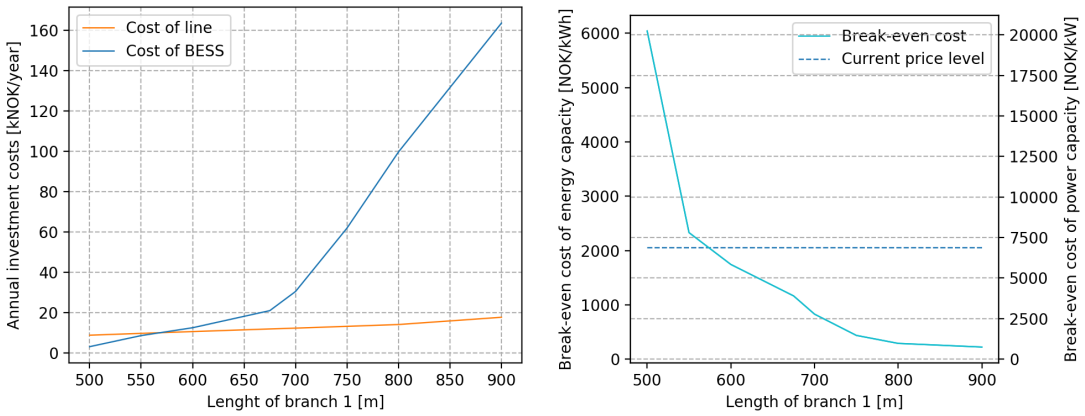

(a) Annual costs for BESS and new line

(b) Break-even cost for BESS

Figure 7.17: S4: Costs as a function of line-length

It should be noted that in this analysis, as well as for the analysis in S2, installing a smaller line than $95mm^2$ have not been studied. For the scenarios where the minimum voltage level is the highest, a smaller line might have been sufficient, causing lower line costs.

7.4.6 S5: Sensitivity to the C-rate

When looking at the importance of the combined power and energy capacity of the BESS, it can be interesting to conclude upon the C-rate for which the BESS is profitable. This section will investigate only the economic outcome of the study without running the model. The method of determining the BESS size used in the study will be dismissed so that the actual C-rate can be found without rounding up the energy capacity to the closest integer divisible by 5. From section 7.4.1 it was found that the cost of the BESS would break even with the line costs for a C-rate of C/2.2, with an energy capacity 2.2 times the power capacity of 10 kW. Based on the findings from the previous analyses, this section will check the economic outcome as a function of the C-rate for three different values of P_{batt} and their associated E_{batt}. For each of the three values of P_{batt}, different lines will be used as a reference, as it is more realistic that a lower P_{max} in the system also will result in smaller line.

The three power ratings chosen were 7 kW, 10 kW and 14 kW. The associated energy capacity for an example C-rate of C/2.5 will be 17.5 kWh, 25 kWh and 35 kWh respectively. The lines required at these power levels are EX3x50, EX3x95 and EX3x150, respectively. In figure 7.18 the annual costs have been plotted as a function of the C-rate.

It can be seen that a higher C-rate increase the likeliness of BESS being the most profitable

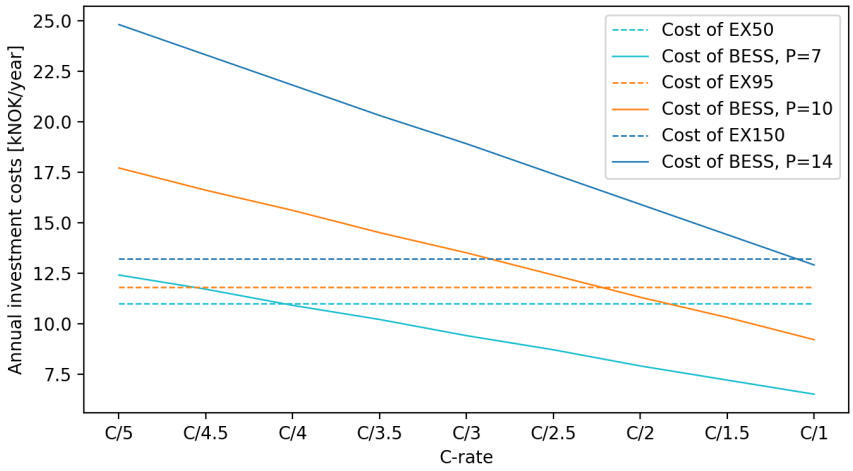

Figure 7.18: S5: The annual cost for various values of system peak power, as a function of the C-rate

solution. A lower required power rating also makes it possible to have a higher energy capacity before the BESS turn unprofitable. For the case where the P_{batt} is 7 kW, the C-rate may be as low as C/4, corresponding to an E_{batt} of 28 kWh, and the BESS is still the optimal solution. However, for the case with where the required power rating is 14 kW, only at a C-rate of 1, is the BESS profitable.

8 | Discussion

This chapter aims to discuss the findings from chapter 7. Since some results were analysed and compared in chapter 7, the primary purpose of this chapter will be to discuss the results in a broader perspective and draw conclusions from the overall study. It is divided into four sections, where the first two sections will discuss the main operational and economic findings, and look at the factors having the most significant impact. Furthermore, a discussion will be carried out to see if the battery can be a suitable solution despite the high investment costs. Finally, the methodology and the limitations of the thesis will be reviewed.

8.1 The Operational Findings

8.1.1 Technical Purposes

Both the alternatives were capable of delivering the required services to ensure that the voltage limit did not violate the critical limit of 0.9 pu. This was ensured by having a large enough cross-section for the line upgrade and a large enough power and energy rating for the BESS. Since the required sizes are determined by the needs of the system, and not what would lead to the lowest installation costs, it was expected that the technical purposes would hold. This has been the typical finding also from previous studies on BESSs in grid [9][12][15][17], and confirms the potential of the BESS being an as good technical solution as the line upgrade. Even if the two alternatives both provide the needed services in this case study, their operational differences are considerable and will be of interest in decision making. The main observed differences from the operational outcome are related to the voltage profile, the peak power consumption and the total energy demand.

8.1.2 Voltage Level

Sustaining the voltage quality in the system has been the main purpose for the alternatives in this study. After the line upgrade, the voltage profile was shifted up along the y-axis to a level above 0.9 pu. Whereas the voltage level when the BESS is operating is stable at around 0.9 pu., both during charging and discharging. As such, the average voltage level with the BESS is lower than with the line upgrade. The BESS-solution is therefore more volatile to changes in the system and can cause voltage drops of strong character. The dimensioning of the BESS will be the most crucial part to avoid such events.

If the power rating is not sufficient to handle some of the power peaks, the BESS will provide as much power as it can, and the voltage level may drop somewhat below 0.9 pu. A similar outcome would be the case if the line was under-dimensioned. Such events are indeed undesirable, but the consequences are not fatal. What will be of greater importance is the energy capacity of the BESS. If the BESS has been emptied before the most significant power peaks appear, suddenly no power can be withdrawn, and the voltage will drop to the present situation-level. The battery will be useless with insufficient storage capacity, whereas such a situation will not be the case for a line upgrade. This finding shows the importance of having a large enough energy capacity for the BESS to be able to perform its purpose.

To avoid these situations, the model can also be developed to prevent the most significant voltage drops. The rule of the algorithm can be changed to prioritise voltage drops that are larger than, for instance, 12% of nominal value, once the SOC level is below a specific limit. This way, the voltage will come below 0.9 pu., but the most substantial and damaging deviations can be avoided.

8.1.3 Energy demand

Due to losses in the BESS and more considerable losses in the old line compared to having two lines, the total energy demand is higher when using BESS than when upgrading the line. The losses were found to be almost twice as large for the BESS as for the line upgrade. Still, they accounted for less than 10% of the total costs and were neglected from the economic study. If the electricity price had been higher, the energy losses may have played a more significant role in the study, and would favour the line upgrade even more, especially with a stable high electricity price and small price variations. The energy losses are low for this situation, but for large-scale applications, the losses may be substantial. Independently of the cost of losses, energy losses are not desired, and the increased losses caused by the BESS should be weighed against the benefits the BESS provide when making a decision.

8.1.4 Peak Power Demand

The battery has proven to be better at reducing the power peaks in the system than the new line. The maximum power drawn from the grid was 12.5% lower when the BESS was operated compared to when the additional line was operated. However, in this study, no gratitude was given for that capability, neither technically nor economically. Since the substation in the case study is dimensioned to handle power flows more than five times as large as the maximum power drawn from the grid, limiting the power peaks was not a necessity. If, however, the substation also would have to be upgraded for the new line to handle the power demand, alternative 0 would cause an even more massive intervention, also making the cost calculation more favourable for the BESS. Besides, if the maximum power demand drawn from the grid were limited, the two radials would both have to be taken into account as also the power demand in radial A would impact the results. Another factor worth mentioning is the power pricing regime proposed by NVE [82]. The peak power tariffs are typically high in the morning and afternoon, when the battery discharges, and low when the battery is recharging. If peak power tariffs had been included in this study, the economic outcome would be more favourable for the battery installation.

8.2 The Economic Outcome

From the investment analysis, it was found that the annual net benefit of installing a BESS in the proposed cabin field is -9'082 NOK/year, equal to a cost that is 76.95% higher than the cost of the line upgrade. This result coincides with the results from previous research, many of which concludes on batteries not being profitable when providing only one service [6][10][12].

The break-even costs were found to be 3900 NOK/kW for power capacity and 1164 NOK/kWh for energy capacity. The costs have to fall with 43.49% compared to today's prices for these values to be achieved. Other studies that have investigated BESSs for voltage regulating purposes and grid planning find profitable solutions for varying costs of energy capacity. Fortenbacher et al. [9] find beneficial solutions for both centralised and distributed placements of BESS in LV grids with PV. The break-even costs for the two scenarios are 1000 NOK/kWh and 2300 NOK/kWh respectively. Böcker et al. [10] include both the cost of energy and power capacity in the study of BESS in congested grids. The BESS is found to be profitable for a variety of situations, with different line lengths and PV feed-in, for an energy cost of 2000 NOK/kWh and a power cost of 1000 NOK/kW. Some few operating conditions still find the BESS profitable when the prices increase to 5000 NOK/kWh and 1200 NOK/kW. The findings from this thesis can be seen not deviating too much from what other studies with similar use cases conclude. Also, this study has shown that the break-even cost is volatile to changes in the system topology and load profile, as will be further investigated in section 8.2.3.

The factors having the most significant impact on the total BESS costs in this study are the cost of energy and power capacity, and the overall size of the BESS. These factors will be discussed below, along with the different circumstances that will impact the sizing.

8.2.1 The Installation Costs

While the costs of installing new lines are well-known and precise for Norwegian conditions, the costs related to the BESS are estimations that in practice will vary greatly depending on the climate and nature where the BESS is to be installed. As such, large uncertainties are associated with what will become the actual investment costs of the BESS for a grid company in Norway. Another factor of interest related to the costs of the alternatives is that the costs of the BESS are linearly dependent on the power and energy ratings. The cost of the line includes many cost-factors such as engineering and construction costs that are more or less equal for all cross-sections. The material costs of the line account for less than 50% of the total costs. Consequently, doubling the cross-section areal will not cause the cost to double, as would be the case for the BESS. This way, the lower the required upgrade is, the more costly will the line be compared to the BESS.

8.2.2 The Size Determination

There are also more substantial uncertainties related to the sizing of the BESS compared to the line. The cross-section of the line and the power ratings of the BESS are dependent upon the maximum power flow in the line. Besides, the BESS requires a specific energy capacity to be able to perform its service, as discussed briefly in section 8.1.2. What factors are essential when determining the energy capacity of the BESS will be analysed further in section 8.2.3.

When neglecting the cost of losses and all the other operational costs in the system, the economic outcome of the two alternatives is only dependent upon the sizing. Large enough capacity is crucial for the technical purpose, at the same time as it is very costly. These conflicting wishes demonstrate the importance of proper planning to neither over- nor under-dimension the BESS.

8.2.3 The Impact From the Load Profile

As the maximum power demand will decide on the cross-section of the line and the power ratings of the BESS, deciding on the correct energy capacity for the BESS is more comprehensive. Interesting findings occurred when studying the sensitivity analyses S2, S3 and S4 concerning the sensitivity in the number of customers, the fluctuations in the power demand, and the length of the supply line. While the total energy demand in the system and the maximum power peak and voltage drop will impact the determination of the BESS's energy capacity, even more critical

is the impact from the load profile and for how many consecutive hours the power demand is high.

While the required power ratings of the BESS increase more or less linearly with the increase of customers or increasing line length, the required energy capacity follows an exponential development. These relationships could be seen in figure 7.11 and 7.15. Common for both of the analyses was that once the power demand become such that it requires for the BESS to supply power for many hours in a row, the required energy capacity exponentially increases. The sensitivity to the load profile was further investigated in S3, section 7.4.4, concluding that a more fluctuating power demand requires a lower battery energy capacity and thus also reduces the total costs.

The sensitivity analyses S2, S3 and S4 demonstrate how costly it is to store energy over time, and how the load increase will impact the energy capacity much more than the power capacity. From small load increases or increasing line length, the required energy capacity quickly escalates to being unaffordably large. In the report on BESSs in grid written by DNV-GL for NVE [5], they state that the BESS is usually a more profitable investment when used for large power ratings and low energy ratings. This conclusion can be verified from this case study as well. In the comparison of BESS and line upgrade for voltage regulating purposes, it comes as a considerable advantage in favour of the line investment that it is independent of the load profile and the overall energy demand in the system.

An investment planning process where a BESS installation is an alternative will indeed be more complex and resource consuming. It can be seen that only performing an estimation of the maximum power transfer in the system will not be sufficient when investigating BESSs for grid-purposes. It is essential with information about the load profile and to have access to time-dependent data. Conveniently, the imposed installation of AMS for all customers in Norway makes hourly data available for all grid companies.

Another outcome of the evident dependency on the load profile when sizing the BESS is that it causes even more substantial uncertainties in the total cost for the BESS, and makes it a less predictable solution. Due to the cabins having a more unpredictable power demand than for instance the load profile of an area with residential household, it can be argued that it might be necessary to install a larger BESS than the analysis gives as the minimum requirement. When it becomes clear how sensitive the size determination is to changes in the load profile, it can not be assured that the power profile will never be more demanding than what was the case in this scenario. At the same time, it is the uncertainty, the large fluctuations and low utilisation in such an area that may give the BESS increased possibilities. Investing in a new line would indeed be to over-dimension the line capacity into the cabin field, especially since the utilisation time for the line is this low, almost only overloaded during the Easter break.

Böcker et al. [10] found that a longer line and larger voltage drops would benefit the BESS installation over a line upgrade in a congested system with distributed PVs. Interestingly, the opposite conclusion can be drawn from this study. The longer the line, the higher are the voltage drops over time, and the larger is the required BESS investment compared to the line. This effect is enhanced as the line costs increase less steep than the BESS costs for the same increase in peak power. Consequently, it will be important to investigate the exact necessities for a system before drawing conclusions and making decisions, again showing the importance of sufficient data access.

8.2.4 The Optimal BESS C-Rate

A general conclusion upon a C-rate of which the battery will be profitable can not be made, looking at the results from S5 in section 7.4.6. However, the analysis verifies that situations, where a higher C-rate of the BESS is required, will be the best economically circumstances for profitable BESS results. The study also shows that the lower the required power rating is, the more beneficial will it be to invest in a BESS rather than a line. This relation is caused by a combination of the fact that high power ratings of the BESS are very expensive, three times the costs of energy capacity, and that the cost curve for the line costs is less steep. Another benefit of a higher C-rate is that the battery recharges from empty to fully charged in a shorter time.

8.2.5 The Placement of BESS and Line

The placement of the BESS and the line may also impact the economic outcome, as the wrong placement may lead to the need for a bigger size. For this specific case, the siting of the line and the BESS were quite prominent. Hence, not much time was spent on considering alternative sitings. For more complex grids, there will be more options, and these should be systematically reviewed. Pandzic et al. [6] propose a method for systematically determining the close-to-optimal placement for grid-installed BESSs. Also in smaller grids with residential PVs, placing the BESS BTM has been found to be more efficient and beneficial than the more central siting used in this study [9]. These possibilities should be explored for cases where PVs are installed.

8.3 Is the BESS Still an Option?

This section will discuss if the BESS can still be considered an option over the line upgrade, despite the poor economic outcome.

8.3.1 A Less Invasive Installation

The BESS may be installed more quickly and with a lower level of bureaucracy involved in the process. Upgrading the lines can be a long process, and often take many years from the first estimations to a line in full operation. In the area of the upgrade, a BESS may also reduce the impact on nature as it causes a smaller intervention. However, without going into an extensive analysis of which materials are the worst to extract from nature, lithium-ion batteries do not have the best reputation when it comes to ethical and environmental issues during the recovering of materials and manufacturing [83]. So even if installing a BESS causes a smaller intervention in Norwegian nature, the impact in other parts of the world should not be disregarded from the decision-making.

Another benefit of the BESS is that it is a less permanent installation. If the BESS is no longer needed were it is installed, it can easily be removed and used for another purpose. The line upgrade is permanent, and making such an investment is typically postponed until it is inevitable that it is needed. A BESS can be used as a temporary solution until the exact demand in an area has been determined. Flexible solutions that postpone permanent decision-making is a value in itself for the grid company.

8.3.2 Additional Services

While a line that is not in use can provide minimal additional purpose, the opportunities are extensive for the BESS. Combining the usage areas may give other economic benefits from the installation [3]. Such an outcome can come as a result of either increased profit from, for instance, market participation, or reduced costs from not having to invest in other equipment. In the area where the battery is installed, it may be used to provide reserve power in the area, to increase short circuit capacity in the system or to avoid over-voltages if PV systems are installed. Böcker et al. [10] found that BESSs are more economically beneficial compared to a line investment, the higher the level of excess PV feed-in in the system. If the battery is to participate in the market, the regulatory aspect of the study may be of greater importance as the grid company can not earn directly from market participation. Also, one could argue that with the decreasing prices in of batteries, they will become economically beneficial in the future, and for a grid company to be prepared, gaining knowledge through the installation of prototypes will be valuable.

8.4 Reviewing the Method and the Limitations

This section will evaluate the input parameters, the model construction and the simplifications made in the study.

8.4.1 Costs

A typical reason for upgrading the line, in addition to a load increase, is due to a significant probability of failure that may account for a large part of the costs when comparing alternatives. This study has neglected the inclusion of costs of energy not supplied (CENS). If the existing line could not be trusted to be used along with the new one, this would affect especially alternative 0. The costs would increase, as a bigger line would have to be installed as a replacement for the two $95mm^2$ lines. The impact on alternative 1 would depend on the estimated reliability of the BESS to provide sufficient capacity through a potential outage. With an energy capacity approximately three times as large as the maximum power demand in the system, for a worst-case scenario, the BESS could provide power for three hours.

Another cost that has not been included, and that often play an important part in other studies on BESS is the cost of battery degradation. Including the cost of battery degradation might be of greater importance if the goal of the study was to optimise the battery operation. A way to account for the degradation in this study can be to install a bigger battery, and exact degradation values are not considered as necessary. The master thesis written by F. Berglund [61] proposes a method for including battery degradation, and demonstrates the importance of including the cost when determining the optimal operation of the BESS.

8.4.2 Input Data

The load profile was put together based on the known AMS data from 8 cabins, to illustrate a grid with a load increase in the cabin field. It may not be very realistic that the profiles were just adjusted some hours, especially not in a cabin field were the load profiles are more unpredictable than for regular household profiles. This approach was used to see the effect of high power peaks more clearly, as this is more interesting for the study than overall high energy demand. Also, limited data access makes it more challenging to conclude upon how a typical load profile is in this area. Instead of adding additional load profiles to the system, high power demand could have been added for parts of the hours to symbolise the increased demand of for power from EVs and HPs. It may be more realistic to install a BESS in such a scenario than for the case with an increase in customers. With significant power peaks and less energy demand over time, the BESS has shown to result in a more positive economic outcome.

Since the exact power demand for the entire operating month was known before running the model, the optimal BESS could be determined for this exact profile. However, for an investment planning situation, it is the forecasted future load that is of the highest interest. With the BESS found to be so sensitive to changes in the load profile, more considerable uncertainty is associated with the size determination of the BESS, and a much larger margin would be needed if the BESS was to be dimensioned for future load profiles.

8.4.3 The Model Construction

The developed model is fast, which is an advantage as it is possible to expand the analysis without the concern of long computational time. The model is built such that it takes in one operating hour at a time, not knowing what will happen for the next hour. This type of operation is realistic in terms of being an operating strategy that could be used for the actual installation.

The main drawbacks of the proposed model are the manual steps. The system topology has to be known before the analysis for the algorithm to work correctly. For the model to work for other systems, adjustments to the code and input data must be made. Also, the determination of power and energy capacity has to be done manually.

8.4.4 Number of Installed Assets

It was assumed that the already existing line may still be used and that the grid reinforcement only involves adding one extra line to the grid. This assumption is realistic since the basis for installing the BESS is that the line can still be used. As such, this perspective would also hold for the grid reinforcement. At the same time, one can argue that because upgrading the line is a more permanent investment the grid company might as well replace the old line too. This decision would cause the line upgrade to become more expensive, and the net benefit of the BESS would increase.

Only the use of one BESS in the grid has been exploited. Since the system is small, this proved to be a valid assumption based on the operational results. For a more extensive network, it might have been necessary with more than one BESS. This alternative would complicate the model, as also a coordinated operation between the BESSs would be required to avoid over-dimensioning the BESSs.

9 | Conclusion

This thesis has investigated the economic and technical possibilities for the DSO to install a BESS in a low-voltage distribution grid with high peak power demand, as an alternative to grid reinforcement. The primary purpose of the BESS is to provide sufficient active power supply in the hours with large voltage drops, to keep the voltage level above the pre-set limit of 0.9 pu. A model has been developed in Python, including a power flow solution model using the BFS-method, and a battery model. The BESS is modelled to regulate the voltage level, and by using an optimal charge and discharge strategy, the model will limit the need for installed capacity. An investment planning analysis has been performed, comparing the alternative of investing in a BESS, with the more traditional alternative of completing a line upgrade. The case study has been carried out in a remote cabin field in southern Norway. The most important conclusions from the results and discussion are drawn below.

It was found that both alternatives are capable of providing the necessary service to maintain proper voltage quality in the system. For the BESS sizing this results in power capacity of 10 kW and energy capacity of 65 kWh. For the grid-reinforcement, an additional line of the type EX3x95 must be installed. The costs of installing a BESS to satisfy the operating requirements were found to be 76.95% higher than the corresponding line costs. For the BESS installation to break even with the line investment, a cost reduction of 43.49% from today's price level is necessary. The break-even power cost is thus 3900 NOK/kW and the break-even energy cost is equal to 1164 NOK/kWh. Looking at the cost projections from NREL, these costs levels may be realised within 2025 in an optimistic price-development scenario, or not at all by 2050 for a pessimistic scenario.

The impact from the BESSs energy and power ratings has been investigated in both a technical and economic perspective. For the operation of the system, it was found that having sufficient energy capacity is more crucial than adequate power capacity. Without enough energy stored in the BESS when it is needed, the battery will be useless in the given operating hour, letting the voltage drop to levels as low as they were before the installation. With lower power ratings than required, the voltage level may fall below 0.9 pu., but as long as there is energy

stored in the BESS, the voltage quality will still be improved relative to the present situation.

While finding the optimal size of the overhead line is dependent on the maximum power transfer, the sizing of the BESS is also dependant upon how much energy it must store during a period to maintain the voltage quality in the system. The results from this thesis have revealed how sensitive the determination of the required energy capacity of the BESS is to changes in the load profile. Even small variations of a few hours may cause significant differences in the required size, which again can change the economic outcome completely. These findings demonstrate how important it is to include the time-perspective when dimensioning the energy capacity of the BESS, and how crucial that determination is for the economic outcome. Such thorough analyses can only be done with sufficient data access. Overall, the process becomes more complicated with BESS as an alternative in investment planning.

For this specific system topology with the given load profile, the BESS does not prove as an economical alternative to the line upgrade. Both the required energy capacity and the power capacity of the BESS are too high in this particular case. A conclusion upon the optimal conditions where the BESS is the better solution can be drawn from the analyses of line length, the power profile, the number of loads in the system and by investigating the C-rate of the BESS. For all the scenarios, it was found that the lower the required energy capacity, the lower the required power capacity and the higher the C-rate, the better is the economic outcome of the BESS. Thus, in systems with few, not too high power peaks, occurring periodically, and preferably not more than 3 hours in a row, the prospects of BESS installations as an alternative to grid reinforcements are looking bright.

10 | Further Work

Some suggestions for further work on the topic are listed based on the shortcomings of the model and the explored expansion possibilities:

- Improve the model so that it can more easily be used for other grid topologies.
- Investigate the use of other assets and methods for mitigation of voltage irregularities. Examples are to include shunt or series compensation in the model or investigate the possibility to exploit consumer flexibility.
- Expand the model to also work for the integration of PVs in the system. This expansion would require the need to change the charging and discharging strategy of the BESS since it will not only be used to avoid voltage drops but also to mitigate over-voltages.
- Investigate the use of the BESS for other services than voltage regulations, to see how the technical and economic outcome changes.
- Determine if it is possible to make probabilistic models for how the load demand in an area is likely to be distributed. This thesis reveals how sensitive the outcome is to changes in the load profile, and having more information about an area will be of high value, especially since the dimensioning in a real situation is done for the future load development, and not for an exact load profile from the past.
- Determine how the computational time increases with increased model complexity.

Bibliography

[1] Olje-og energidepartementet, "Vi bygger Norge - om utbygging av strømnettet," *Melding til Stortinget*, vol. 14, 2012. [Online]. Available: https://www.regjeringen.no/no/dokumenter/meld-st-14-20112012/id673807/sec2

[2] ——, "Et bedre organisert strømnett," Oslo, Tech. Rep., 2014. [Online]. Available: https://www.regjeringen.no/globalassets/upload/oed/pdf_filer_2/rapport_et_bedre_organisert_stroemnett.pdf

[3] P. Ahcin, K. Berg, and I. Petersen, "Techno-economic analyis of battery storage for peak shaving and frequency containment reserve," in *2019 16th International Conference on the European Energy Market (EEM)*. IEEE, 9 2019, pp. 1–5. [Online]. Available: https://ieeexplore.ieee.org/document/8916380/

[4] J. Haas, F. Cebulla, K. Cao, W. Nowak, R. Palma-Behnke, C. Rahmann, and P. Mancarella, "Challenges and trends of energy storage expansion planning for flexibility provision in low-carbon power systems – a review," *Renewable and Sustainable Energy Reviews*, vol. 80, pp. 603–619, 2017. [Online]. Available: https://www.sciencedirect.com/science/article/pii/S1364032117308377

[5] DNV GL, "Batterier i distribusjonsnettet," NVE, Tech. Rep., 2018. [Online]. Available: http://publikasjoner.nve.no/rapport/2018/rapport2018_02.pdf

[6] H. Pandzic, Y. Wang, T. Qiu, Y. Dvorkin, and D. S. Kirschen, "Near-Optimal Method for Siting and Sizing of Distributed Storage in a Transmission Network," *IEEE Transactions on Power Systems*, vol. 30, no. 5, pp. 2288–2300, 2015. [Online]. Available: https://ieeexplore.ieee.org/abstract/document/6936940

[7] Y. J. A. Zhang, C. Zhao, W. Tang, and S. H. Low, "Profit-maximizing planning and control of battery energy storage systems for primary frequency control," *IEEE Transactions on Smart Grid*, vol. 9, no. 2, pp. 712–723, 2018. [Online]. Available: https://ieeexplore.ieee.org/document/7464879

[8] Y. Yang, H. Li, A. Aichhorn, J. Zheng, and M. Greenleaf, "Sizing strategy of distributed battery storage system with high penetration of photovoltaic for voltage regulation and peak load shaving," *IEEE Transactions on Smart Grid*, vol. 5, no. 2, pp. 982–991, 3 2014. [Online]. Available: https://ieeexplore.ieee.org/document/6609116

[9] P. Fortenbacher, M. Zellner, and G. Andersson, "Optimal sizing and placement of distributed storage in low voltage networks," in *19th Power Systems Computation Conference, PSCC 2016*. Institute of Electrical and Electronics Engineers Inc., 8 2016. [Online]. Available: https://ieeexplore.ieee.org/abstract/document/7540850

[10] B. Böcker, S. Kippelt, C. Weber, and C. Rehtanz, "Storage valuation in congested grids," *IEEE Transactions on Smart Grid*, vol. 9, no. 6, pp. 6742–6751, 2018. [Online]. Available: https://ieeexplore.ieee.org/document/7964735

[11] J. A. Aguado, S. de la Torre, and A. Triviño, "Battery energy storage systems in transmission network expansion planning," *Electric Power Systems Research*, vol. 145, pp. 63–72, 2017. [Online]. Available: https://www.sciencedirect.com/science/article/pii/S0378779616304874

[12] L. Wang, D. H. Liang, A. F. Crossland, P. C. Taylor, D. Jones, and N. S. Wade, "Coordination of Multiple Energy Storage Units in a Low-Voltage Distribution Network," *IEEE Transactions on Smart Grid*, vol. 6, no. 6, pp. 2906–2918, 2015. [Online]. Available: https://ieeexplore.ieee.org/document/7172552

[13] P. Fortenbacher, A. Ulbig, and G. Andersson, "Optimal Placement and Sizing of Distributed Battery Storage in Low Voltage Grids Using Receding Horizon Control Strategies," *IEEE Transactions on Power Systems*, vol. 33, no. 3, pp. 2383–2394, 2018.

[14] I. Ranaweera and O. M. Midtgård, "Optimization of operational cost for a grid-supporting PV system with battery storage," *Renewable Energy*, vol. 88, pp. 262–272, 2016. [Online]. Available: https://www.sciencedirect.com/science/article/pii/S0960148115304651

[15] M. A. Kashem and G. Ledwich, "Energy requirement for distributed energy resources with battery energy storage for voltage support in three-phase distribution lines," *Electric Power Systems Research*, vol. 77, no. 1, pp. 10–23, 2007. [Online]. Available: https://www.sciencedirect.com/science/article/pii/S0378779606000150

[16] M. J. Alam, K. M. Muttaqi, and D. Sutanto, "Distributed energy storage for mitigation of voltage-rise impact caused by rooftop solar PV," *IEEE Power and Energy Society General Meeting*, pp. 1–8, 2012. [Online]. Available: https://ieeexplore.ieee.org/document/6345726

[17] M. N. Kabir, Y. Mishra, G. Ledwich, Z. Y. Dong, and K. P. Wong, "Coordinated control of grid-connected photovoltaic reactive power and battery energy storage systems

to improve the voltage profile of a residential distribution feeder," *IEEE Transactions on Industrial Informatics*, vol. 10, no. 2, pp. 967–977, 2014. [Online]. Available: https://ieeexplore.ieee.org/abstract/document/6708466

[18] D. Shirmohammadi, H. W. Hong, A. Semlyen, and G. X. Luo, "A compensation-based power flow method for weakly meshed distribution and transmission networks," *IEEE Transactions on Power Systems*, vol. 3, no. 2, pp. 753–762, 1988. [Online]. Available: https://ieeexplore.ieee.org/document/192932

[19] Y. Zhu and K. Tomsovic, "Adaptive power flow method for distribution systems with dispersed generation," *IEEE Transactions on Power Delivery*, vol. 17, no. 3, pp. 822–827, 2002. [Online]. Available: https://ieeexplore.ieee.org/abstract/document/1022810

[20] M. H. Haque, "Load flow solution of distribution systems with voltage dependent load models," *Electric Power Systems Research*, vol. 36, no. 3, pp. 151–156, 1996. [Online]. Available: https://www.sciencedirect.com/science/article/pii/0378779695010254

[21] A. Augugliaro, L. Dusonchet, S. Favuzza, M. G. Ippolito, and E. R. Sanseverino, "A backward sweep method for power flow solution in distribution networks," *International Journal of Electrical Power and Energy Systems*, vol. 32, no. 4, pp. 271–280, 2010. [Online]. Available: https://www.sciencedirect.com/science/article/pii/S0142061509001495

[22] C. S. Cheng and D. Shirmohammadi, "A three-phase power flow method for real-time distribution system analysis," *IEEE Transactions on Power Systems*, vol. 10, no. 2, pp. 671–679, 1995. [Online]. Available: https://ieeexplore.ieee.org/document/387902

[23] L. Zhang, W. Tang, and H. Guan, "The back/forward sweep-based power flow method for distribution networks with DGs," in *PEITS 2009 - 2009 2nd Conference on Power Electronics and Intelligent Transportation System*, vol. 1, 2009, pp. 145–149. [Online]. Available: https://ieeexplore.ieee.org/abstract/document/5407048

[24] G. Diaz, J. Gomez-Aleixandre, and J. Coto, "Direct Backward/Forward Sweep Algorithm for Solving Load Power Flows in AC Droop-Regulated Microgrids," *IEEE Transactions on Smart Grid*, vol. 7, no. 5, pp. 2208–2217, 9 2016. [Online]. Available: https://ieeexplore.ieee.org/document/7283640

[25] M. R. Brubæk, "Optimal Integration of Battery Energy Storage System in Weak Distribution Grid," *Unpublished work*, 2019.

[26] Energifakta-Norge, "The Electricity Grid," p. 2019. [Online]. Available: https://energifaktanorge.no/en/norsk-energiforsyning/kraftnett/

[27] Norwegian Water Resources and Energy Directorate (NVE), "Network regulation," 2019. [Online]. Available: https://www.nve.no/norwegian-energy-regulatory-authority/network-regulation/

[28] I. Wangensteen, *Power System Economics - the Nordic Electricity Market*, 2nd ed. Fagbokforlaget, 2011.

[29] Lovdata, "Lov om produksjon, omforming, overføring, omsetning, fordeling og bruk av energi m.m. (energiloven)," 2019. [Online]. Available: https://lovdata.no/dokument/NL/lov/1990-06-29-50#KAPITTEL_1

[30] Norwegian Water Resources and Energy Directorate (NVE), "Om RME," 2019. [Online]. Available: https://www.nve.no/reguleringsmyndigheten/om-rme/

[31] ——, "Spenningskvalitet," 2020. [Online]. Available: https://www.nve.no/reguleringsmyndigheten/nettjenester/leveringskvalitet/spenningskvalitet/

[32] Lovdata, "Forskrift om leveringskvalitet i kraftsystemet," pp. 1–4, 2004. [Online]. Available: https://lovdata.no/dokument/SF/forskrift/2004-11-30-1557/KAPITTEL_1#\T1\textsection1-4

[33] K. A. Rosvold, "Spenningskvalitet," 2019. [Online]. Available: https://snl.no/spenningskvalitet

[34] Norwegian Water Resources and Energy Directorate (NVE), "Leveringspålitelighet," 2020. [Online]. Available: https://www.nve.no/reguleringsmyndigheten/nettjenester/leveringskvalitet/leveringspalitelighet/

[35] B. Wasowicz, S. Koopmann, T. Dederichs, A. Schnettler, and U. Spaetling, "Evaluating regulatory and market frameworks for energy storage deployment in electricity grids with high renewable energy penetration," in *9th International Conference on the European Energy Market, EEM 12*, 2012. [Online]. Available: https://ieeexplore.ieee.org/document/6254811

[36] K. Hartwig and I. Kockar, "Impact of Strategic Behavior and Ownership of Energy Storage on Provision of Flexibility," *IEEE Transactions on Sustainable Energy*, vol. 7, no. 2, pp. 744–754, 4 2016. [Online]. Available: https://ieeexplore.ieee.org/document/7360228

[37] EnergiNorge, "Nettstruktur og organisering," 2020. [Online]. Available: https://www.energinorge.no/fagomrader/stromnett/kraftsystemet/nettstruktur-og-organisering/

[38] Norwegian Water Resources and Energy Directorate (NVE), "Utforming av overføringsnettet i Norge," 2019.

[39] R. A. Nordeng, J. Tjersland, L. E. Eilifsen, H. S. Fadum, T. N. Gange, and K. Ness, "Driften av kraftsystemet 2018," Tech. Rep. 27, 2019. [Online]. Available: https://www.nve.no/nytt-fra-nve/nyheter-energi/arlige-rapporter-om-kraftsystemet/

[40] Energi Norge, "Nett: Optimal håndtering av utfordringer i lavspenningsnett," 2019. [Online]. Available: https://www.energinorge.no/forskning/forskningsprosjekter/nett/optinett/

[41] Norwegian Water Resources and Energy Directorate (NVE), "Forklaring på noen begreper brukt innen spenningskvalitet," p. 4, 2019. [Online]. Available: https://www.nve.no/Media/3121/definisjoner-spenningskvalitet_v2.pdf

[42] G. M. Masters, "Transmission and Distribution," in *Renewable and Efficient Electric Power Systems*, 2nd ed. John Wiley & Sons, 2013, ch. 3.7, pp. 148–157.

[43] H. Saadat, "Power Flow Analysis," in *Power System Analysis*, 3rd ed. PSA Publishing, 2010, ch. 6, pp. 228–295.

[44] K. Sand, "Supply voltage variations," in *Course Slides ELK-10: Quality of supply in electrical power systems*. NTNU, 2018.

[45] D. Mondal and A. Sengupta, "Shunt Compensation," 2014. [Online]. Available: https://www.sciencedirect.com/topics/engineering/shunt-compensation

[46] A. K. Singh and B. C. Pal, "Flexible AC Transmission Systems," 2019. [Online]. Available: https://www.sciencedirect.com/topics/engineering/flexible-ac-transmission-systems

[47] IRENA, "Battery Storage for Renewables : Market Status and Technology Outlook," *Irena*, no. January, p. 60, 2015. [Online]. Available: https://www.irena.org/publications/2015/Jan/Battery-Storage-for-Renewables-Market-Status-and-Technology-Outlook

[48] ——, *Enabling Technologies*. International Renewable Energy Agency, 2019. [Online]. Available: https://www.irena.org/-/media/Files/IRENA/Agency/Publication/2019/Sep/IRENA_Enabling-Technologies_Collection_2019.pdf

[49] H. Ibrahim, A. Ilinca, and J. Perron, "Energy storage systems-Characteristics and comparisons," *Renewable and Sustainable Energy Reviews*, vol. 12, no. 5, pp. 1221–1250, 2008. [Online]. Available: https://www.sciencedirect.com/science/article/pii/S1364032107000238

[50] D. Wu, C. Jin, P. Balducci, and M. Kintner-Meyer, "An energy storage assessment: Using optimal control strategies to capture multiple services," in *2015 IEEE Power and Energy Society General Meeting*, Denver, 2015. [Online]. Available: https://ieeexplore.ieee.org/document/7285820

[51] B. Xu, A. Oudalov, A. Ulbig, G. Andersson, and D. S. Kirschen, "Modeling of lithium-ion battery degradation for cell life assessment," *IEEE Transactions on Smart Grid*, vol. 9, no. 2, pp. 1131–1140, 2018. [Online]. Available: https://ieeexplore.ieee.org/document/7488267

[52] Y. Yang, S. Bremner, C. Menictas, and M. Kay, "Battery energy storage system size determination in renewable energy systems: A review," *Renewable and Sustainable Energy Reviews*, vol. 91, pp. 109–125, 2018. [Online]. Available: https://www.sciencedirect.com/science/article/pii/S1364032118301436

[53] J. Hole and H. Horne, "Batterier vil bli en del av kraftsystemet," *NVE FAKTA*, no. 14, pp. 1–4, 2019. [Online]. Available: http://publikasjoner.nve.no/faktaark/2019/faktaark2019_14.pdf

[54] IRENA, *Electricity storage and renewables: Costs and markets to 2030*, 2017, no. October. [Online]. Available: http://irena.org/publications/2017/Oct/Electricity-storage-and-renewables-costs-and-markets

[55] W. Cole and A. W. Frazier, "Cost Projections for Utility- Scale Battery Storage," National Renewable Energy Laboratory (NREL), Golden, CO, Tech. Rep., 2019. [Online]. Available: https://www.nrel.gov/docs/fy19osti/73222.pdf

[56] Norges Bank, "Valutakurser," 2020. [Online]. Available: https://www.norges-bank.no/tema/Statistikk/Valutakurser/

[57] M. R. Aghamohammadi and H. Abdolahinia, "A new approach for optimal sizing of battery energy storage system for primary frequency control of islanded Microgrid," *International Journal of Electrical Power and Energy Systems*, vol. 54, pp. 325–333, 2014. [Online]. Available: https://www.sciencedirect.com/science/article/pii/S0142061513003025

[58] H. B. Kvandal, K. Sagen, and E. Solvang, "Prosjektnotat Kartlegging av alternativer til nettforsterkning," *Unpublished work from Sintef Energi*, pp. 1–33, 2019.

[59] A. Malhotra, B. Battke, M. Beuse, A. Stephan, and T. Schmidt, "Use cases for stationary battery technologies: A review of the literature and existing projects," *Renewable and Sustainable Energy Reviews*, vol. 56, pp. 705–721, 2016. [Online]. Available: https://www.sciencedirect.com/science/article/pii/S1364032115013520

[60] A. Nottrott, J. Kleissl, and B. Washom, "Energy dispatch schedule optimization and cost benefit analysis for grid-connected, photovoltaic-battery storage systems," *Renewable Energy*, vol. 55, pp. 230–240, 2013. [Online]. Available: https://www.sciencedirect.com/science/article/pii/S0960148112008026

[61] F. Berglund, "Optimal Operation of Battery Storage for Peak Shaving Applications," no. June, 2018. [Online]. Available: https://ntnuopen.ntnu.no/ntnu-xmlui/handle/11250/2566723?locale-attribute=en

[62] H. Dagdougui, N. Mary, A. Beraud-Sudreau, and L. Dessaint, "Power management strategy for sizing battery system for peak load limiting in a university campus," *2016 4th IEEE International Conference on Smart Energy Grid Engineering, SEGE 2016*, pp. 308–312, 2016. [Online]. Available: https://ieeexplore.ieee.org/abstract/document/7589542

[63] V. V. Vadlamudi, "Load Flow Studies," in *Compendium - Infrastructure for Energy Transmission and Distribution*. Trondheim: Department of Electric Power Engineering, NTNU, 2016, ch. 8, pp. 130–145.

[64] Lovdata, "Forskrift om energiutredninger," 2012. [Online]. Available: https://lovdata.no/dokument/SF/forskrift/2012-12-07-1158#KAPITTEL_3

[65] SINTEF Energi AS, "Systematikk ved planlegging av kraftnett," in *Planleggingsbok for kraftnett*. SINTEF, 2010, pp. 1–8.

[66] H. Falaghi, C. Singh, M. R. Haghifam, and M. Ramezani, "DG integrated multistage distribution system expansion planning," *International Journal of Electrical Power and Energy Systems*, vol. 33, no. 8, pp. 1489–1497, 2011. [Online]. Available: https://www.sciencedirect.com/science/article/pii/S0142061511001402

[67] S. Lumbreras and A. Ramos, "The new challenges to transmission expansion planning. Survey of recent practice and literature review," *Electric Power Systems Research*, vol. 134, pp. 19–29, 2016. [Online]. Available: https://www.sciencedirect.com/science/article/pii/S0378779615003090

[68] Direktoratet for økonomistyring, *Veileder i samfunnsøkonomiske analyser*. Fagbokforlaget, 2014.

[69] SINTEF Energi AS, "Tapskostnader," in *Planleggingsbok for kraftnett*. SINTEF, 2014, pp. 1–29.

[70] E. Bompard, E. Carpaneto, G. Chicco, and R. Napoli, "Convergence of the backward/forward sweep method for the load-flow analysis of radial distribution systems," *International Journal of Electrical Power and Energy Systems*, vol. 22, no. 7, pp. 521–530, 2000. [Online]. Available: https://www.sciencedirect.com/science/article/abs/pii/S0142061500000090

[71] G. M. Masters, "Power Factor," in *Renewable and Efficient Electric Power Systems*, 2nd ed. John Wiley & Sons, 2013, ch. 3.5, pp. 125–143.

[72] J. W. Nilsson and S. A. Riedel, "Instantaneous Power," in *Electric Circuits*. Pearson Education, 2015, ch. 10.1, pp. 382–387.

[73] A. Dukpa, B. Venkatesh, and M. El-Hawary, "Application of continuation power flow method in radial distribution systems," *Electric Power Systems Research*, vol. 79, no. 11, pp. 1503–1510, 2009. [Online]. Available: https://www.sciencedirect.com/science/article/pii/S0378779609001242

[74] J. H. Teng, "A direct approach for distribution system load flow solutions," *IEEE Transactions on Power Delivery*, vol. 18, no. 3, pp. 882–887, 2003. [Online]. Available: https://ieeexplore.ieee.org/document/1208371?arnumber=1208371

[75] J. A. Martinez and J. Mahseredjian, "Load flow calculations in distribution systems with distributed resources. A review," in *IEEE Power and Energy Society General Meeting*. Detroit: IEEE, 2011, pp. 1–8. [Online]. Available: https://ieeexplore.ieee.org/abstract/document/6039172

[76] J. W. Nilsson and S. A. Riedel, "Power Calculations," in *Electric Circuits*, 10th ed. Pearson Education, 2015, ch. 10.5, pp. 391–394.

[77] ——, "Kirchhoff's Laws," in *Electric Circuits*, 10th ed. Pearson Education, 2015, ch. 2.4, pp. 59 – 61.

[78] Nordpool, "Day-ahead prices," 2019. [Online]. Available: https://www.nordpoolgroup.com/Market-data1/Dayahead/Area-Prices/NO/Monthly/?view=table

[79] M. Buvik, J. Hole, A. M. Østenby, V. Koestler, O. K. Isachsen, and T. B. Ericson, "Kostnader for kraftproduksjon 2018," *Teknologianalyser 2019*, no. 7, pp. 1–2, 2019. [Online]. Available: http://publikasjoner.nve.no/faktaark/2019/faktaark2019_07.pdf

[80] SINTEF Energi AS, "Kostnadskatalog distribusjonsnett," in *Planleggingsbok for kraftnett*, 9th ed. SINTEF, 2016, pp. 1–24.

[81] Tesla, "Powerwall," 2019. [Online]. Available: https://www.tesla.com/sites/default/files/pdfs/powerwall/Powerwall2_AC_Datasheet_en_northamerica.pdf

[82] A. Bjelland Eriksen, H. Hansen, J. Hole, T. Jonassen, V. Mook, S. Steinnes, and L. Varden, *Endringer i nettleiestrukturen*. NVE, 2020. [Online]. Available: http://publikasjoner.nve.no/rme_hoeringsdokument/2020/rme_hoeringsdokument2020_01.pdf

[83] Amnesty International, "Amnesty challenges industry leaders to clean up their batteries," 2019. [Online]. Available: https://www.amnesty.org/en/latest/news/2019/03/amnesty-challenges-industry-leaders-to-clean-up-their-batteries/

[84] H. H. Faanes, G. Doorman, M. Korpås, and M. N. Hjelmeland, "Economic Project Analysis," in *Compendium - Energy Systems Planning and Operation.* Trondheim: Department of Electric Power Engineering, NTNU, 2016, ch. 3.5, pp. 86–94.

[85] W. Kenton, "Net Present Value (NPV)," 2019. [Online]. Available: https://www.investopedia.com/terms/n/npv.asp

[86] R. A. Adams and C. Essex, "Continuity," in *Calculus 1*, 8th ed. Pearson Education, 2013, ch. 1.4, pp. 79–87.

A | Economic Factors

A.1 Net Benefit (NB) and Net Present Value (NPV)

The net benefit (NB) of a project is the Net Present Value (NPV) of all costs and benefits related to the project, compared with the reference alternative [84].

The net present value is used to analyse the profitability of a projected investment or project. By calculating the NPV of different investment alternatives, they can all be compared in today's value of money. NPV is given as [85]:

$$NPV = \sum_{n}^{N} \frac{R_n}{(1+d)^n} \tag{A.1}$$

where

R_t is the net cash inflow minus outflow during a single period, t, [NOK]
d is the discount rate [-]
n is the time period [year]
N is the total number of time periods

In general the NPV is positive if the project is viable. However in some cases for investment planning purposes, the basis scenario is not to do nothing, but it may be that some kind of upgrading has to be done, regardless of economic viability. The alternative to be chosen is thus the one with the lowest total costs, or highest NPV.

The NPV of a project is, as the name indicates, the total costs seen with today's value of money. The net benefit can be given as both the total net benefit, equal to the NPV, or as the annual net benefit (nb), where total costs are annualised by using the annuity factor, defined in equation (A.5). This is the method used in this thesis.

A.2 Discount, Capitalisation and Annuity Factors

The discount factor, $\alpha_{n,d}$ is used to calculate the present value of a future cost or income given n years from now at the specified discount rate,d. It is defined as:

$$\alpha_{n,d} = \frac{1}{(1+d)^n} \tag{A.2}$$

so that the present value of a future cost can be found by:

$$PV = \alpha_{n,d} \cdot FV \tag{A.3}$$

where PV is the present value and FV is the future value.

If a payment is to be received annually for N number of years, the summarised value today can be expressed as the payment times the sum of a geometric series with N elements, which is equal to the capitalisation factor:

$$\lambda_{n,d} = \sum_{n=1}^{N} \frac{1}{(1+d)^n} = \frac{1-(1+d)^{-n}}{d} \tag{A.4}$$

The opposite can be obtained if the annual cost of an investment is to be determined. How big the annual payments are for a given investment cost in year one, can be found by multiplying the initial cost with the annuity factor, $\epsilon_{n,d}$. This factor is the inverse of the capitalisation factor and can be found as:

$$\epsilon_{n,d} = \frac{1}{\lambda_{n,d}} = \frac{1}{\sum_{n=1}^{N} \frac{1}{(1+d)^n}} = \frac{d}{1-(1+d)^{-n}} \tag{A.5}$$

B | Mathematical Methods

B.1 The Bisection Method

The bisection method is an iterative procedure for finding the root of a function f. Meaning that the $f(x) = 0$ is found. The method is built on *the intermediate-value theorem* given as [86]:

> If $f(x)$ is continuous on the interval $[a, b]$ and if s is a number between $f(a)$ and $f(b)$, then there exists a number $c \in [a, b]$ such that $f(c) = s$.

If $s = 0$, c will be the root of the function f. This is the case demonstrated in figure B.1. When finding the root, $s = 0$, the following statement has to hold:

$$f(a) \cdot f(b) < 0$$

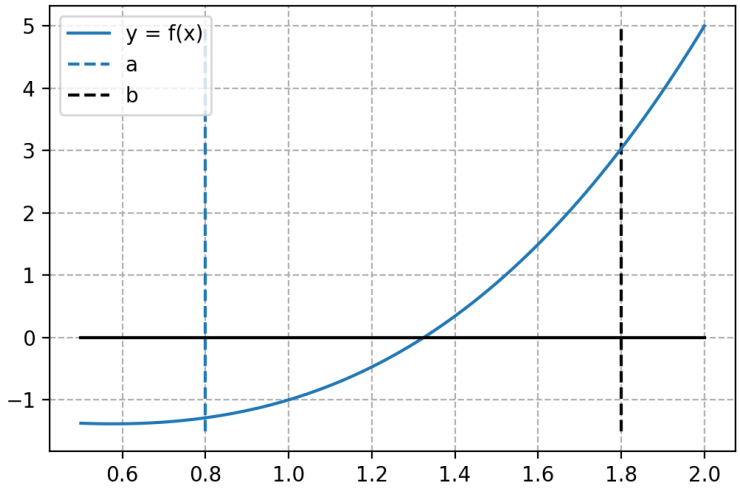

Figure B.1: The continuous function f takes on the value 0 at some point c between a and b

When finding the root with the bisection method, the root c will be an approximation of the actual root. How far away from the solution it is, depends on the value of the tolerance, ϵ set for the algorithm. The steps for solving the bisection method are as follows:

- **Step 1:** For a continuous function $f(x)$, two values a and b are chosen so that $f(a) > 0$ and $f(b) < 0$ or vice versa. The value c is set to be equal either a or b.
- **Step 2:** If the $f(c) = 0$ the root is found.
- **Step 3:** If the $f(c) \leq \epsilon$, c is close enough to the root.
- **Step 4:** If neither of step 2 or 3 are true, the arithmetic mean between a and b is found:

$$c = \frac{a+b}{2} \tag{B.1}$$

  and step 2 og 3 are repeated.

- **Step 5:** If step 2 or 3 are still not true, the sign $f(c)$ is checked, so that either of the following two steps are performed.
- **Step 6:** If $f(c) > 0$, the value of a is replaced by the value of c, while b keeps the same value.
- **Step 7:** If $f(c) < 0$, the value of b is replaced by the value of c, while a keeps the same value.
- Step 4 - 7 are repeated until either step 2 or 3 holds true.

C | System Information

C.1 Overview of operating hours and their corresponding dates

Table C.1: Overview of dates according to which hours

Dates	Simulation hours	Note
Monday 1^{st} of April	0 – 23	
Tuesday 2^{nd} of April	24 – 47	
Wednesday 3^{rd} of April	48 – 71	
Thursday 4^{th} of April	72 – 95	
Friday 5^{th} of April	96 – 119	
Saturday 6^{th} of April	120 – 143	
Sunday 7^{th} of April	144 – 167	
Monday 8^{th} of April	168 – 191	
Tuesday 9^{th} of April	192 – 215	
Wednesday 10^{th} of April	216 – 239	
Thursday 11^{th} of April	240 – 263	
Friday 12^{th} of April	264 – 287	Start Easter
Saturday 13^{th} of April	288 – 311	
Sunday 14^{th} of April	312 – 335	Palm Sunday
Monday 15^{th} of April	336 – 359	
Tuesday 16^{th} of April	360 – 383	
Wednesday 17^{th} of April	384 – 407	
Thursday 18^{th} of April	408 – 431	Holy Thursday
Friday 19^{th} of April	432 – 455	Good Friday
Saturday 20^{th} of April	456 – 479	
Sunday 21^{st} of April	480 – 503	
Monday 22^{nd} of April	504 – 527	
Tuesday 23^{rd} of April	528 – 551	
Wednesday 24^{th} of April	552 – 575	
Thursday 25^{th} of April	576 – 599	
Friday 26^{th} of April	600 – 623	
Saturday 27^{th} of April	624 – 647	
Sunday 28^{th} of April	648 – 672	
Monday 29^{th} of April	672 – 695	
Tuesday 30^{th} of April	696 – 719	

D | Additional Results

D.1 Voltage Profiles at all Buses

D.1.1 A0: Voltages With New Line

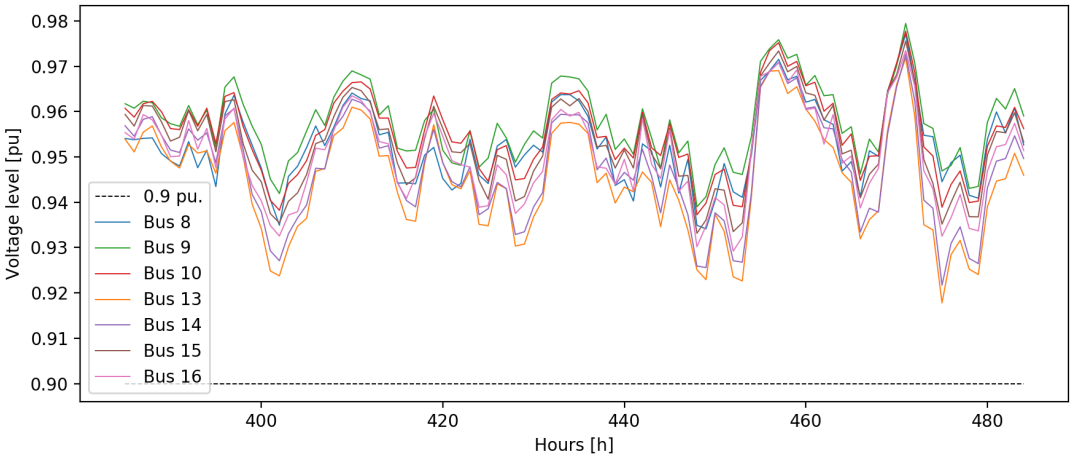

Figure D.1: A0: The voltage profiles of the seven load buses in radial B

D.1.2 A1: Voltages With BESS

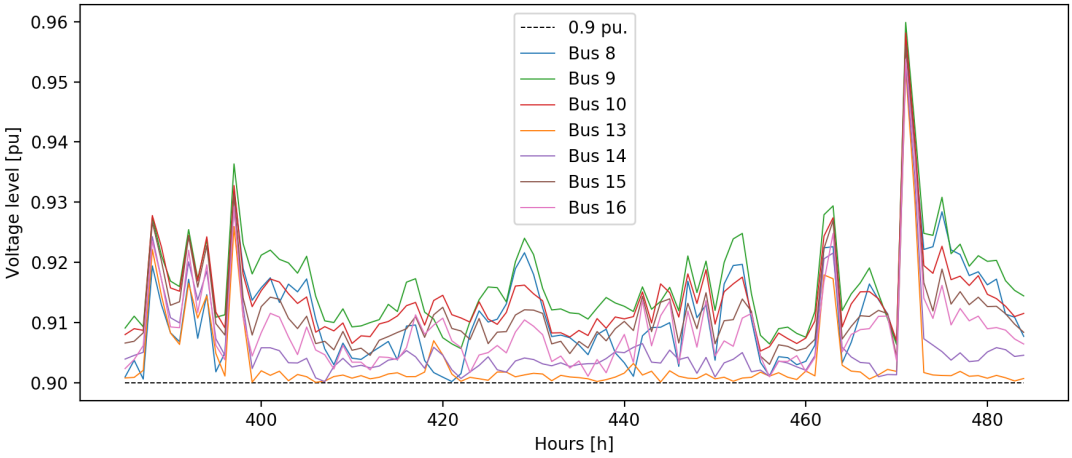

Figure D.2: A1: The voltage profiles of the seven load buses in radial B

Maren Refsnes Brubæk

Battery Storage as Alternative to Grid Reinforcement in the Low-Voltage Network

NTNU
Norwegian University of
Science and Technology